

C55.13: NESS 58

NOAA TR NESS 58

A UNITED STATES
DEPARTMENT OF
COMMERCE
PUBLICATION

NOAA Technical Report NESS 58

U.S. DEPARTMENT OF COMMERCE
National Oceanic and Atmospheric Administration
National Environmental Satellite Service

The Airborne ITPR Brassboard Experiment

W. L. Smith
D. T. Hilleary
E. C. Baldwin
W. Jacob
H. Jacobowitz
G. Nelson
S. Soules
D. Q. Wark



WASHINGTON, D.C.
March 1972

NOAA TECHNICAL REPORTS

National Environmental Satellite Service Series

The National Environmental Satellite Service (NESS) is responsible for the establishment and operation of the National Operational Meteorological Satellite System and of the environmental satellite systems of NOAA. The three principal Offices of NESS are Operations, Systems Engineering, and Research. The NOAA Technical Report NESS series is used by these Offices to facilitate early distribution of research results, data handling procedures, systems analyses, and other information of interest to NOAA organizations.

Publication of a Report in NOAA Technical Report NESS series will not preclude later publication in an expanded or modified form in scientific journals. NESS series of NOAA Technical Reports is a continuation of, and retains the consecutive numbering sequence of, the former series, ESSA Technical Report National Environmental Satellite Center (NESC), and of the earlier series, Weather Bureau Meteorological Satellite Laboratory (MSL) Report. Reports 1 to 37 are listed in publication NESC 56 of this series.

Reports 1 to 50 in the series are available from the National Technical Information Service, U.S. Department of Commerce, Sills Bldg., 5285 Port Royal Road, Springfield, Va. 22151. Price: \$3.00 paper copy; \$0.95 microfiche. Order by accession number, when given, at end of each entry. Beginning with 51, Reports are available through the Superintendent of Documents, U.S. Government Printing Office, Washington, D.C. 20402.

ESSA Technical Reports

- NESC 38. Angular Distribution of Solar Radiation Reflected from Clouds as Determined from TIROS IV Radiometer Measurements, I. Ruff, R. Koffler, S. Fritz, J. S. Winston, and P. K. Rao, March 1967. (PB 174 729)
- NESC 39. Motions in the Upper Troposphere as Revealed by Satellite Observed Cirrus Formation, H. McClure Johnson, October 1966. (PB 173,996)
- NESC 40. Cloud Measurements Using Aircraft Time-Lapse Photography, L. F. Whitney, Jr., and E. Paul McClain, April 1967. (PB 174 728)
- NESC 41. The SINAP Problem: Present Status and Future Prospects. Proceedings of a Conference held at the National Environmental Satellite Center, Suitland, Md., January 18-20, 1967, E. Paul McClain, Reporter, October 1967. (PB 176 570)
- NESC 42. Operational Processing of Low Resolution Infrared (LRIR) Data from ESSA Satellites, Louis Rubin, February 1968. (PB 178 123)
- NESC 43. Atlas of World Maps of Long-Wave Radiation and Albedo -- For Seasons and Months Based on Measurements from TIROS IV and TIROS VII, J. S. Winston and V. Ray Taylor, September 1967. (PB 176 569)
- NESC 44. Processing and Display Experiments Using Digitized ATS-1 Spin Scan Camera Data, M. B. Whitney, R. C. Doolittle, and B. Goddard, April 1968. (PB 178 424)
- NESC 45. The Nature of Intermediate-Scale Cloud Spirals, Linwood F. Whitney, Jr., and Leroy D. Herman, May 1968. (AD-673 681)
- NESC 46. Monthly and Seasonal Mean Global Charts of Brightness From ESSA 3 and ESSA 5 Digitized Pictures, February 1967-February 1968, V. Ray Taylor and Jay S. Winston, November 1968. (PB 180 717)
- NESC 47. A Polynomial Representation of Carbon Dioxide and Water Vapor Transmission, William L. Smith, February 1969. (PB-183 296)
- NESC 48. Statistical Estimation of the Atmosphere's Geopotential Height Distribution From Satellite Radiation Measurements, William L. Smith, February 1969. (PB 183 297)
- NESC 49. Synoptic/Dynamic Diagnosis of a Developing Low-Level Cyclone and Its Satellite-Viewed Cloud Patterns, Harold J. Brodrick and E. Paul McClain, May 1969. (PB 184 612)
- NESC 50. Estimating Maximum Wind Speed of Tropical Storms from High Resolution Infrared Data, L. F. Hubert, A. Timchalk, and S. Fritz, May 1969. (PB 184 611)
- NESC 51. Application of Meteorological Satellite Data in Analysis and Forecasting, R. K. Anderson, J. P. Ashman, F. Bittner, G. R. Farr, E. W. Ferguson, V. J. Oliver, and A. H. Smith, September 1969. (AD-697 033)
- NESC 52. Data Reduction Processes for Spinning Flat-Plate Satellite-Borne Radiometers, Torrence H. MacDonald, July 1970.

(Continued inside back cover)



U.S. DEPARTMENT OF COMMERCE
Peter G. Peterson, Secretary

NATIONAL OCEANIC AND ATMOSPHERIC ADMINISTRATION
Robert M. White, Administrator

NATIONAL ENVIRONMENTAL SATELLITE SERVICE
David S. Johnson, Director

NOAA Technical Report NESS 58

The Airborne ITPR Brassboard Experiment

W. L. Smith
D. T. Hilleary
E. C. Baldwin
W. Jacob
H. Jacobowitz
G. Nelson
S. Soules
D. Q. Wark

WASHINGTON, D.C.
MARCH 1972

UDC 551.508.25:551.507.352:551.507.362.2

551.5	Meteorology
.508	Instruments
.25	Radiance measurement
.507	Instrument carriers
.352	Aircraft observations
.362.2	Satellite observations

The inclusion of the name or description of any product does not constitute an endorsement by the NOAA National Environmental Satellite Service. Use for publicity or advertising purposes of information from this publication concerning proprietary products or the tests of such products is not authorized.

CONTENTS

Acknowledgements	iv
I. Introduction (W. L. Smith, S. D. Soules, and D. Q. Wark).....	1
Objectives.....	1
The CV-990 Expedition.....	2
II. Engineering description and evaluation (D. T. Hilleary and G. J. Nelson).....	2
The instrument.....	2
Aircraft installation and flight testing.....	18
III. Measurement characteristics (W. L. Smith).....	19
IV. Data reduction and accuracy (W. L. Smith, W. J. Jacob, and E. C. Baldwin).....	21
Introduction.....	21
The calibration equations.....	21
V. Clear-column radiance determination (W. L. Smith).....	24
Introduction.....	24
Analytical solution.....	24
Aircraft test results.....	26
Conclusion.....	28
VI. Aircraft-deduced atmospheric transmittances (W. L. Smith).....	28
Introduction.....	28
Mathematical solution.....	32
Computational procedure.....	34
Results.....	38
Summary.....	44
VII. Determination of cloud transmittance (H. Jacobowitz).....	44
Introduction.....	44

Numerical method.....	45
Results of the aircraft measurements.....	48
Conclusions and recommendations.....	55
References.....	59
Appendix Flight plan and ITPR data for June 12, 1970, (flight 7).....	60
I Flight plan.....	60
II Flight data.....	61

Acknowledgements

We would like to express our sincere gratitude to Earl Peterson and his staff at the Airborne Science Office of the NASA Ames Research Center, and William Nordberg of the NASA Goddard Space Flight Center for their collaboration which enabled the successful accomplishment of the Airborne ITPR Experiment. We also acknowledge the assistance L. Mannello, P. Pellegrino, and R. Ryan in the reduction and analysis of the data.

THE AIRBORNE ITPR BRASSBOARD EXPERIMENT

W. L. Smith, D. T. Hilleary, E. C. Baldwin, W. Jacob, H. Jacobowitz,
G. Nelson, S. Soules, and D. Q. Wark

National Environmental Satellite Service
National Oceanic and Atmospheric Administration
Washington, D.C.

ABSTRACT. A preprototype (brassboard model) Infrared Temperature Profile Radiometer (ITPR) was tested on the NASA Convair-990 aircraft expedition during June 1970. The objectives of the airborne ITPR experiment were to obtain data to test various techniques planned for deriving temperature soundings from spaceborne ITPR measurements and to specify the transmission characteristics of the atmosphere and clouds. This paper describes the instrument and shows various results obtained from the airborne measurements.

I. INTRODUCTION

Objectives

A preprototype (brassboard model) Infrared Temperature Profile Radiometer (ITPR) was tested on the NASA Convair-990 aircraft during June 1970. The ITPR measures the earth-atmosphere upwelling radiance in five narrow spectral channels whose detailed spectral characteristics are summarized in Section II of this report. The spectral intervals were chosen to obtain radiance observations similar to those collected by spacecraft instruments designed for sounding the distribution of the atmosphere's temperature and water vapor. A spacecraft version of the ITPR is assembled for the Nimbus 5 spacecraft to be launched in 1972. The objective of the airborne ITPR brassboard experiment was to provide data for detailed study of various problems of atmospheric remote sensing. The specific objectives of the ITPR experiment in the CV-990 were:

- (1) To obtain data to test a proposed technique for the deduction of clear-column radiances, and hence the atmospheric profile down to the earth's surface, from cloud-contaminated remote observations. (Section V summarizes some of the results of this test.)
- (2) To obtain radiance measurements in a cloudless atmosphere so that the atmospheric transmission characteristics of the ITPR spectral intervals could be determined. (Section VI summarizes these results.)
- (3) To obtain radiance measurements through various types of clouds so that the spectral transmittance characteristics of clouds could be studied. (Section VII summarizes these results.)

The CV-990 Expedition

The ITPR was flown aboard the NASA Convair-990 during the June 1970 meteorological expedition conducted by the Goddard Space Flight Center and the Airborne Science Office of the Ames Research Center. The CV-990 meteorological expedition consisted of 10 flights, each with a duration of about 5 hours. Figures I-1, I-2, I-3, and I-4 show the date, time, and ground track of each flight. The expedition covered a wide range of latitude (28°N-80°N) and terrain (desert, mountains, vegetated land, ocean, and ice); a wide variety of weather conditions was also sampled. The 10 flights collected a sample of airborne radiance data almost as diverse as radiance data obtained by earth-orbiting satellites. This report describes the ITPR instrument, its airborne radiance measurements, and the application of these data to solutions of various atmospheric radiative transfer problems.

II. ENGINEERING DESCRIPTION AND EVALUATION

The Instrument

The preprototype Infrared Temperature Profile Radiometer (ITPR) is a five-channel filter radiometer. Each channel measures radiances in a different spectral interval. The channel spectral characteristics and the pertinent atmospheric absorption bands are shown in Table II-1. Figure II-1 shows the measured transmittance of the spectral filters in channels 1 through 5.

The instrument collects infrared energy with five identical optical telescopes, all of which are oriented to view a common field via a scan mirror. Table II-2 is a summary of the ITPR optical characteristics, figure II-2 is a system block diagram of the instrument electronics, and figure II-3 shows the optical design of a typical channel.

The radiation beams sensed by the five telescopes are chopped by a common mechanical chopper operating at 23.5 Hz, and are then spectrally filtered. A thermistor bolometer detector behind each telescope converts the chopped radiation energy into a proportional AC electrical signal. The signals are amplified and processed through separate electronic channels, each including a synchronous demodulator and a post-demodulation filter.

The ITPR is composed of two units: the optics unit (fig. II-4) which contains the scan mirror drive assembly, optics deck, a.c. amplifiers, a thermistor bolometer bias power supply, and a housing calibration surface; and the electronics unit, which contains the channel demodulators, scan logic, temperature monitor circuits, clocks, command relays, and an instrument power supply.

The optics deck (fig. II-5) contains the channel telescopes, an optical chopper assembly, and the detectors. In the chopper assembly an arrangement, utilizing a gallium arsenide light-emitting diode and a photo transistor, generates a phase reference signal for the synchronous demodulator of each channel.

The ITPR analog signal channel (the preamplifier, amplifier, and

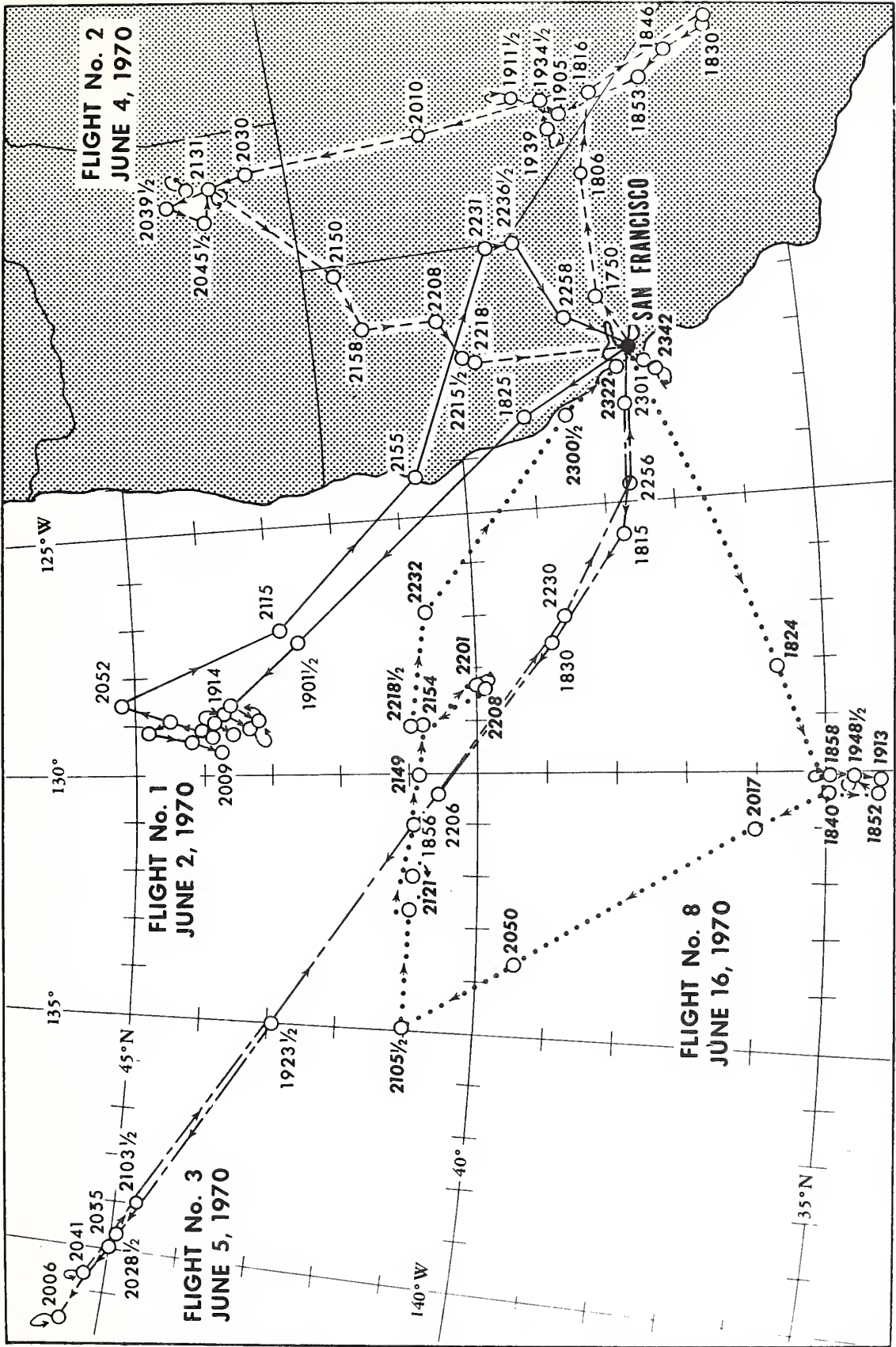


Figure I-1.---Ground-tracks for Convair-990 Flights No. 1, 2, 3, and 8.

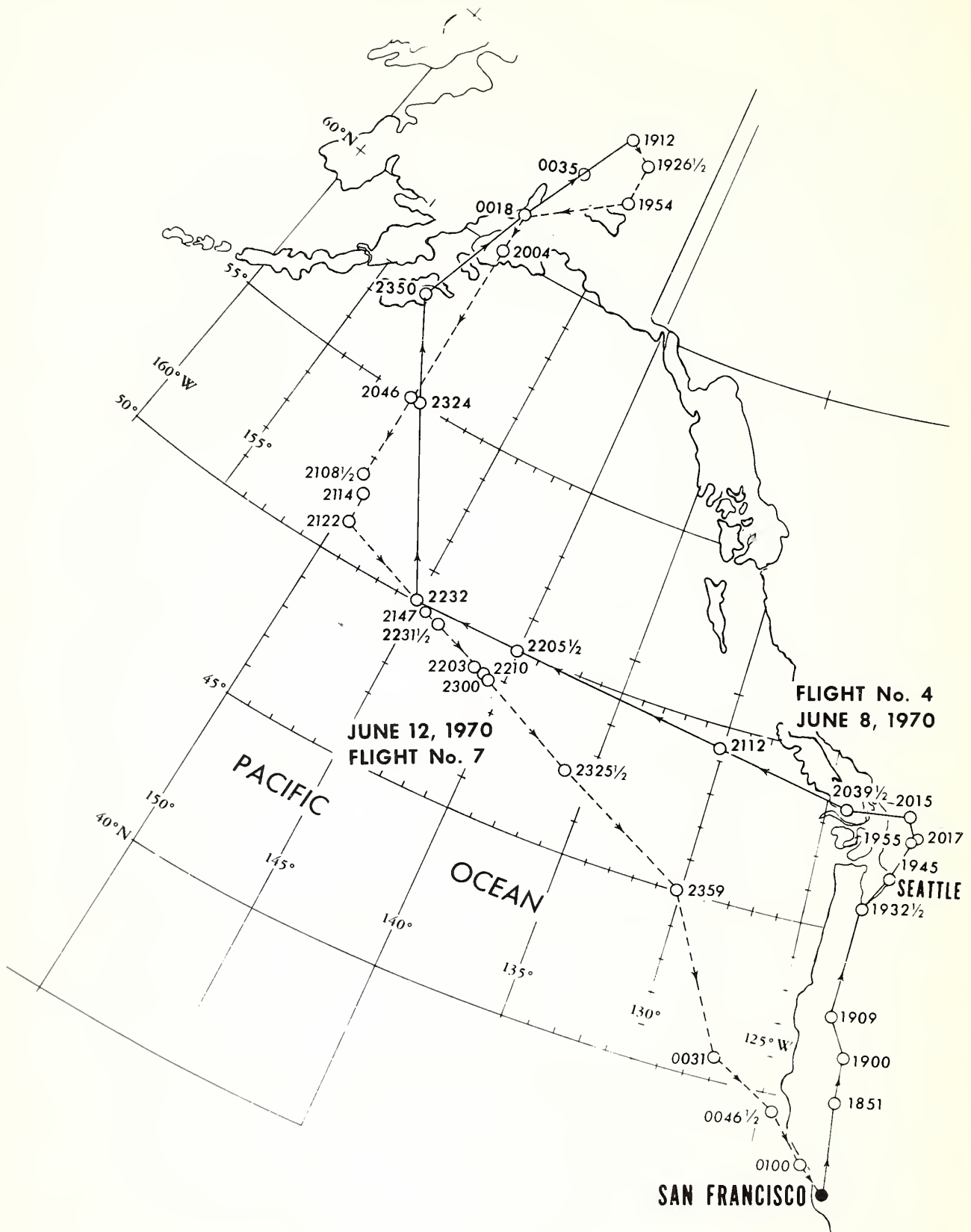


Figure I-2.--Ground-tracks for Convair-990 Flights No. 4 and 7.

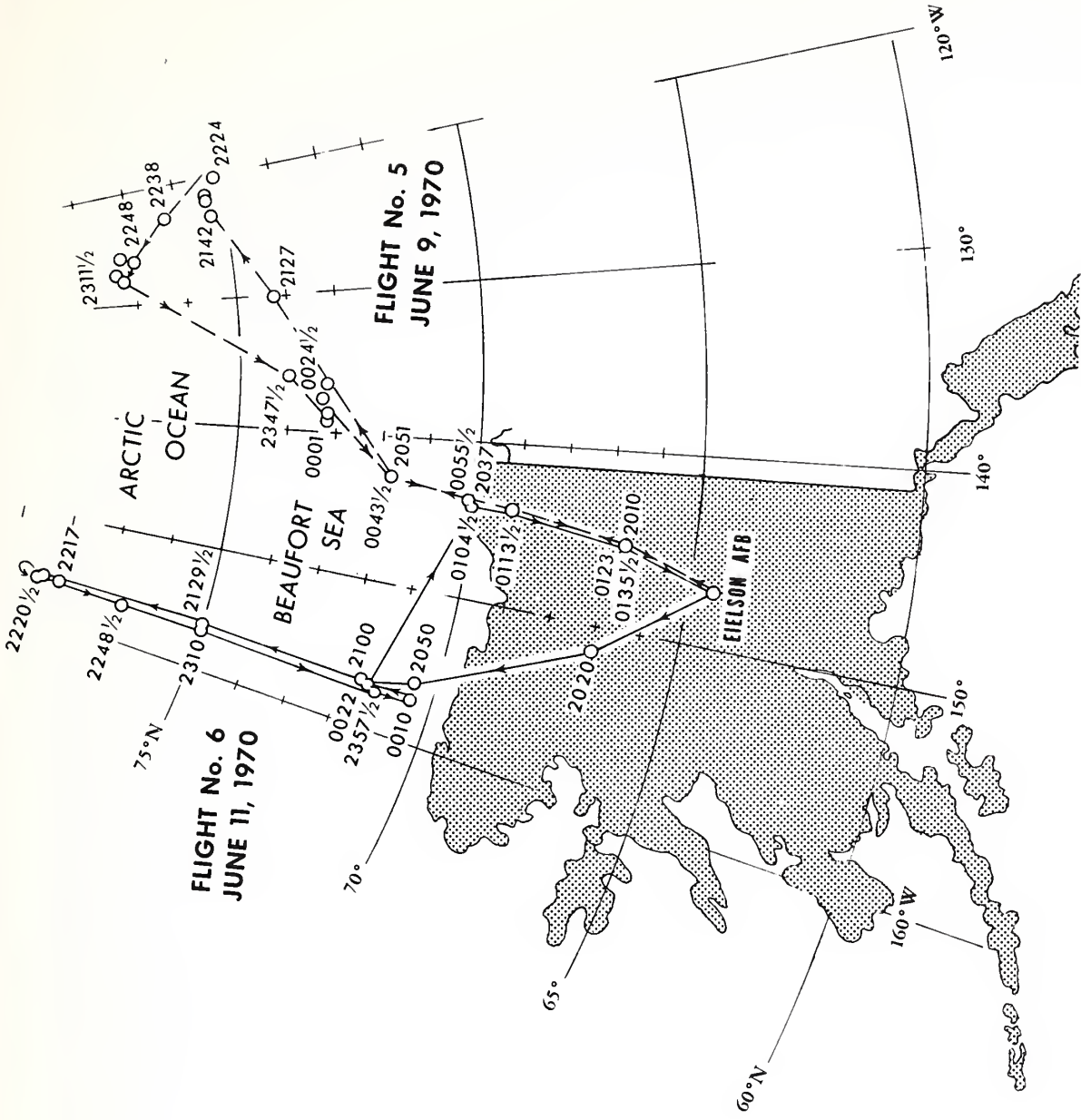


Figure I-3.--Ground tracks for Convair-990 Flights No. 5 and 6.

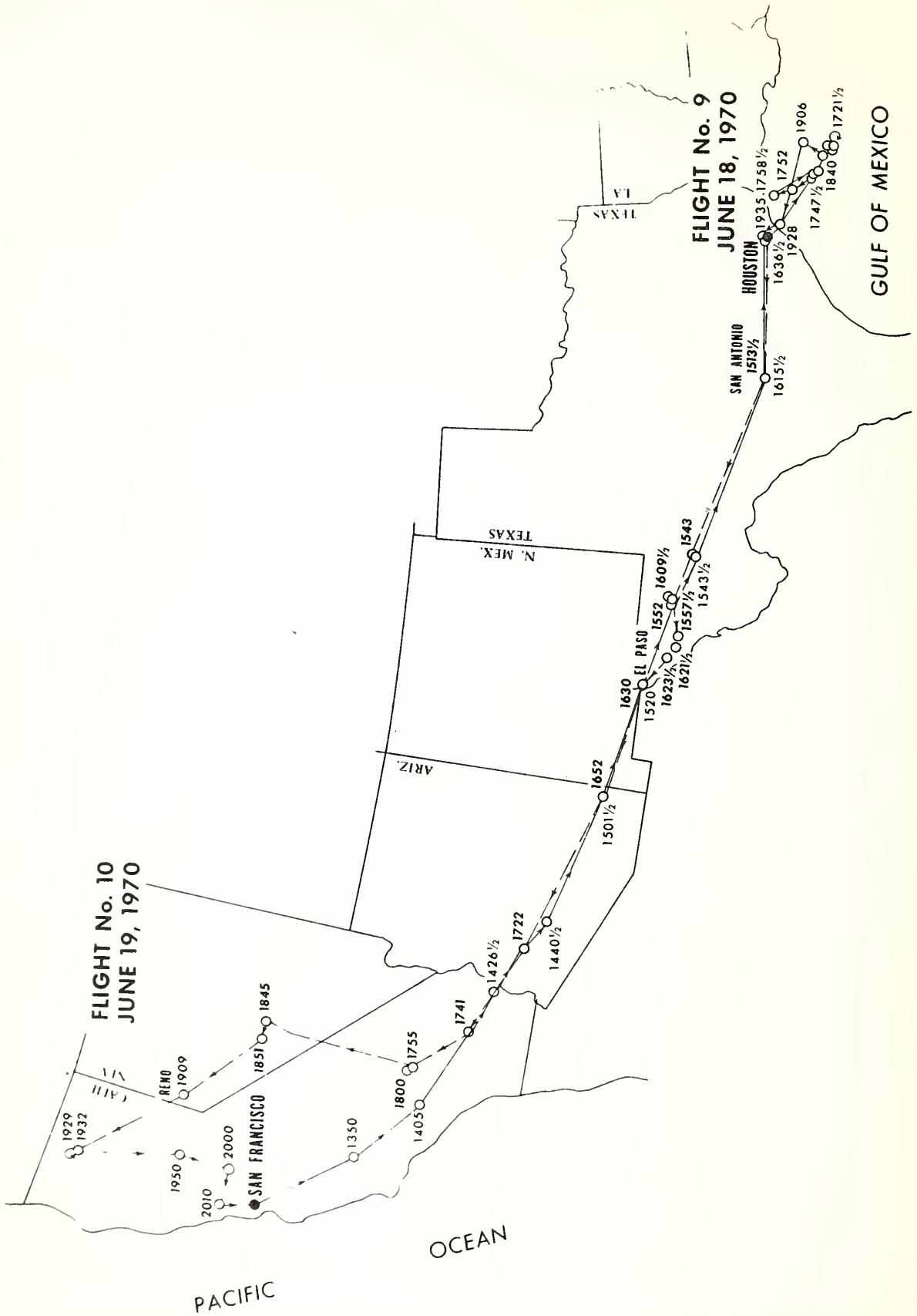


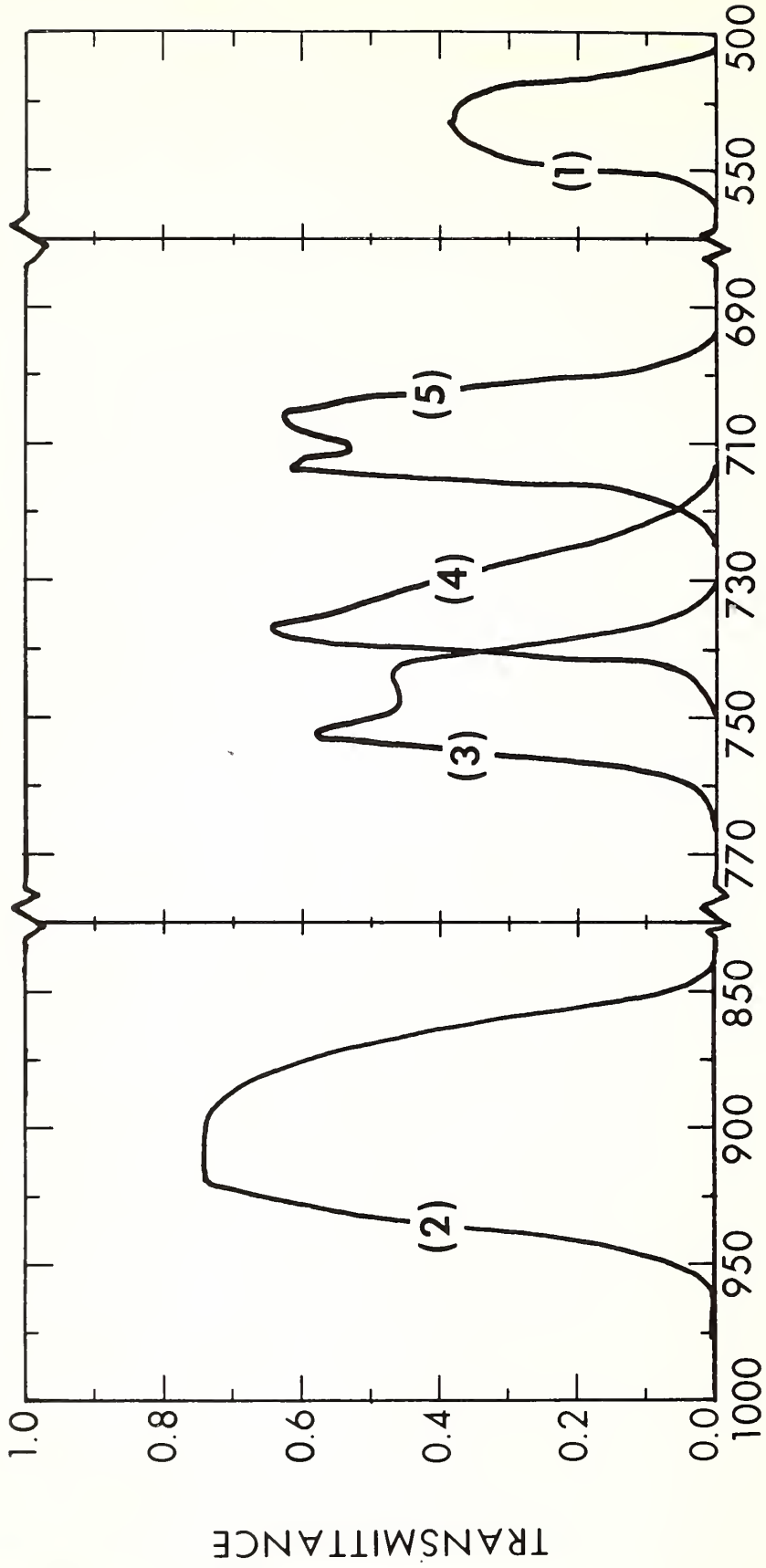
Figure I-4.--Ground-tracks for Convair-990 Flights No. 9 and 10.

Table II-1.--Summary of ITPR spectral characteristics

<u>Channel</u>	<u>Energy-weighted central wavenumber cm⁻¹</u>	<u>Half-power bandwidth cm⁻¹</u>	<u>Absorption band</u>
1	532.5 (18.8 μ m)	30	H ₂ O
2	898.5 (11.1 μ m)	80	Window
3	747.0 (13.4 μ m)	20	CO ₂
4	732.5 (13.7 μ m)	20	CO ₂
5	708.0 (14.1 μ m)	20	CO ₂

Table II-2.--Summary of ITPR optical characteristics

Number of channels	Five, each with separate telescope
Optical FOV (half power)	3.0°
Objective optics	Aspheric Cassegranian
Entrance aperture diameter	4.52 cm
Focal length	14.50 cm
Optical speed	f/3.2
Effective aperture	11.9 cm ²
Condensing optics	Refractive (Entrance aperture imaged on detector)
Scan mirror	Flat Ni-plated aluminum alloy substrate-overcoated with Al and SiO



WAVE NUMBER (cm⁻¹)

Figure II-1.--Measured transmittances of the spectral filters in ITPR channels 1 through 5.

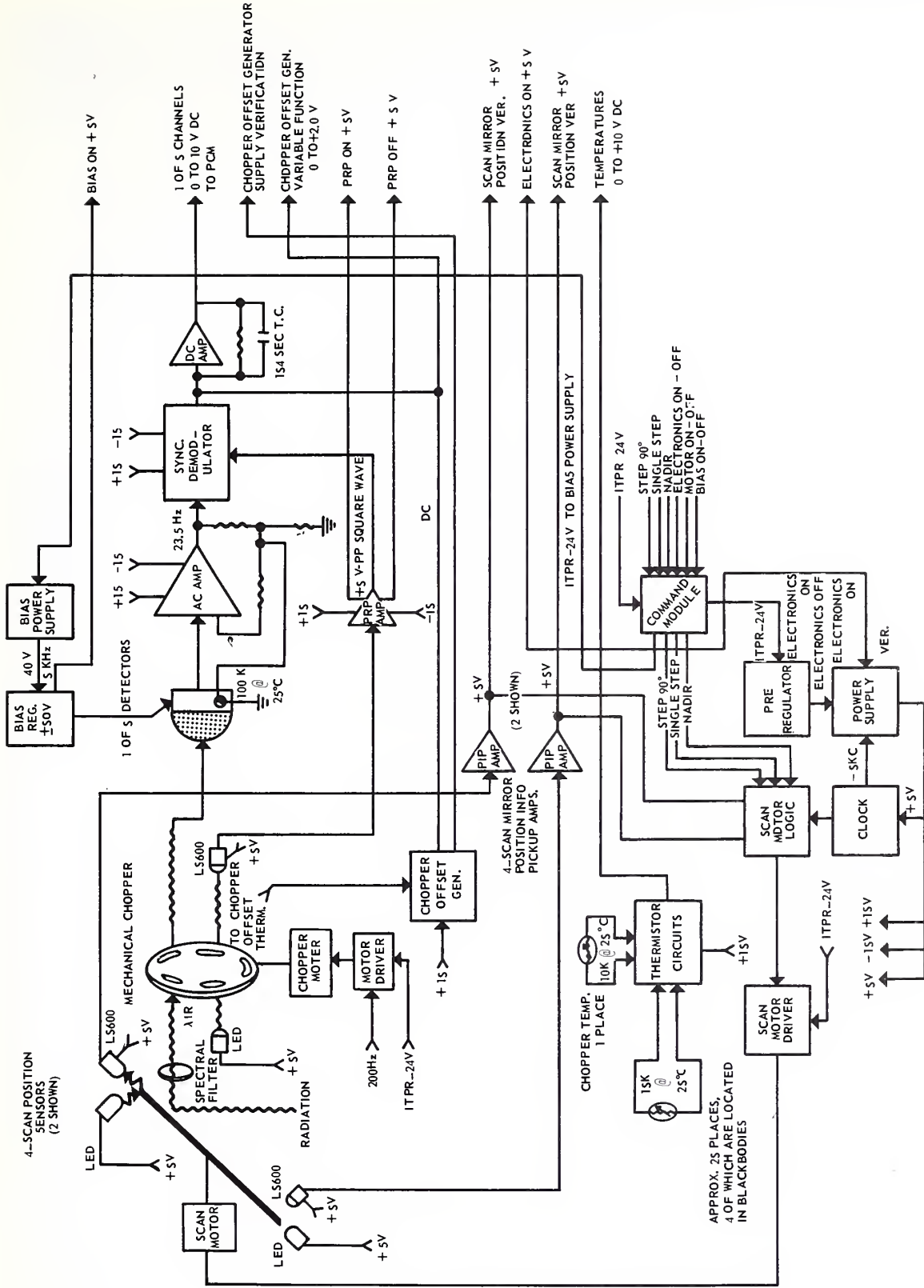


Figure II-2.--ITPR electronics block diagram.

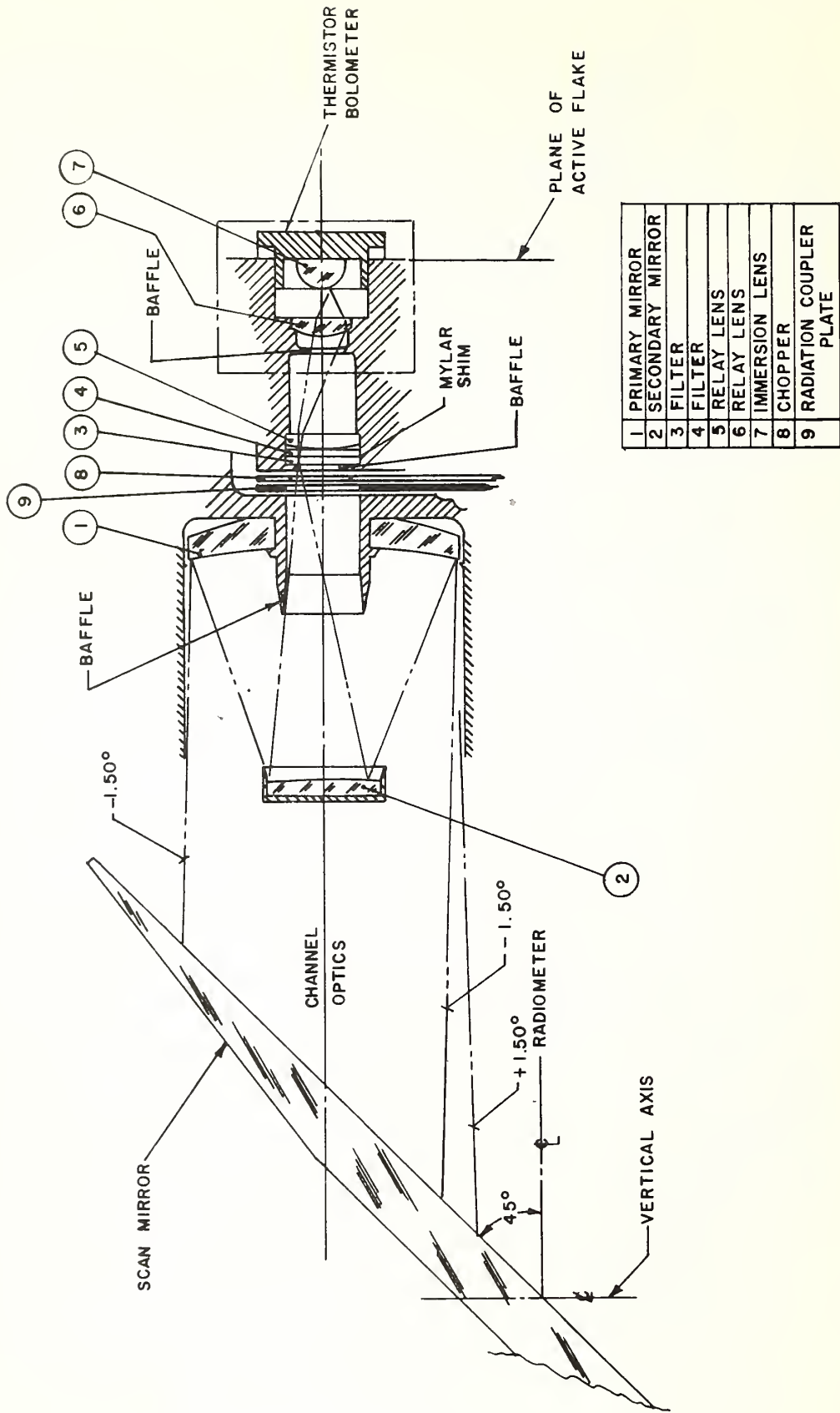


Figure II-3.--Illustration of a typical channel optics layout.

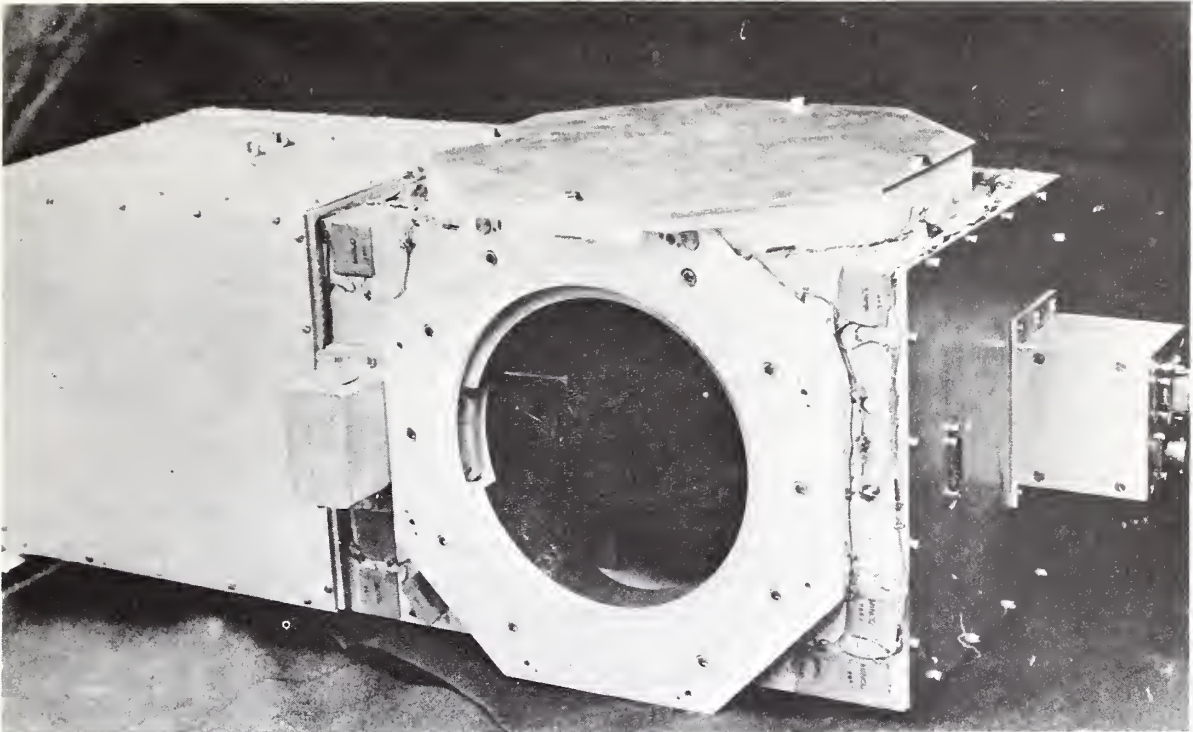


Figure II-4.--ITPR optics unit.

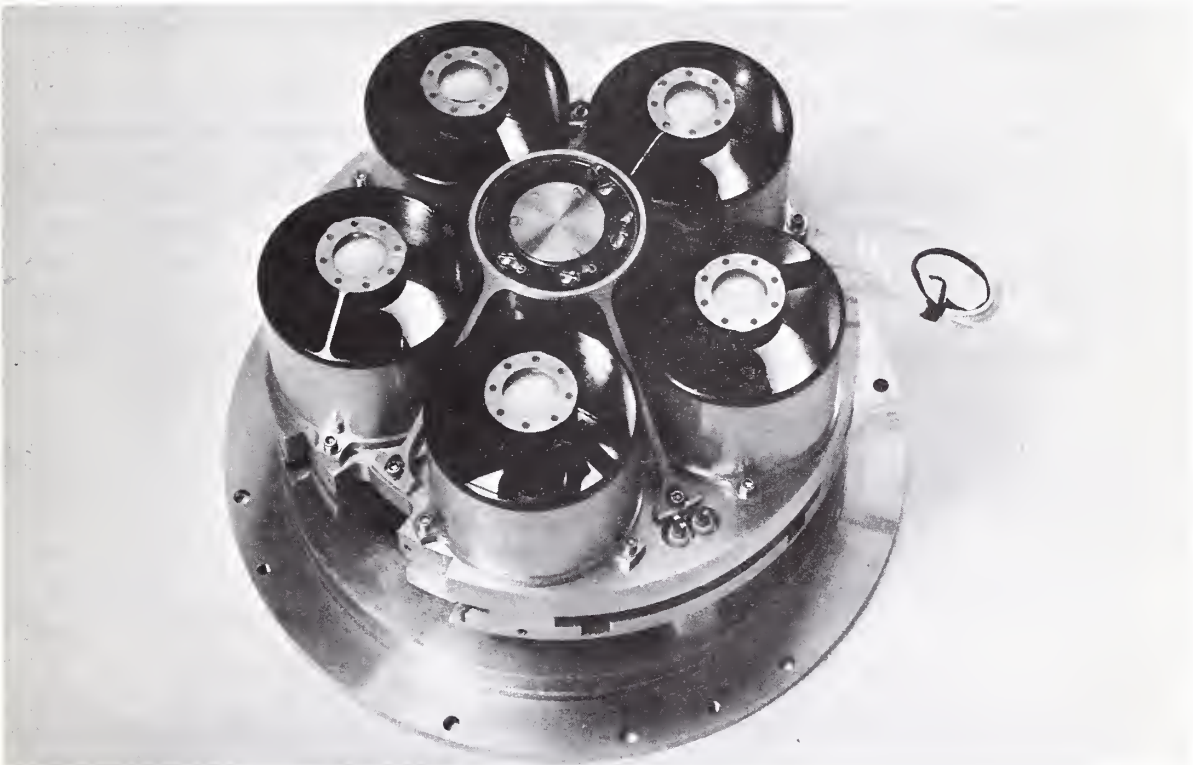


Figure II-5.--ITPR optics deck containing the channel telescopes.

synchronous demodulator) is a modified version of the circuitry designed for the NIMBUS 4 SIRS (Wark et al. 1970). The input stage is a differential amplifier in the Middlebrook configuration using a matched pair of Field Effect Transistors selected for low noise and high transconductance (Middlebrook and Taylor/1961). As in the NIMBUS 4 SIRS, the three-stage amplifier section is capable of producing total gains of 1.4×10^6 . Individual hybrid voltage regulators are used to decouple each amplifier from the power supply to reduce noise and to limit channel crosstalk to better than -60db. A thermistor mounted on the detector case, but electrically a part of the feedback loop of the amplifier second stage, is used to adjust the gain to compensate for the change of detector responsivity as a function of temperature (Barnes Engineering Company/1958). ITPR had a gain compensation to within 2 percent.

One of the problems inherent in a radiometer in which an opaque mechanical chopper is used to modulate incoming scene radiances is the need to correct the signal component caused by sensed radiant energy emitted by the chopper. Since the modulated energy reaching the detector is basically a function of the difference between the temperatures of the scene and the chopper, the instrument channel calibrations are affected by changes in the chopper temperature. In the ITPR, the chopper temperature is sensed by a thermistor embedded in a "radiation coupler plate" adjacent to the chopper. The thermistor is designed into a compensation network (chopper offset generator) which produces a d.c. offset signal. The offset signal is summed with the radiation difference signal to reduce the dynamic range of the measurement and optimize signal telemetry. The offset signals generated for each ITPR channel compensate the output signals for the spectral radiance of the chopper to within 2 percent. A more detailed description of the chopper offset generator and its function appears below.

The following radiometric analysis indicates how a channel calibration should change as a function of varying instrument component temperatures. Each channel senses the chopped radiation (or the difference in radiant power at the detector which results from opening the chopper). The first equation below applies when a chopper port passes all of the sensed beam, and the second equation is applicable when the chopper completely obscures the beam.

$$P_1 = A \Omega \eta \Delta v [0.74 \rho_{ms} \rho_{m1} \rho_{m2} B(T_s) + 0.26 \rho_{m2} B(T_o) + 0.74 \rho_{m1} \rho_{m2} \epsilon_{ms} B(T_{ms}) + 0.74 \rho_{m2} \epsilon_{m1} B(T_{m1}) + \epsilon_{m2} B(T_{m2})] + P_a \quad (\text{II-1})$$

$$P_2 = A \Omega \eta \Delta v B(T_c) + P_a \quad (\text{II-2})$$

where:

P_1 is the radiative power reaching the detector with the chopper completely open and P_2 is the radiative power reaching the detector with the chopper completely closed;

$A = \pi D^2/4$ and D is the outside diameter of the effective primary mirror stop (11.9 cm²);

Ω is the solid angle of the "half power" field of view of the channel (2.16 x 10⁻³ steradian);

η is the effective transmission of the filter and lenses weighted for the associated spectral bandwidth;

τ_f and τ_l are the spectral transmissions of the filter and lenses, respectively;

$B(T)$ is the effective blackbody radiance in the spectral interval $\Delta\nu$ at blackbody temperature T and

$$\eta \Delta\nu B(T) = \int \tau_f \tau_l B(\nu, T) d\nu;$$

T_s and T_c are the effective blackbody temperatures of the scene and the chopper, respectively;

T_o is the blackbody temperature of the channel components whose emissions reach the detector via the central portion of the primary aperture obscured by the secondary mirror;

T_{m1} , T_{m2} , T_{ms} are temperatures of the primary, secondary, and scan mirrors, respectively;

ρ_{m1} , ρ_{m2} , ρ_{ms} are reflectances of the primary, secondary, and scan mirrors;

P_a is the sensed radiation emitted by components on the detector side of the chopper~

The numerical constant 0.74 is necessary because 26 percent of the channel entrance aperture, A , is obscured by the secondary mirror and spider as shown in figures II-3 and II-5. The second term in the brackets occurs because the detector views the obscured portion of the aperture. It senses radiation emitted by the cylindrical baffle tube and other components in reflections from the central part of the secondary mirror.

The other terms in equation (II-1) represent radiation emitted by the mirrors. The radiation power, P_a , emitted by components on the detector side of the chopper and reaching the detector is eliminated by subtracting equation (II-2) from equation (II-1). Equation (II-3) was written in terms of the root-mean-square value of the chopped radiant power on the detector. Matched mirror reflectances and equal primary and secondary mirror temperatures have been assumed.

$$\begin{aligned} P_{rms} = C_1 (P_1 - P_2) = C_1 A \Omega \eta \Delta\nu [& 0.74 \rho^3 B(T_s) + \\ & 0.26 \rho B(T_o) + 0.74 \rho^2 \epsilon B(T_{ms}) + \\ & (1.74\epsilon - 0.74\epsilon^2) B(T_{m1}) - B(T_c)] \end{aligned} \quad (II-3)$$

C_1 is a factor to convert the amplitude of the radiant power waveform ($P_1 - P_2$), to its root-mean-square, P_{rms} . The factor depends upon the shape of the radiant power waveform created by the chopper port passing through the sensed beam and depends upon the relative sizes of the beam and the port.

The higher order emissivity term has been dropped from equation (II-4). This equation has been arranged to show that the channel must be considered to measure not only the differences between the chopper radiance and that of the scene, but also to some extent the differences between the chopper radiance and the obscuration and mirror radiances.

$$\begin{aligned}
 P_{rms} = & C_1 A \Omega \eta \Delta v \{ [0.74 - 2.22\epsilon] [B(T_S) - B(T_C)] \\
 & + [0.26 - 0.26\epsilon] [B(T_O) - B(T_C)] \\
 & + 0.74\epsilon [B(T_{ms}) - B(T_C)] \\
 & + 1.74\epsilon [B(T_{m1}) - B(T_C)] \}
 \end{aligned}
 \tag{II-4}$$

, where $\epsilon = 1 - \rho$

The relative sensitivities of the signal to target radiances, and to mirror emissions, can be estimated by assuming mirror reflectances and emissivities. The ITPR mirror surfaces are aluminum overcoated with a 0.15-micron thickness of silicon monoxide. Reflectivities of 96 percent and emissivities of 4 percent were assumed to obtain equation (II-5). These values may be pessimistic, but the cleanliness of the mirrors could not be maintained during the flight test program.

$$\begin{aligned}
 P_{rms} = & C_1 A \Omega \eta \Delta v \{ 0.65 [B(T_S) - B(T_C)] \\
 & + 0.25 [B(T_O) - B(T_C)] + 0.03 [B(T_{ms}) - B(T_C)] \\
 & + 0.07 [B(T_{m1}) - B(T_C)] \}
 \end{aligned}
 \tag{II-5}$$

It is apparent that the instrument calibration can be affected significantly by temperature changes in the chopper, obscuration, telescope mirror, and scan mirror. The chopper temperature is indirectly sensed in the ITPR. The rotating chopper is radiatively coupled to a "radiation coupler plate" which contains thermistor temperature sensors. One thermistor circuit output is used only as a monitor; another is used with the chopper offset generator circuitry mentioned above.

The chopper temperature monitor was calibrated indirectly. The optics deck was mounted in a temperature-controlled fixture and set up to measure spectral radiances from a blackbody source. The optical path was purged with nitrogen. The amplitudes of the AC signals were brought to zero, at the output of the amplifiers, by adjusting the blackbody temperature. This procedure was repeated for several instrument temperatures. In each instance, the instrument and source were allowed to reach thermal equilibrium.

The relationship of the channel output signal to the chopped radiance

can be simplified to the following equation:

$$S_{dc} = C_2 R(T_d) G_1(T_d) H G_2 P_{rms} + X(T_c) \quad (II-6)$$

where:

S_{dc} is the d.c. voltage at the analog electronic channel output.

$R(T_d)$ is the single flake thermistor bolometer responsivity in volts rms/watt rms (including all harmonic components) which is a function of detector temperature (Barnes Engineering Company 1958).

C_2 is a constant factor necessary to adjust the single flake responsivity specified by the bolometer manufacturer. It corrects the responsivity for the bolometer bias voltage, the chopping frequency, and the signal loading by the compensating thermistor flake (Barnes Engineering Company 1958).

$G_1(T_d)$ is the a.c. amplifier gain which has been made a function of detector temperature so that the product $R(T_d) G_1(T_d)$ is approximately constant (Barnes Engineering Company 1969).

H is a factor which relates the DC output of the synchronous demodulator to the rms of the AC signal waveform. The amplifier bandwidth passes all of the significant signal components.

G_2 is the effective signal gain in the post-demodulation filter which includes a DC amplifier.

$X(T_c)$ is the chopper-offset-generator signal component as measured at the channel output.

Combining (II-5) and (II-6):

$$S_{dc} = C_1 C_2 A \Omega \eta \Delta v R(T_d) G_1(T_d) H G_2 \{ 0.65 B(T_s) + 0.25 B(T_o) + 0.07 B(T_{ml}) + 0.03 B(T_{ms}) - B(T_c) \} + X(T_c) \quad (II-7)$$

The changes of detector responsivity with temperature are partially compensated as mentioned above. The circuitry was adjusted empirically to make the product of detector responsivity and AC amplifier gain constant, within ± 2 percent, over the temperature range 10° to 40°C . The slope of each channel's output versus the pertinent spectral radiance of a blackbody test source was determined from instrument temperatures of 10° , 25° and 40°C . The 10° and 40°C slopes were finally equalized by adjusting the value of a resistor in series with the thermistor. The slope at 25°C was about 2 percent greater than at other temperatures.

The chopper offset generator signal is expressed in equations (II-6) and (II-7) in terms of its effect at the channel output, because the d.c.

amplifier actually amplifies the fixed offset signal component, the variable offset signal component, and the synchronous demodulator output signal by different factors. Different input resistors are used at the summing junction of the d.c. operational amplifier for the various signal components.

Equation (II-8) shows the desired offset term assuming that $T = T_c$. Equations (II-9) and (II-10) show the form of the offset signals generated by the chopper offset generator circuitry shown in figure II-6.

$$X(T_c) = 0.74 \rho^3 A \Omega \eta \Delta v R(T_d) G_1(T_d) H G_2 B(T_c) \quad (\text{II-8})$$

$$X(T_c) = \left[G_3 \frac{R_7 E_1}{\frac{R_6 T}{R_6 + R_T} + R_7} \right] + G_4 E_1 \left(\frac{R_3 + R_4 + R_5}{R_2 + R_3 + R_4 + R_5} \right) \quad (\text{II-9})$$

$$R_T = R_o \exp \beta \left(\frac{1}{T_c} - \frac{1}{T_o} \right) \quad (\text{II-10})$$

where:

G_3 is the d.c. amplifier gain for the variable chopper offset signal.

G_4 is the d.c. amplifier gain for the fixed chopper offset signal.

R_6 and R_7 are resistances as indicated in figure II-6.

R_T is the resistance of thermistor temperature sensor mounted on the radiation coupler plate. R_o is its resistance at temperature T_o .

β is a property of the thermistor material.

The chopper offset term has not been combined with other terms in equation (II-7) because of the manner in which the flight data were processed. The fixed voltage E_1 and the variable voltage corresponding to the bracketed portion of equation (II-9) were separately digitized and recorded with the channel output data and used to compute $X(T_c)$ from equation (II-9). The computed $X(T_c)$ was then subtracted from the recorded channel output, S_{dc} . In practice, the offset generator circuitry only served to compress the range of the recorded data. The proper performance of the generator circuitry was checked by comparing the variable portion of $X(T_c)$ against the values of T_c measured by the monitoring thermistor.

It can be shown from equation (II-7) that the primary and secondary mirror temperatures could be allowed to change about 1.5°C, or that the scan mirror temperature could change about 3°C before the spectral radiances deduced from an initial instrument calibration would err by more than 0.25 ergs/cm² s sr cm⁻¹. The mirror temperatures were not measured.

Variations in the chopper and obscuration temperatures would be much more serious. The temperature of the radiation coupler plate was measured

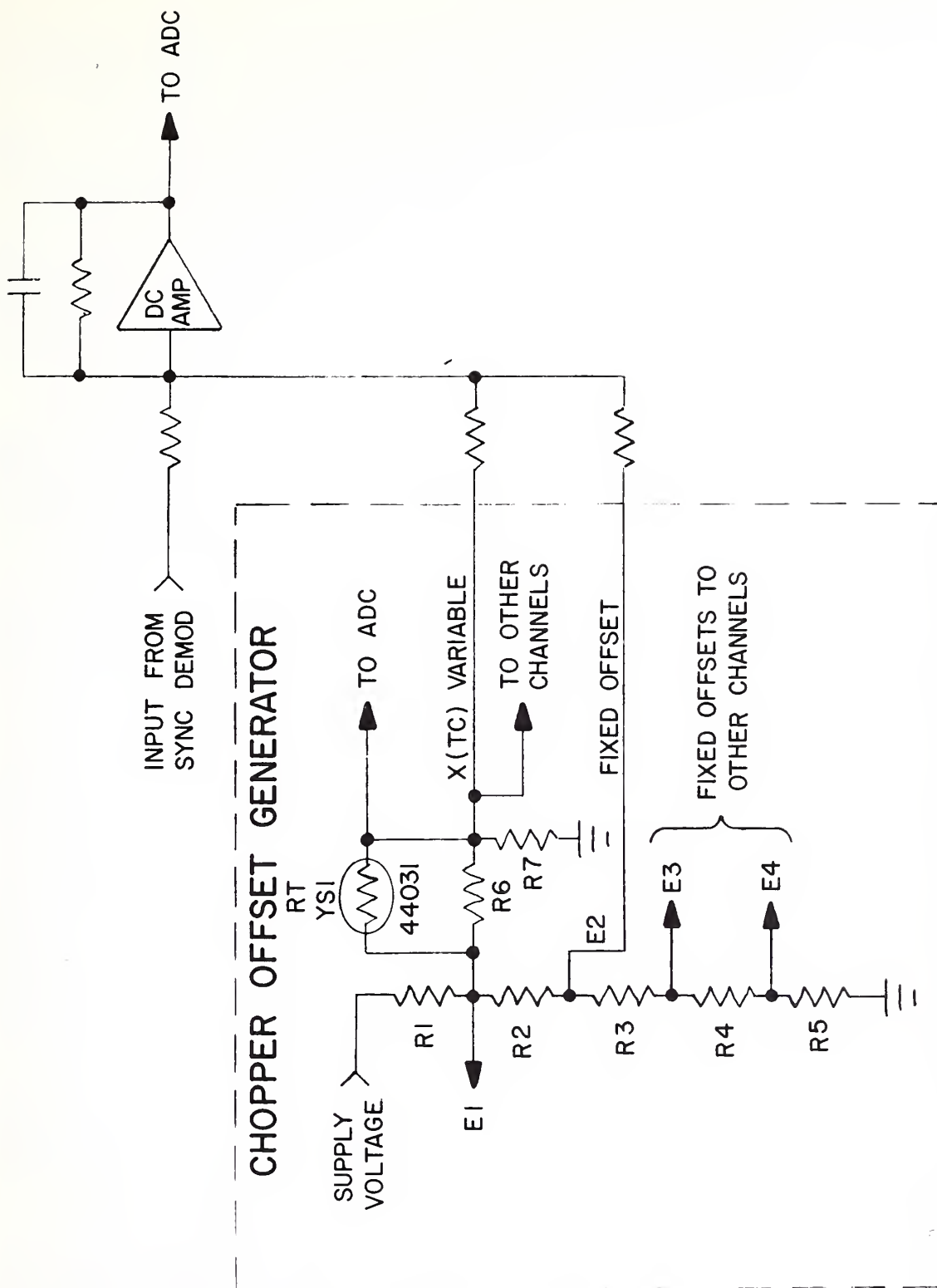


Figure II-6.--Schematic of chopper offset generator circuit typical for one channel.

but could not be considered a satisfactory indicator of chopper or obscuration temperature except when the instrument temperature was not changing.

Aircraft Installation and Flight Testing

The instrument, attached to a special frame which included a remotely controlled door assembly, was mounted in the forward cargo compartment of the aircraft. The NASA Convair-990 is fitted with windows near the bottom of its cargo compartments. A tubular section of the frame penetrated the aircraft fuselage through a mating sleeve in a dummy window plate, allowing the radiometer a clear view of the earth beneath the aircraft. O-ring seals between the instrument and frame and the tube and window sleeve maintained the pressure integrity of the cargo compartment.

Two blackbody radiation sources were installed with the radiometer. The scan mirror indicated in figure II-3 could be rotated on command so that the channels viewed (1) the earth beneath the aircraft, (2) a warm blackbody operated at about 50°C, (3) the instrument's housing calibration surface, or (4) a cold blackbody operated at a temperature between 0° and -40°C. The radiating surfaces of the blackbodies consisted of V-grooves milled into copper plates and coated with 3M401 "Black Velvet" paint.

The cold blackbody was designed as an integral part of a small 5-liter dewar and was cooled by liquid nitrogen (LN₂). A larger (45-liter) storage dewar contained enough LN₂ for flights of 4 to 6 hours. Thermistors sensed the liquid level in the small blackbody dewar, and a liquid level controller automatically valved LN₂ from the larger dewar when it was required. Nitrogen gas boiled off from the small dewar was used to purge the instrument's optical path prior to opening the remotely controlled door, and to cool the warm blackbody thermal sink.

The blackbody temperatures were controlled to about 0.2°C. Commercial thermocouple deviation amplifiers were used to sense the blackbody temperatures and to drive temperature controllers which provided signals to Silicon Control Rectifier power units that powered the blackbody resistance heaters. Thermistors embedded in the radiator plates were used to read out the radiator temperatures. The thermistors were calibrated in situ against certified thermocouples, also embedded in the plates; however, these thermocouples were not read out during the flights.

During the flight attempts were made to determine the channel calibrations (using two blackbody temperatures) whenever the instrument temperature changed significantly. The housing calibration surface proved to be unreliable for calibration because of internal thermal gradients.

The instrument, the blackbodies, the LN₂ supply, and other auxillary equipment were controlled and monitored from a console located in the aircraft passenger cabin. The instrument's infrared and housekeeping data were multiplexed, digitized, formatted, and recorded on a digital tape recorder. An auxillary multiplexer and analog-to-digital converter transferred data to a paper tape printer which generated an inflight printout of the infrared data and selected housekeeping data.

III. MEASUREMENT CHARACTERISTICS

The spectral radiance, $I_{\nu_0}(p_t)$, measured in any spectral channel of the airborne ITPR at the pressure level, p_t over a cloudless atmosphere is given by the radiative transfer equation

$$I_{\nu_0}(p_t) = B_{\nu_0}(p_0)\tau_{\nu_0}(p_t, p_0) - \int_{p_t}^{p_0} B_{\nu_0}(p) \frac{d\tau_{\nu_0}(p_t, p)}{d \ln p} d \ln p \quad (\text{III-1})$$

where $B_{\nu_0}(p)$ is the Planck radiance source function at pressure level p and the channel central wave number, ν_0 . $\tau_{\nu_0}(p_t, p)$ is the mean spectral transmittance of the atmosphere between the pressure levels defined by

$$\tau_{\nu_0}(p_t, p) = \int_0^{\infty} \phi_{\nu} \tau_{\nu}(p_t, p) d\nu / \int_0^{\infty} \phi_{\nu} d\nu \quad (\text{III-2})$$

where ϕ_{ν} is the channel response function. The Planck radiance is given by

$$B_{\nu_0}(p) = 2hc^2\nu_0^3 / \{\exp(hc\nu_0/k T(p)) - 1\} \quad (\text{III-3})$$

where $h = 6.6237 \times 10^{-27}$ erg sec, $c = 2.99791 \times 10^{10}$ cm sec⁻¹ and $k = 1.38024 \times 10^{-16}$ erg deg⁻¹. $T(p)$ is the atmospheric temperature at the pressure level p . The equivalent blackbody (brightness) temperature sensed by any channel is

$$T_{\nu_0}^B(p_t) = hc\nu_0/k \ln \{2hc^2\nu_0^3 / I_{\nu_0}(p_t) + 1\} \quad (\text{III-4})$$

Channel 1 ($\nu_0 = 532.5$ cm⁻¹) measures the radiation upwelling from the earth and atmosphere within a semitransparent spectral region of the rotational water vapor band. The radiance measured in this spectral interval can be interpreted in terms of the total amount of water vapor in the atmospheric column below the instrument sensor.

Channel 2 ($\nu_0 = 898.0$ cm⁻¹) measures most of the radiation emitted from the earth's surface and clouds below the sensor. The radiation measured in this "atmospheric window" channel is only slightly attenuated by atmospheric gases (primarily water vapor) and so can provide a good measure of cloud-top and surface temperatures as well as cloud cover. Channels 3 ($\nu_0 = 747.0$ cm⁻¹), 4 ($\nu_0 = 732.5$ cm⁻¹), and 5 ($\nu_0 = 708.0$ cm⁻¹) sense the radiation upwelling in semitransparent regions of the 15 μ m CO₂ band. Since the atmospheric CO₂ distribution is known, these spectral measurements can be interpreted in terms of the temperatures of lower, middle, and upper layers of the atmosphere below the instrument.

Figure III-1 shows the variation of the effective radiating altitude for each channel at varying aircraft altitudes. The "effective-radiating-altitude" is defined here as that atmospheric level where the air temperature is equal to the measured equivalent blackbody temperature. Channel 5 measurements provide a good means for determining the air temperature at aircraft level (i.e., the effective radiating pressure equals the aircraft pressure) up to about 5,000 ft. The window channel, channel 2, senses temperatures at and close to the earth's surface, even under fairly moist

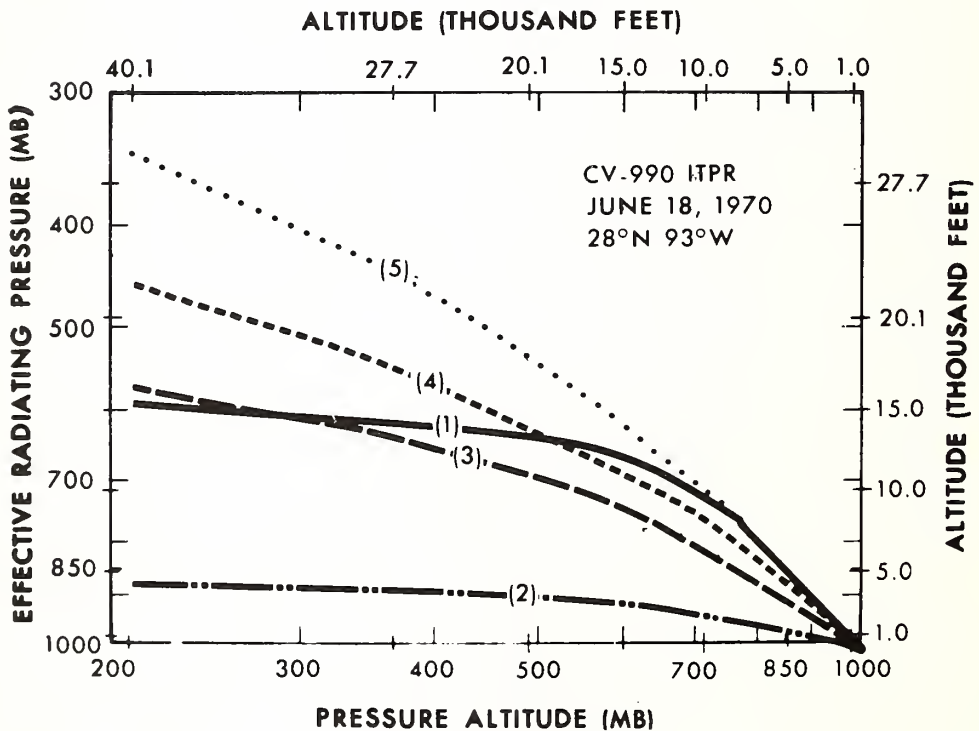
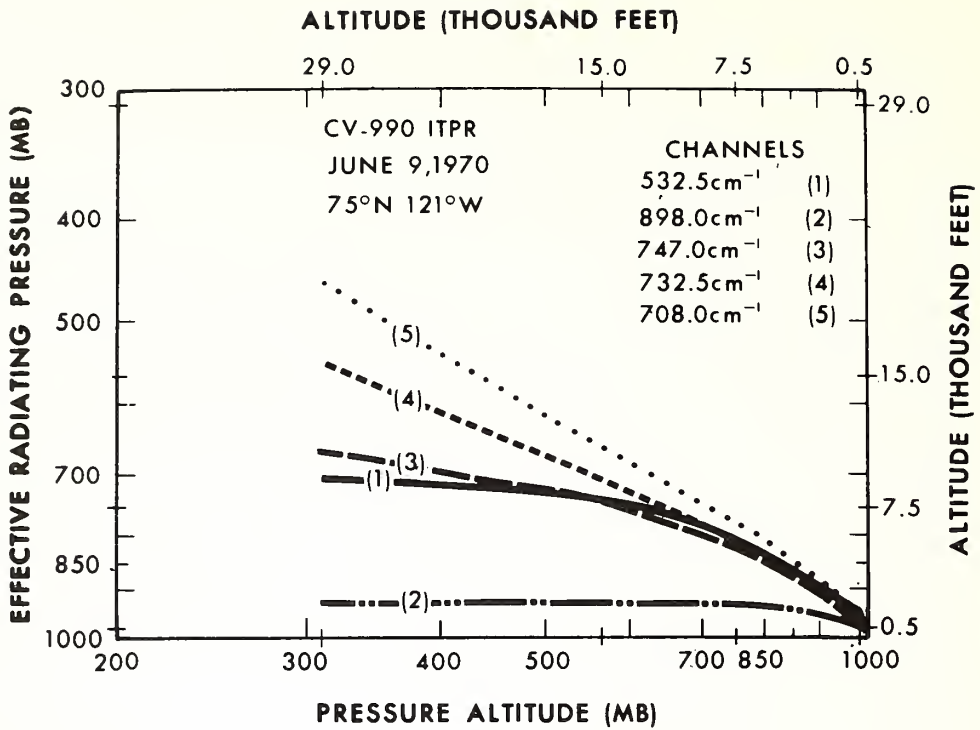


Figure III-1.--Variation of effective altitude with aircraft altitude for five channels of ITPR. High latitude (Top), Subtropical (Bottom).

atmospheric conditions. At high aircraft altitudes, the water vapor channel senses radiances originating lower in the atmosphere than any of the CO₂ channels. However, from low aircraft altitudes, the water vapor channel does not probe as deeply into the atmosphere as channels 3 or 4, because of the relatively large concentrations of water vapor near the surface.

IV. DATA REDUCTION AND ACCURACY

Introduction

There were almost continuous temperature variations of the ITPR optics unit because of large variations in the environmental air temperature during the CV-990 flights. Therefore, accurate determination of scene spectral radiance from a channel output required that the instantaneous thermal state of the instrument be taken into account in the output voltage-to-radiance transformation. Preflight calibration relations could not be applied to inflight data because they were not obtained for the thermal conditions encountered during flight. Furthermore, inflight calibrations, obtained by viewing the warm and cold blackbody reference targets, could not be applied directly to subsequent scene data unless the thermal environment remained constant. The CV-990 experiments generally required almost continuous variations in aircraft altitude so it was impossible to have specific inflight calibration data for every thermal situation. As a consequence, a multivariable calibration relationship had to be formulated for each channel to account for all the thermal energy transfer processes affecting the output signal. The coefficients of the calibration equations were determined by least-square multiple regression from the entire sample of inflight calibration data. The inflight calibrations were conducted under thermal conditions covering the entire range of those encountered during scene measurements.

The Calibration Equations

As discussed in section II, the ITPR electronics were designed so that the output of each channel would vary linearly with the spectral scene radiance when the instrument was in thermal equilibrium. That is

$$B(T_s) = A_0 + A_1 S_{dc} \quad (\text{IV-1})$$

As indicated in equations (II-7) - (II-10), A_0 and A_1 , are functions of the detector responsivity, the chopper radiation, and any radiation from components located in front of the chopper (e.g., the mirrors and portions of the instrument reflected in the cassegrain obscuration), as well as the chopper offset generator variable. Expressing the detector responsivity in terms of a cubic function of the detector temperature, the chopper radiation in terms of the Planck function of the chopper temperature, and the remaining radiation in terms of the Planck function of the housing temperature, then

$$A_0 = C_0 + \sum_{i=1}^6 C_i f_i, \text{ and } A_1 = d_0 + \sum_{i=1}^6 d_i f_i \quad (\text{IV-2})$$

where the C's and d's are constants, $f_1 = T_d$, $f_2 = T_d^2$, $f_3 = T_d^3$,

$f_4 = B(T_c)$, $f_5 = B(T_h)$, and $f_6 = X(T_c)$. (The symbols are defined in section II.) The Planck function of the housing temperature, T_h , is used to account for all other radiation components because the mirror temperatures were not measured. Substituting (IV-2) into (IV-1) yields the calibration equation for each channel

$$B(T_s) = \sum_{i=0}^6 f_i (C_i + d_i S_{dc}) \quad (IV-3)$$

where f_0 is equal to unity.

The cold and warm blackbody calibration data obtained throughout all 10 CV-990 flights were used to obtain the 14 coefficients of (IV-3) by multiple regression. $B(T_s)$ is merely the Planck radiance of the thermistor-measured blackbody temperature when viewing a calibration blackbody. All the f_i 's and blackbody temperatures were measured and telemetered simultaneously with S_{dc} , permitting the empirical determination of (IV-3) and its application to scene radiance data.

The resulting calibration equations were tested by application to the calibration channel outputs, S_{dc} , from which they were derived. They permitted specification of blackbody temperatures by the output of each channel to within 0.5°C rms of that obtained independently by the blackbody thermistors. The root-mean-square error of the blackbody thermistor temperatures were judged to be about 0.4°C. The random error of the channel output derived scene temperatures were found to be about 0.3°C for an individual 4-second sample.

Figure IV-1 shows a sample of calibration data obtained for channel 3. The dots are values of channel 3 output dc voltage, S_{dc} , obtained by viewing the warm blackbody whose radiance was calculated from the thermistor-monitored temperatures. There is generally a 10.0 ergs/cm² s sr cm⁻¹ disparity of blackbody radiance for a given output voltage of the channel. The X's show the same output voltages transformed into scene radiance by equation (IV-3). The 10.0 ergs/cm² s sr cm⁻¹ disparity has been reduced to well within 1.0 ergs/cm² s sr cm⁻¹ after accounting for the thermal conditions of the instrument by means of equation (IV-3).

As mentioned above, the random error of a 4-second radiance sample obtained by any channel was found to be about 0.5 ergs/cm² s sr cm⁻¹ (i.e., 0.3°C of scene temperature). Comparisons of the calibrated output radiances indicated interchannel relative accuracies of better than 0.5 ergs/cm² s sr cm⁻¹.

The absolute accuracy of channel output radiance is more difficult to assess because it depends upon the effective emissivity of the blackbodies as well as on the absolute accuracy of the blackbody thermistors. An estimate of the absolute accuracy of the output radiance was obtained by comparing the scene brightness temperature, measured by channel 5, the most opaque CO₂ channel, with the temperature, measured by the aircraft platinum-wire thermometer. The brightness temperature measured by channel 5 at low altitudes, where the atmosphere is opaque to 15-μm radiation, or within opaque clouds, should be close to the environmental air temperature. Figure IV-2,

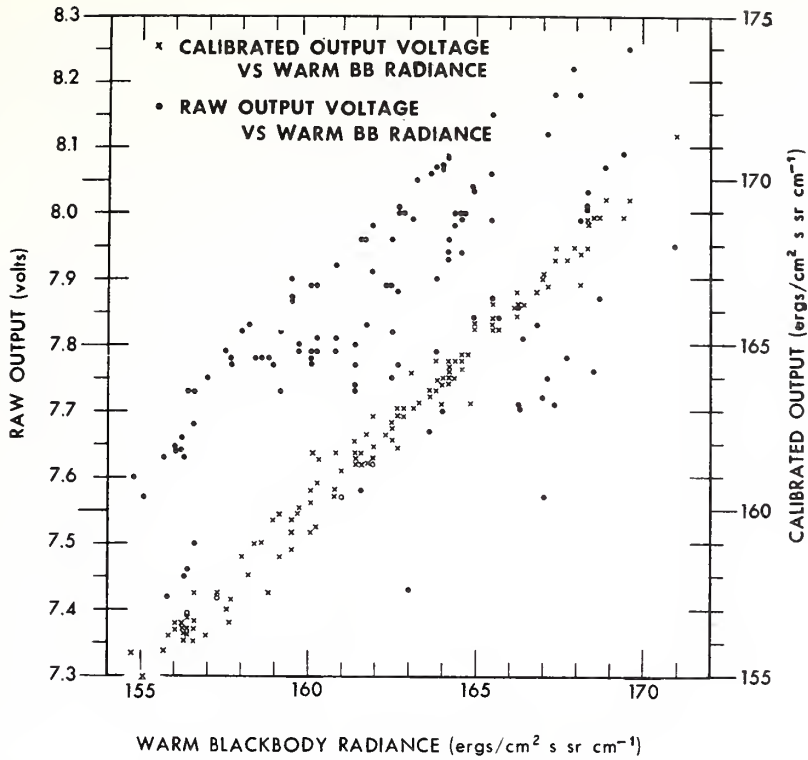


Figure IV-1.--Warm blackbody calibration data obtained for ITPR channel 3 (13.4- μm).

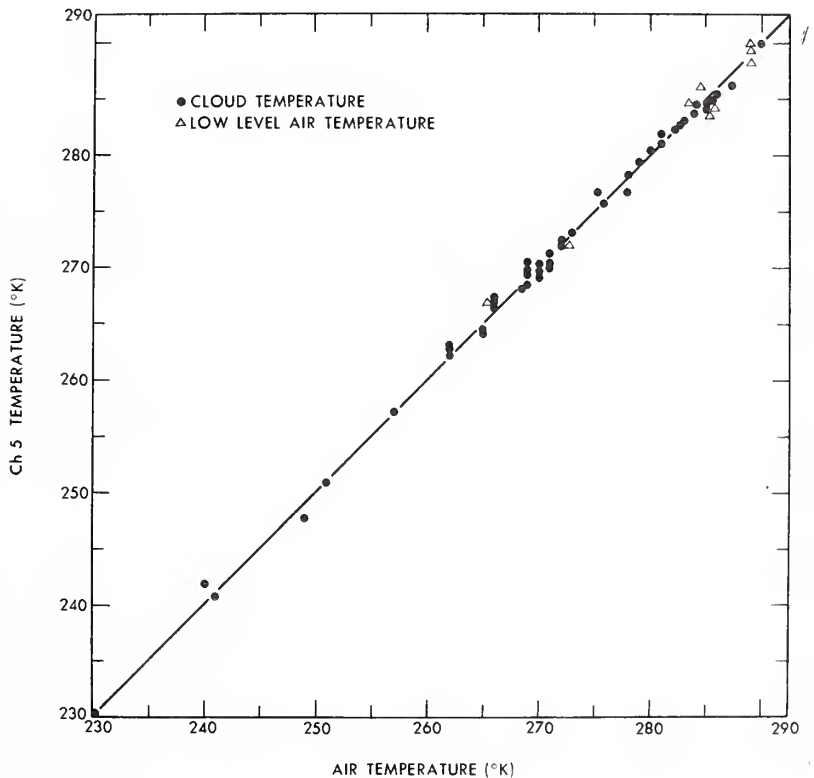


Figure IV-2.--ITPR channel 5 (14.1- μm) measurements of cloud temperature and low level air temperature vs. Rosemont measured air temperature.

which shows the comparison of the two independent air temperature measurements, indicates that the absolute accuracy of the ITPR brightness temperature measurements is within the 1°C absolute accuracy of the Rosemont thermometer measurements. The apparent achievement of 1 percent absolute accuracy and 1/2 percent relative accuracy for radiance observations in the highly unstable aircraft environment is considered remarkable.

Finally, figure (IV-3) is an example of a computer plot of measured brightness temperatures for a small portion of flight 3 over the eastern Pacific. Low stratus clouds existed during the observation period. The 3-step "staircases" are measurements of the temperatures of the cold housing, and warm blackbody calibration targets. The other "brightness temperatures" are the earth-atmosphere scene temperatures. The high relative accuracy of the brightness temperatures measured by the various channels is clear from the calibration data. The stability of the observations is indicated by the lack of significant variation in brightness temperatures in the atmospheric window channel (channel 2) during large variations in aircraft altitude. At low altitudes all channels observe the same brightness temperature because there is little vertical temperature variation in the atmosphere beneath the aircraft, and the ocean and air temperatures are nearly the same. The close examination of the ITPR data, a sample of which is given in the appendix, will permit the reader to judge for himself the reliability of the airborne ITPR radiance observations.

V. CLEAR-COLUMN RADIANCE DETERMINATION

Introduction

Future Nimbus satellites will carry an Infrared Temperature Profile Radiometer (ITPR), and ITOS weather satellites a similar Vertical Temperature Profile Radiometer (VTPR) instrument to measure vertical profiles of temperature and water vapor in the earth's atmosphere. The radiation from clear columns of air is required for the derivation of temperature and moisture profiles from high in the atmosphere to the earth's surface. Because most of the earth is covered by varying amounts of clouds, a method is needed for estimating the equivalent clear-column radiance for the many areas where the radiometer's field of view is partially filled by clouds. A method for calculating the clear-column radiance from the observed total radiance has been suggested previously (Smith, 1968). One of the primary objectives of NASA Convair-990 brassboard ITPR flights during June 1970 was to collect data to test this technique.

Analytical Solution

The solution for calculating the clear-air radiance contribution to the total radiance measured over a partly cloudy atmosphere was presented by Smith (1969). Briefly, the clear-column radiance for any frequency, ν , is obtained from two spatially independent radiance measurements through the solution of

$$I_{\text{clr}}(\nu) = \frac{I_1(\nu) - N^*I_2(\nu)}{(1-N^*)} \quad (\text{V-1})$$

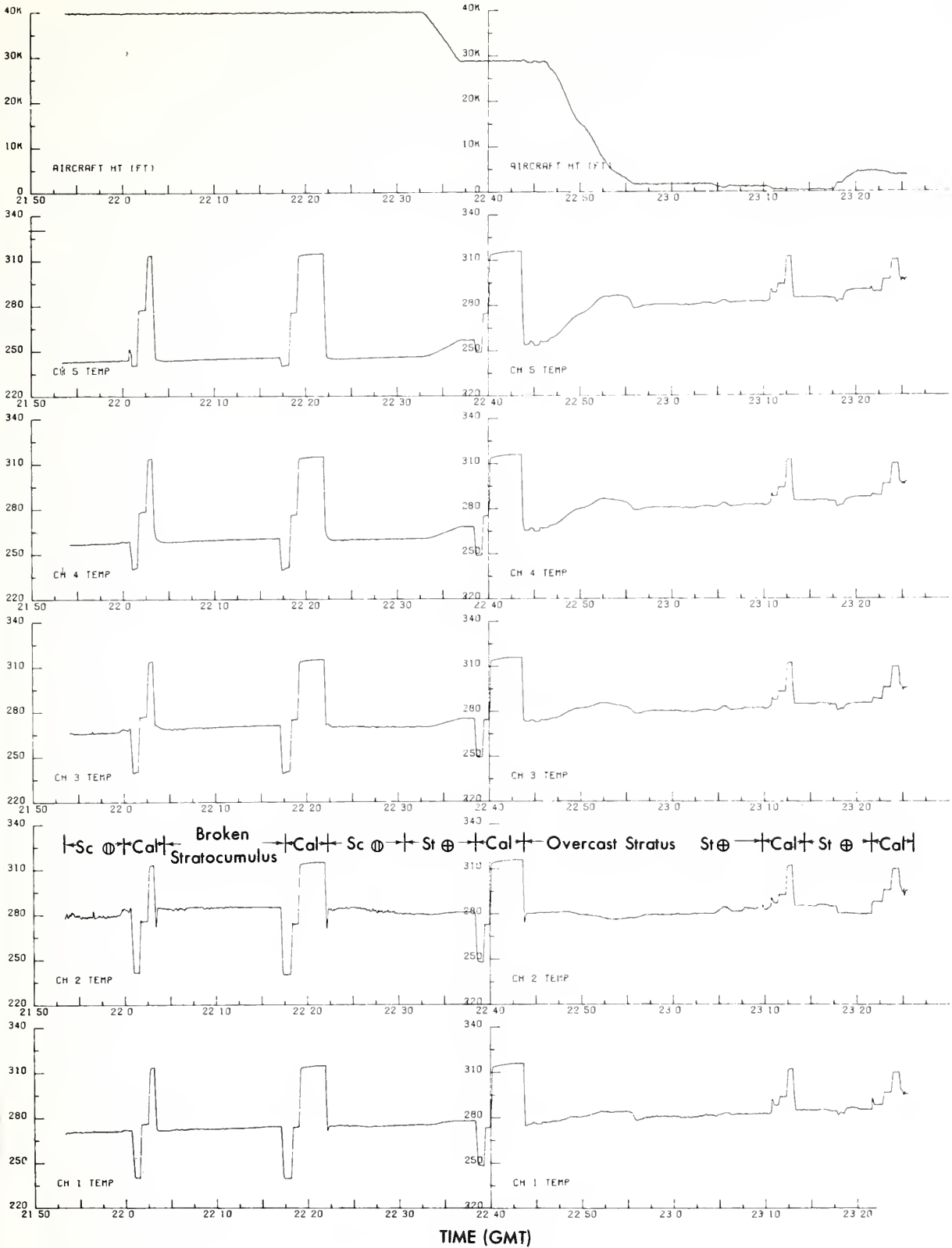


Figure IV-3.--Computerized plot of measured brightness temperature for all ITPR channels during a portion of Flight 3.

where $I_{clr}(v)$ is the clear-column radiance and $I_1(v)$ and $I_2(v)$ are the two spatially independent radiance measurements. The parameter N^* is the ratio of the fractional cloud covers of the two fields of view. N^* is determined from corresponding atmospheric "window" radiometric observations, $I(w)$. It follows from (V-1), applied to the window region, that

$$N^* = \frac{N_1}{N_2} = \frac{I_{clr}(w) - I_1(w)}{I_{clr}(w) - I_2(w)} \quad (V-2)$$

where the clear-air radiance for the window region is assumed known. $I_{clr}(w)$ will be determined from the simultaneous 11- μ m and 3.7- μ m window measurements to be obtained by the spacecraft version of the ITPR (Smith and Jacob, 1972). Elements 1 and 2 are chosen so that $I_1(w) > I_2(w)$, which restricts N^* to $1 > N^* > 0$.

The above solution for the clear-column radiance is valid only when the geographical variation of observed radiance is due to a variation of fractional cloud cover in the adjacent fields sampled. A variation of either atmospheric temperature or cloud height would produce erroneous values of N^* and $I_{clr}(v)$. Therefore, the two spatially independent observations should be geographically close to each other so that variations in the observed radiance will tend to be caused only by cloud cover variations. The ITPR and VTPR are designed for high spatial resolution and contiguous sampling to ensure geographically close observations, to increase the probability of clear fields of view, and to produce a large number of independent estimates of clear-air radiance for a given geographical area.

The "noise" level of the deduced clear-air radiances will be larger than the measurement noise. It can be seen from equation (V-1) that the clear-air radiance noise level is about $1/(1-N^*)$ times as large as the measurement noise. Consequently, the instrument noise level must be kept relatively low. On the other hand, the spatial resolution must be sufficiently high so that most of the N^* values will be much less than unity. The satellite versions of the ITPR and VTPR temperature sounding radiometers have been designed to scan spatially and contiguously with instantaneous resolutions of 21 and 30 n.mi., respectively, and to achieve noise levels of less than 0.5 percent of the signal levels (i.e., 200/1 signal-to-noise ratios).

Aircraft Test Results

On June 12, 1970, high-altitude (41,000 ft) ITPR radiance observations were obtained above broken altocumulus and stratocumulus clouds over the Pacific Ocean at 46°N, 133°W. Clear-air measurements were obtained on either side of the broken cloud region, and clear-air radiances were calculated from the cloud-contaminated observations.

Figure V-1 shows the measured window radiances (ergs/cm² s sr cm⁻¹) during the period. Clear observations were obtained near 23:37:20 and 23:44:20 GMT. The actual clear-air radiance measured by channel 2 was about 84.0 ergs/cm² s sr cm⁻¹ (279°K). Cloud-contaminated radiances measured in the window channel were as low as 50 ergs/cm² s sr cm⁻¹ (250°K).

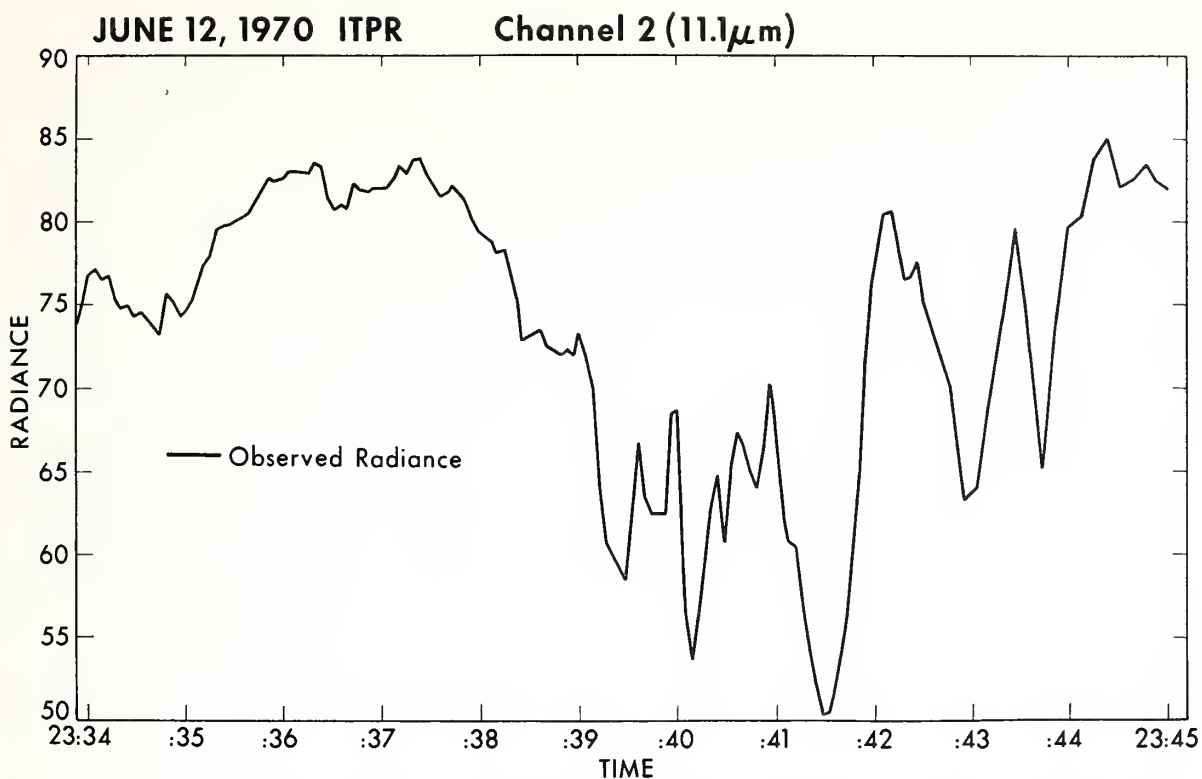


Figure V-1.--"Window" radiances measured by ITPR 11.1- μ m CO₂ channel.

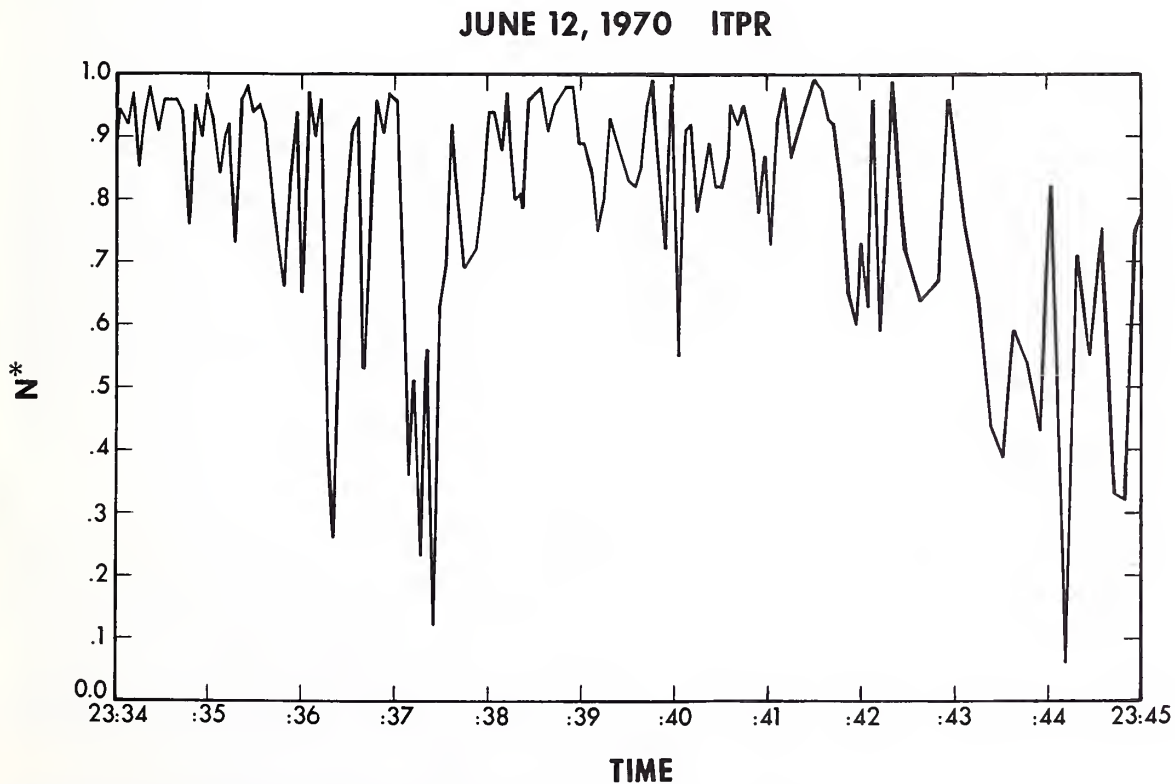


Figure V-2.--N* distribution calculated for adjacent fields of view from 11.1- μ m radiance measurements.

Assuming a clear-air window spectral radiance of 84.0, we calculated N^* for the adjacent fields of view which were observed about 4 seconds apart. Figure V-2 shows the resulting distribution of N^* . Values of the clear-column radiances were then calculated from the adjacent observed radiances in the three-temperature-sounding CO_2 channels. The values for $N^* > 0.8$ are shown together with the measured radiance distributions in figures V-3, V-4, and V-5.

It can be seen from figures V-3, V-4, and V-5 that some of the infrared clear-air radiances are erroneous, particularly in the region where a large amount of cloudiness exists (e.g., 23:38 to 23:44 GMT). Some erroneous values were calculated because N^* is relatively high (greater than 0.5 between 23:38 and 23:44 GMT), and in some cases the variation in radiance probably resulted from variations in cloud heights rather than differences in cloud amounts (the field of view contained both altocumulus and stratocumulus). However, many of the estimates of clear-column radiance are in fair agreement with the observed clear-air radiances measured at 23:37:20 and 23:44:20 GMT.

Figures V-6, V-7, and V-8 show histograms of the clear-column radiances deduced from the cloud-contaminated radiances measured between 23:38 and 23:44 GMT. The values of the most frequently occurring estimates agree closely with the observed clear-air radiances. The mean clear-column radiance values, $I_{\text{clr}}(\nu)$, defined as the frequency-weighted average of the mode value and values of the two adjacent class intervals, agree with the measured values of clear-air radiance quite well considering the instrument noise.

Conclusion

The aircraft test results presented here indicate that the clear-air radiance contribution to radiances observed with a partial cloud cover within the field of view can be deduced with the accuracy needed for calculating temperature profiles down to the earth's surface. (This conclusion is also borne out by other examples not presented here.) Since the earth's atmosphere, when viewed on a synoptic scale (i.e., horizontal scale of 300 to 500 km), is covered by broken clouds, this method applied to appropriate satellite measurements should make possible the determination of atmospheric temperature distribution on a synoptic scale over almost the entire globe.

VI. AIRCRAFT-DEDUCED ATMOSPHERIC TRANSMITTANCES

Introduction

Vertical profiles of upwelling (or downwelling) radiance, as observed by an airborne radiometer, can be used to determine the transmittance of the atmosphere to the sensed radiation. The solution for atmospheric transmittance from the radiance profile is obtained through a solution of the differential equation of radiative transfer. The inference of the physical properties of the atmosphere (e.g., distribution of its temperature and water vapor) from satellite radiance observations requires knowledge of the atmosphere's transmission as a function of optical depth, pressure, and temperature. The observation of the radiative transmittance properties of

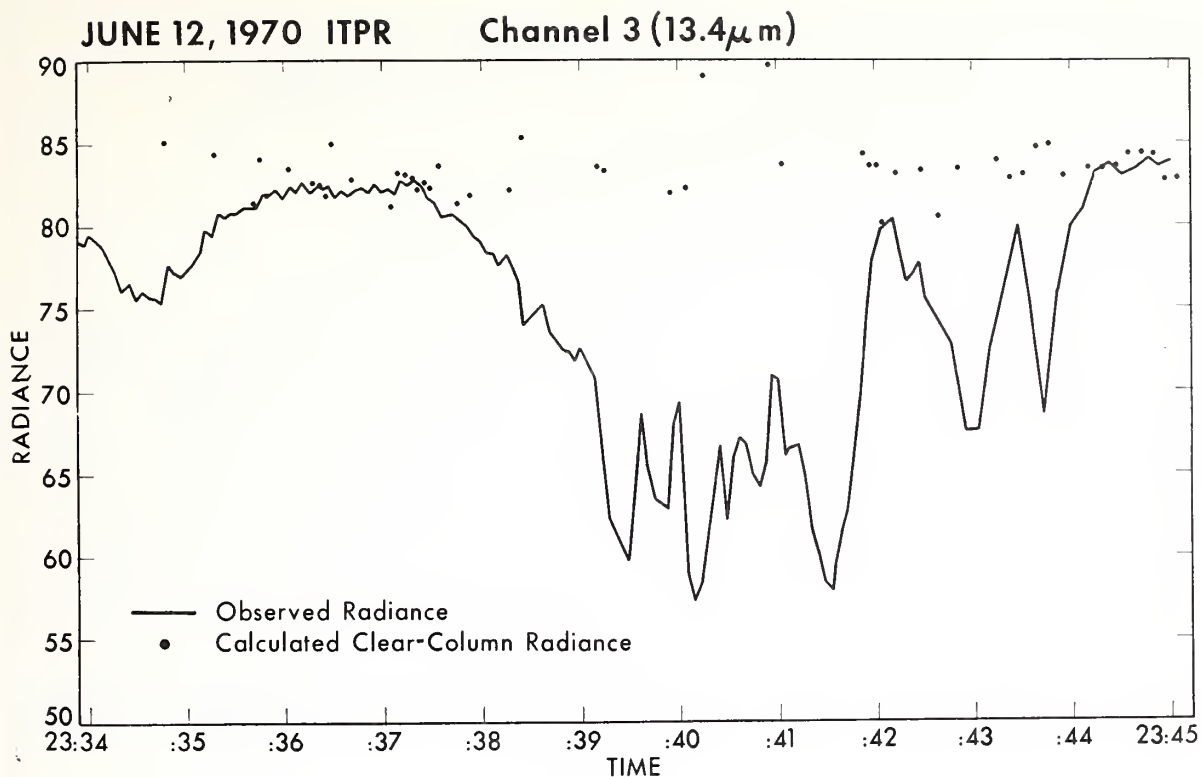


Figure V-3.--Observed radiances (solid line) and calculated clear-column radiance (dots) for the ITPR 13.4- μ m CO₂ channel.

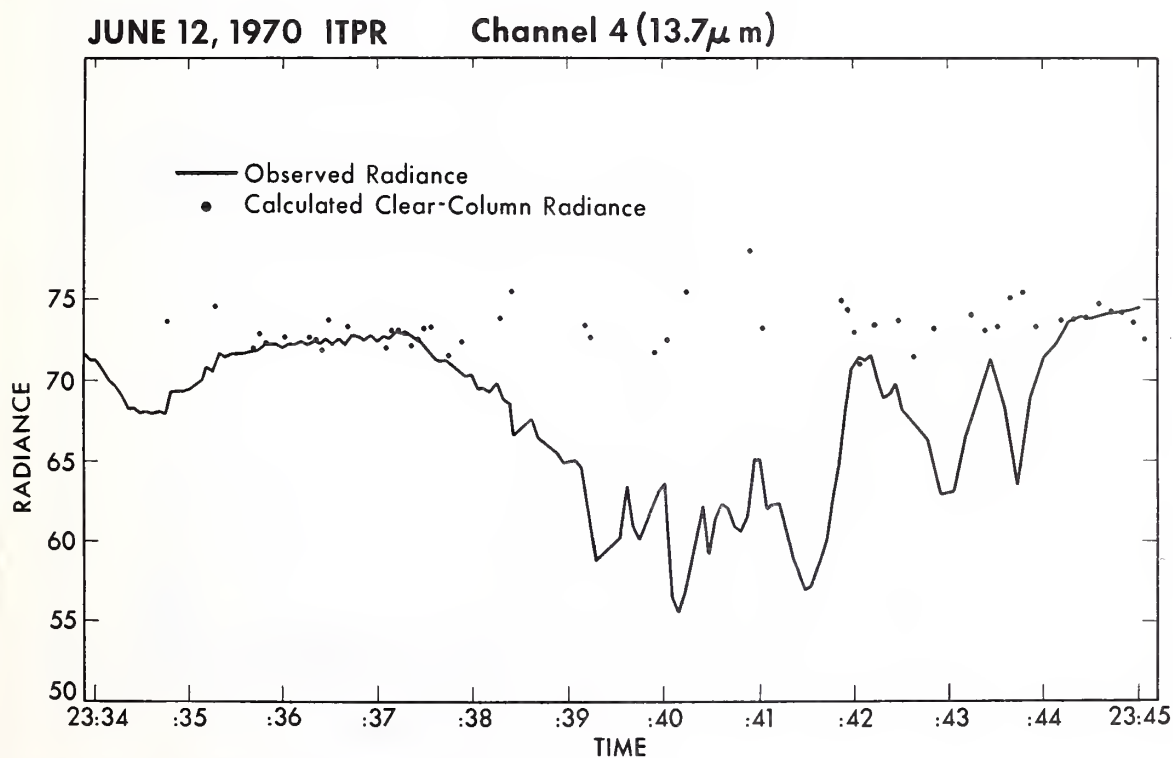


Figure V-4.--Observed radiances (solid line) and calculated clear-column (dots) for the ITPR 13.7- μ m CO₂ channel.

JUNE 12, 1970 ITPR Channel 5 ($14.1\mu\text{m}$)

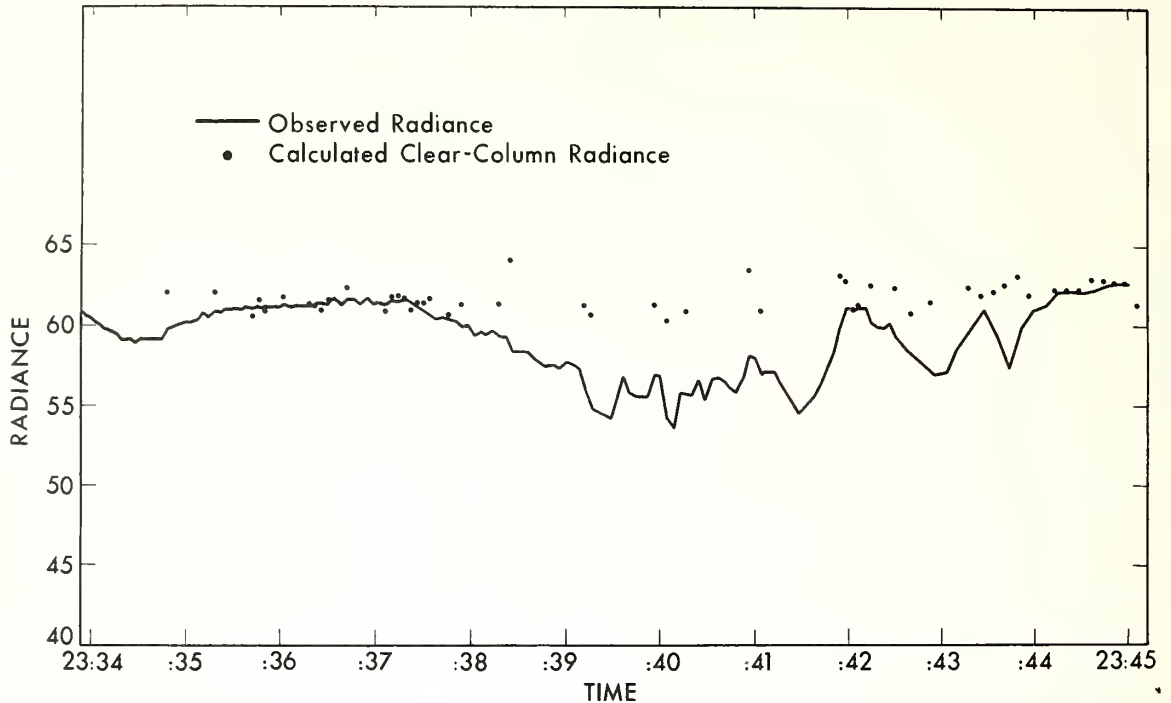


Figure V-5.--Observed radiances (solid line) and calculated clear-column radiance (dots) for the ITPR $14.1\text{-}\mu\text{m}$ CO_2 channel.

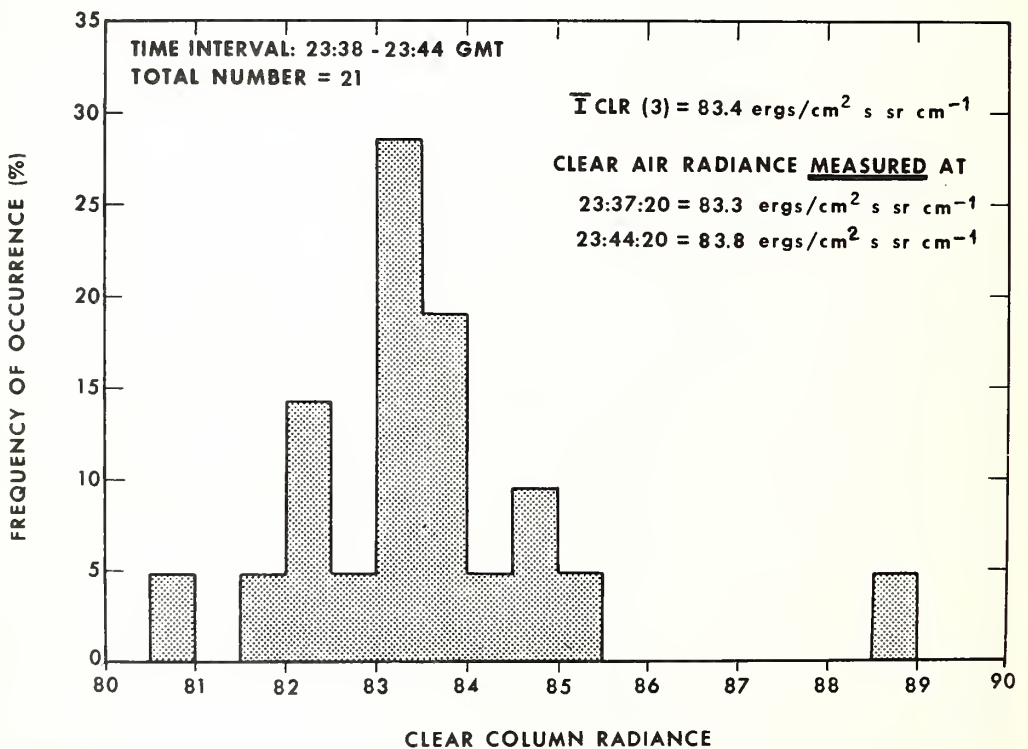


Figure V-6.--Histogram of clear-column radiances deduced from cloud-contaminated radiances measured in the $13.4\text{-}\mu\text{m}$ CO_2 channel.

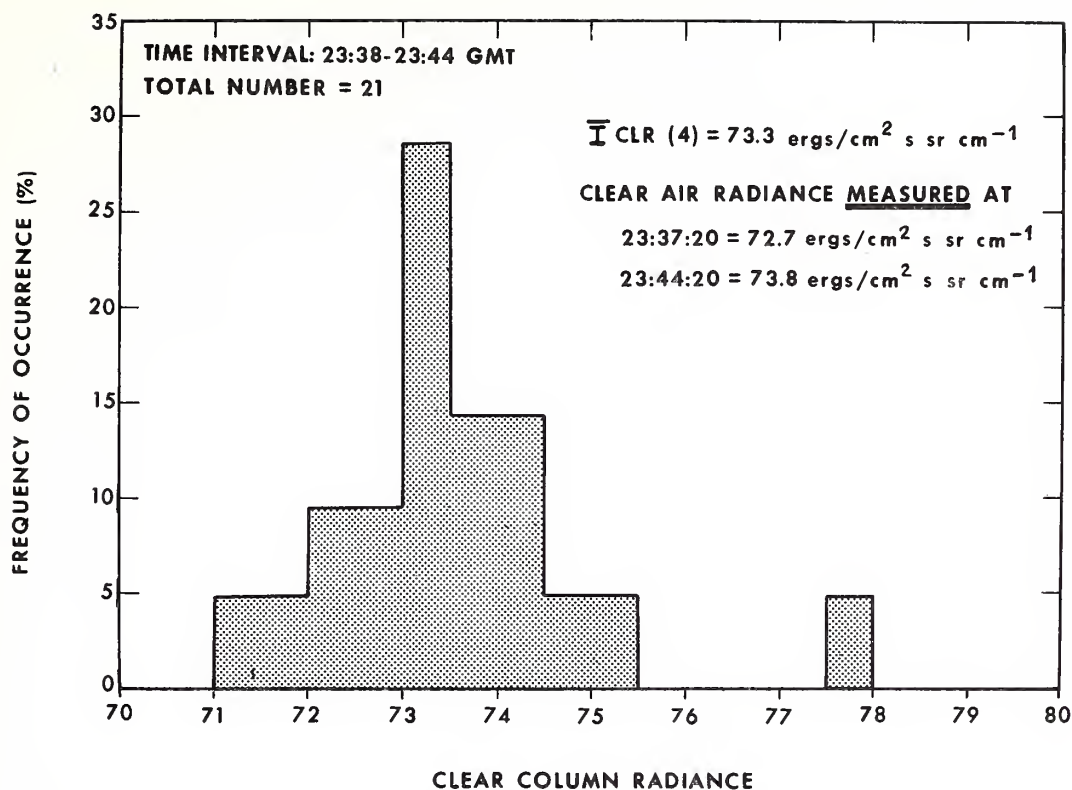


Figure V-7.--Histogram of clear-column radiances deduced from cloud-contaminated radiance measured in the 13.7- μm CO₂ channel.

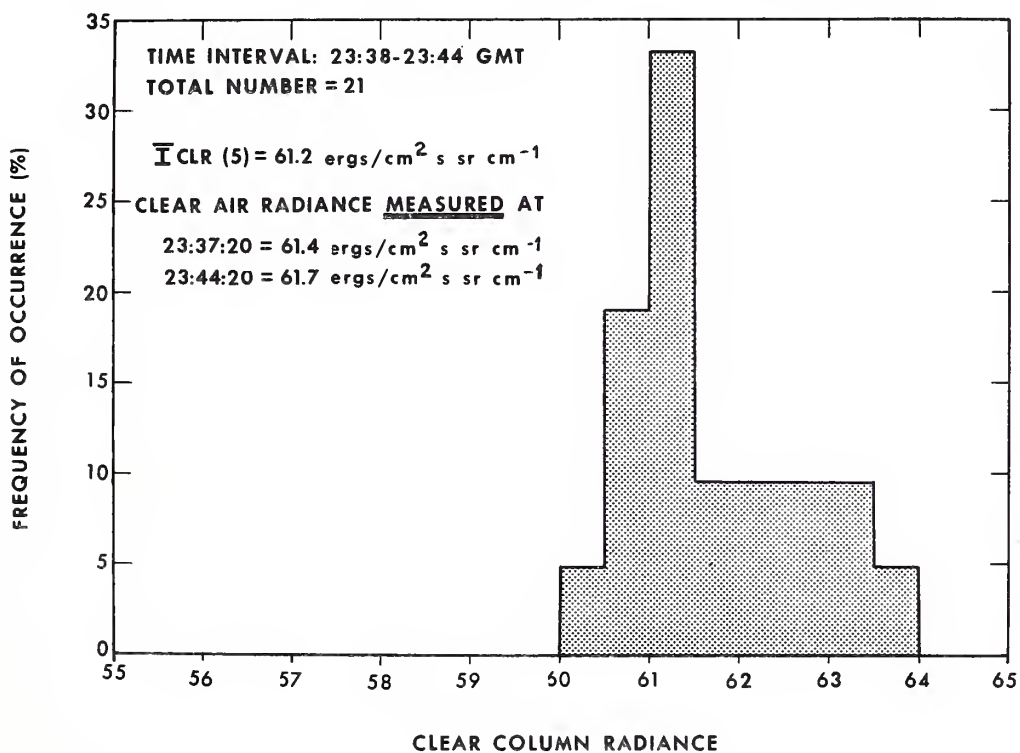


Figure V-8.--Histogram of clear-column radiances deduced from cloud contaminated radiances measured in the 14.1- μm CO₂ channel.

the real atmosphere has obvious advantages over the estimation of atmospheric transmission solely from theory or laboratory measurements.

Mathematical Solution

The differential equation of radiative transfer, known as Schwarzschild's Equation, can be written for an atmosphere in local thermodynamic equilibrium as

$$dI_\nu = k_\nu (B_\nu - I_\nu) du \quad (\text{VI-1})$$

where I_ν is the monochromatic radiance, B_ν is the monochromatic source function which is the Planck radiance for a medium in thermodynamic equilibrium, and k_ν is the monochromatic mass absorption coefficient. The incremental optical path length

$$du = \rho dz \quad (\text{VI-2})$$

where ρ is the density of absorbing medium and dz is the incremental geometric path length.

The monochromatic transmittance of the medium is given by

$$\tau_\nu = \exp(-\int k_\nu du) \quad (\text{VI-3})$$

thus (VI-1) may be written as

$$\tau_\nu(p) \frac{dI_\nu(p)}{d \ln p} + [B_\nu(p) - I_\nu(p)] \frac{d\tau_\nu(p)}{d \ln p} = 0 \quad (\text{VI-4})$$

where $\ln p$, the natural logarithm of pressure, has been chosen as the vertical coordinate. Integrating (VI-4) over the frequency interval sensed by a particular channel of the ITPR we have

$$\int_0^\infty \frac{dI_\nu(p)}{d \ln p} \phi_\nu d\nu + \int_0^\infty [B_\nu(p) - I_\nu(p)] \frac{d\tau_\nu(p)}{d \ln p} \phi_\nu d\nu = 0 \quad (\text{VI-5})$$

where ϕ_ν is the spectral response function (see figure II-1).

Consider the following definitions for a spectral mean of any quantity, Q ,

$$\bar{Q} = \int_0^\infty Q \phi_\nu d\nu / \int_0^\infty \phi_\nu d\nu, \quad (\text{VI-6})$$

and the departure of the quantity from its mean;

$$Q'_\nu = Q_\nu - \bar{Q}; \quad (\text{VI-7})$$

such that,

$$\int_0^\infty Q'_\nu \phi_\nu d\nu = 0. \quad (\text{VI-8})$$

Making use of (VI-6), (VI-7), and (VI-8), Equation (VI-5) may then be written as

$$\frac{d\bar{I}(p)}{d \ln p} + [\bar{B}(p) - \bar{I}(p)] \frac{d \ln \bar{\tau}(p)}{d \ln p} = C(p)$$

where

$$C(p) = \frac{1}{\bar{\tau}} \left[I'_V(p) \frac{d\tau'_V(p)}{d \ln p} - B'_V(p) \frac{d\tau'_V(p)}{d \ln p} - \tau'_V \frac{dI'_V(p)}{d \ln p} \right] \quad (\text{VI-9})$$

We wish to solve (VI-9) for $\bar{\tau}$ given observations of \bar{I} and \bar{B} as functions of $\ln p$. The solution, however, is complicated by the fact that the covariance terms on the right of (VI-9) are not observed. Let us for the moment assume no variation of monochromatic transmittance with frequency so that the right-hand side of (VI-9) becomes zero. This case yields a first order approximation of the mean transmittance, denoted as τ_0 . Integrating (VI-9), with $C(p) = 0$, gives

$$\tau_0(p_0, p) = \exp \left\{ \int_{p_0}^p \frac{1}{[\bar{B}(p) - \bar{I}(p)]} \frac{d\bar{I}(p)}{d \ln p} d \ln p \right\} \quad (\text{VI-10})$$

where p_0 is any boundary pressure level. By definition, $\tau_0(p_0, p_0) = 1$. The first order approximation of the transmittance profile, $\tau_0(p_0, p)$, can be calculated directly from a measured radiance and temperature (Planck radiance) profile.

The actual transmittance profile, $\bar{\tau}(p_0, p)$, in which $C(p) \neq 0$, is then

$$\bar{\tau}(p_0, p) = \tau_0(p_0, p) \exp \left\{ \int_{p_0}^p \frac{C(p)}{[\bar{B}(p) - \bar{I}(p)]} d \ln p \right\} \quad (\text{VI-11})$$

The exponential factor can be thought of as a correction term. Since the covariance term, $C(p)$, is not observable, it must be estimated from theoretical principles. The correction term is estimated from theoretically calculated radiances and transmittances. Using (VI-9),

$$C(p) \approx \frac{d\hat{I}(p)}{d \ln p} + [\bar{B}(p) - \hat{I}(p)] \frac{d \ln \hat{\tau}(p)}{d \ln p} \quad (\text{VI-12})$$

where the circumflex ($\hat{}$) indicates a calculated value. Combining (VI-9), (VI-11), and (VI-12) yields

$$\bar{\tau}(p_0, p) = \exp \left[- \int_{p_0}^p \frac{1}{[\bar{B}(p) - \bar{I}(p)]} \left\{ \frac{d[\bar{I}(p) - \hat{I}(p)]}{d \ln p} - [\bar{B}(p) - \hat{I}(p)] \frac{d \ln \bar{\tau}(p)}{d \ln p} \right\} d \ln p \right] \quad (\text{VI-13})$$

Equation (VI-13) is used to calculate the atmospheric transmittance profiles pertaining to the ITPR spectral intervals from the observed radiance and temperature (Planck radiance) profiles.

Computational Procedure

The ITPR aboard the CV-990 measured the upward radiance, \bar{I} , as a function of pressure in its five spectral channels. Other instrumentation provided measures of air temperature and relative humidity. Vertical profiles were obtained over a cloudless sea on three occasions, during flights 1, 8, and 9. The observational procedure was one of flying 5-minute legs at various altitudes above a specific earth location. Table VI-1 summarizes the average values of radiance, air temperature, and relative humidity for each altitude leg of the three vertical profiles.

Each profile variable was interpolated to 100 levels equally spaced in the natural logarithm of pressure, in order to ensure accurate quadrature in the numerical computations. Air temperature and relative humidity were interpolated linearly with respect to $\ln p$. The measured radiances were interpolated on the basis of the theoretically calculated radiances by assuming that the discrepancy between measured and calculated radiance within each layer is linear with respect to the logarithm of pressure.

The theoretically calculated radiances are obtained from the equation of radiative transfer in integral form;

$$\hat{I}(p_a) = \bar{B}(p_s) \hat{\tau}(p_a, p_s) - \int_p^{p_s} \bar{B}(p) \frac{d\hat{\tau}(p_a, p)}{d \ln p} d \ln p \quad (\text{VI-14})$$

where p_a and p_s are the pressures at the instrument and surface altitudes, respectively.

The transmission of atmospheric water vapor, for the rotational H_2O band, is assumed to be given by the "Random Band Model",

$$\hat{\tau}_w(p_a, p) = \exp \left\{ \frac{-(S/\delta)U_w}{\sqrt{1 + (S/\pi\alpha)U_w}} \right\} \quad (\text{VI-15})$$

where S is the mean line strength, δ is the mean line spacing and α is the mean half-width of the lines. The path length of water vapor

$$U_w = \frac{1}{g} \int_{p_a}^p w(p) dp \quad (\text{VI-16})$$

where g is the acceleration of gravity and w is the water vapor mixing ratio.

The transmission of the atmospheric carbon dioxide for the $15\text{-}\mu\text{m}$ CO_2 band is assumed to be given by the "Ordered Band Model",

$$\hat{\tau}_c(p_a, p) = 1 - \text{erf} \left\{ \sqrt{(\pi\alpha S/\delta^2)U_c} \right\} \quad (\text{VI-17})$$

The path length of carbon dioxide, $U_c(p)$, is assumed to be a constant 0.247 atm cm/mb. Assuming no selective absorption, the transmission in the $11\text{-}\mu\text{m}$ "window" spectral region is expressible in terms of the continuum absorption

Table VI-1.--Measured radiances, temperature, and relative humidity

Pressure (mb)	Measured Radiances (ergs/cm ² s sr cm ⁻¹)					Temp °K	Rel. Hum. Percent
	Ch 1	Ch 2	Ch 3	Ch 4	Ch 5		
<u>FLT-1 (44°N, 129°W)</u>							
997	134.93	100.94	121.94	124.49	126.82	289.1	73
970	136.00	100.15	122.42	125.30	128.10	291.0	48
926	137.08	100.78	123.07	125.95	129.39	292.0	55
854	136.81	101.41	123.07	125.78	128.25	291.0	39
698	131.99	99.37	118.57	119.68	119.55	284.0	35
573	124.62	97.97	110.88	109.28	105.64	271.0	50
466	120.99	97.63	105.10	100.95	94.93	262.0	29
337	120.99	97.22	99.63	91.31	81.44	246.0	22
<u>FLT-8 (34°N, 130°W)</u>							
1017	138.05	100.80	124.35	126.90	129.72	290.0	85
1003	136.74	100.17	123.62	125.85	128.54	289.6	63
932	132.84	100.25	120.86	122.79	124.00	285.0	62
754	129.41	99.40	117.87	118.92	119.08	281.3	45
505	113.87	98.19	105.74	102.34	97.82	264.0	35
238	104.43	95.09	91.81	82.05	70.00	224.0	18
<u>FLT-9 (28°N, 93°W)</u>							
1017	153.61	120.10	144.39	146.21	148.98	301.5	100
983	150.53	119.41	141.94	142.73	145.20	299.0	88
853	140.33	115.98	134.88	133.87	132.81	292.9	60
716	131.59	112.94	126.34	123.68	120.95	285.0	47
601	125.79	110.95	119.36	115.28	109.48	275.2	30
490	122.28	109.79	113.21	107.02	98.72	265.0	22
365	119.96	108.64	106.46	96.64	84.94	249.0	20
209	117.15	107.82	98.03	84.14	67.51	218.6	37

coefficient, β , by

$$\hat{\tau}_{wD}(p_a, p) = \exp \{ - k U_w \} \quad (\text{VI-18})$$

where k is the continuum absorption coefficient. The temperature and pressure dependence of the line parameters S , α , and k is assumed to be accounted for by the usual forms (Smith, 1969)

$$S = S_o \left(\frac{T_e}{T_o} \right)^n, \quad \alpha = \alpha_o \left(\frac{p_e}{p_o} \right)^m \left(\frac{T_e}{T_o} \right)^{-1/2}, \quad k = k_o \left(\frac{T_e}{T_o} \right)^n \left(\frac{p_e}{p_o} \right)^m \quad (\text{VI-19})$$

where S_o , α_o , and k_o are fixed values for standard temperature and pressure, T_o and p_o , values of 273°K and 1000 mb. The effective temperature and pressure, T_e and p_e , of an absorbing layer (p_a, p) are defined by

$$\left. \begin{aligned} T_e &= \int_{p_a}^p T \frac{du}{dp} dp / \int_{p_a}^p \frac{du}{dp} dp \\ p_e &= \int_{p_a}^p p \frac{du}{dp} dp / \int_{p_a}^p \frac{du}{dp} dp \end{aligned} \right\} \quad (\text{VI-20})$$

Howard, Burch, and Williams (1955) showed from empirical data that (VI-15) can be expressed as

$$\hat{\tau}_w(p_a, p) = \exp \left\{ \frac{-1.97 L U_w}{\sqrt{1 + 6.57 L U_w}} \right\} \quad (\text{VI-21})$$

for a given temperature and pressure, where L is a generalized absorption coefficient. It then follows from (VI-15), (VI-19), and (VI-21) that

$$\hat{\tau}_w(p_a, p) = \exp \left\{ \frac{-1.97 L_o (T_e/T_o)^n U_w}{\sqrt{1 + 6.57 L_o (T_e/T_o)^{n+1/2} (p_e/p_o)^{-m} U_w}} \right\} \quad (\text{VI-22})$$

where L_o is the generalized absorption coefficient for standard pressure and temperature. In a similar manner (VI-17) can be expressed as

$$\hat{\tau}_c(p_a, p) = 1 - \operatorname{erf} \left\{ \sqrt{L_o \left(\frac{T_e}{T_o} \right)^n \left(\frac{p_e}{p_o} \right)^m U_c} \right\} \quad (\text{VI-23})$$

and (VI-18) by

$$\hat{\tau}_{wD}(p_a, p) = \exp \left\{ - L_o \left(\frac{T_e}{T_o} \right)^n \left(\frac{p_e}{p_o} \right)^m U_w \right\} \quad (\text{VI-24})$$

where in (VI-23) the $-1/2$ temperature exponent has been absorbed by the n .

Thus the atmospheric transmissions for spectral channels 1 and 2 are calculated by equation (VI-22) and (VI-24). The atmospheric transmissions for the 15- μm carbon dioxide channels, (3), (4), and (5), which are influenced by H_2O as well as CO_2 lines, are calculated as the product of (VI-22) and (VI-23), (i.e., $\hat{\tau} = \hat{\tau}_c \cdot \hat{\tau}_w$). The transmission model parameters (L_o , n , and m) were determined from the theoretical data given by Möller and Raschke (1963) and are presented in table VI-2 below.

Table VI-2.--Theoretical transmission model parameters

Channel	Water vapor			Carbon dioxide		
	L_o	m	n	L_o	m	n
1	3.550	0.72	1	-	-	-
2	0.158	1.00	0	-	-	-
3	0.347	.72	0	0.003	.66	7
4	0.380	.72	0	0.010	.66	6
5	0.437	.72	0	0.028	.66	5

As mentioned earlier, the measured radiances were interpolated to levels within a measurement layer assuming that

$$\frac{d[\bar{I}(p) - \hat{I}(p)]}{d \ln p} = K = \text{constant} \quad (\text{VI-25})$$

Integrating (VI-25) between the limits p_L and p , where p_L is the layer base pressure, gives the interpolated measured radiances

$$\bar{I}(p) = \hat{I}(p) + [\bar{I}(p_L) - \hat{I}(p_L)] + K \ln (p/p_L) \quad (\text{VI-26})$$

The slope K is found from (VI-26) for $p=p_u$ where p_u is the pressure at the top of the layer.

$$K = \frac{[\bar{I}(p_u) - \hat{I}(p_u)] - [\bar{I}(p_L) - \hat{I}(p_L)]}{\ln (p_u/p_L)} \quad (\text{VI-27})$$

To ensure that the calculated radiance profile will be a close approximation of the true profile, the generalized water vapor absorption coefficients for channels (1) and (2) and the generalized CO_2 absorption coefficients for channels (3), (4), and (5) were specified for each flight as those values which yielded agreement between $\hat{I}(p)$ and $\bar{I}(p)$ for the highest level of the profile.

The transmission for each layer was computed on the basis of the measured and calculated radiance profiles using (VI-13) written in its numerical form

$$\bar{\tau}(p_L, p_U) = \exp \left\{ - \sum_{i=1}^{N-1} \left\{ [I(i+1) - \hat{I}(i+1)] - [I(i) - \hat{I}(i)] - [B(i+1/2) - \hat{I}(i+1/2)] [\ln \hat{\tau}(i+1) - \ln \hat{\tau}(i)] \right\} / \{ B(i+1/2) - I(i+1/2) \} \right\} \quad (\text{VI-28})$$

where N is the number of the quadrature levels for the layer and

$$Q(i+1/2) \equiv [Q(i) + Q(i+1)]/2 \quad (\text{VI-29})$$

where Q denotes any quantity.

Results

Table VI-3 lists the atmospheric transmittances computed from the measured radiances and the corresponding optical properties of the observed layers. The pure CO_2 transmittances for channels 3, 4, and 5 were obtained by dividing the total transmittance values by the model-determined water vapor transmittances. It is somewhat difficult to assess the reliability of these transmittances. One immediately questions their dependence upon the theoretically calculated values used in (VI-13). To assess this dependence, the transmittances for flight 9 were recomputed using different absorption coefficients in the theoretical band models. Table VI-4 shows the results. The first-order approximation, τ_0 , is independent of the model transmittance and calculated radiance profile except for their minor influence (<.001 percent) on the measured radiance interpolation. As may be seen from table VI-4, the final transmittance values are only weakly dependent upon the model values used.

Figures VI-1 through VI-5 shows plots of the radiance derived H_2O and CO_2 transmittance values versus the pressure and temperature scaled mass of these gases. Here the pressure exponent was assumed to be unity. The temperature exponent was assumed to be zero for channels 1 and 2.

For channels 3, 4, and 5 the temperature exponent and the generalized absorption coefficients of the ordered band model were determined by a non-linear least-squares procedure. The result minimizes the rms difference between the observed transmittances and those calculated using the ordered band model.

The scatter revealed in these figures appear to be due primarily to inaccuracies in the estimated water vapor path lengths. This is because the scatter becomes successively smaller for those spectral channels which are less affected by water vapor. For instance, channel 1, whose radiation is completely dependent on the water vapor distribution, has the greatest amount of scatter. On the other hand, channel 5, whose radiation is almost independent of water vapor, has the least amount of scatter. Channel 3, whose radiation is due to both water vapor and carbon dioxide, has an

Table VI-3.--Transmittances computed from measured radiances and corresponding path length, effective pressures and temperatures for the layers observed

Pressure Layer (mb)	Total transmittance					CO ₂ transmittance					Path length		Effective pressure		Effective temperature		
	Ch 1	Ch 2	Ch 3	Ch 4	Ch 5	Ch 3	Ch 4	Ch 5	Ch 4	Ch 5	U _w	U _c	P _e	P _e	T _e	T _e	
											g/cm ²	atm cm	H ₂ O	CO ₂	H ₂ O	CO ₂	
FLT 1																	
337-446	0.940	0.995	0.767	0.582	0.280	0.792	0.601	0.291	0.09	31.4	413	400	255.9	254.4			
337-573	.682	.971	.579	.356	.073	.641	.396	.083	.29	58.6	497	455	264.2	260.0			
337-698	.336	.869	.355	.189	.018	.449	.242	.024	.74	90.0	585	519	272.8	266.2			
466-573	.680	.977	.670	.498	.172	.724	.540	.189	.20	26.5	528	519	267.4	266.6			
466-698	.358	.880	.390	.239	.036	.485	.300	.047	.65	57.5	604	582	274.7	272.6			
573-698	-	.905	.470	-	-	.557	-	-	.45	31.0	639	636	278.1	277.7			
FLT 8																	
238-505	.478	.933	.603	.425	.169	.633	.447	.179	.14	65.3	426	371	255.1	247.1			
FLT 9																	
209-365	.902	.988	.772	.639	.401	.779	.645	.405	.03	38.0	307	286	239.0	235.0			
209-490	.760	.965	.640	.452	.160	.662	.468	.167	.10	69.3	406	349	254.0	245.0			
209-601	.532	.933	.518	.312	-	.572	.346	-	.28	97.5	500	406	264.7	252.2			
365-490	.813	.978	.752	.593	.269	.773	.611	.279	.08	30.8	438	427	258.7	257.3			
365-601	.560	.944	.582	.379	-	.640	.419	-	.26	59.0	519	484	267.4	263.5			
490-601	.580	.968	.688	.533	-	.739	.575	-	.18	27.6	553	546	271.0	270.3			

Table VI-4.--Transmittances computed from flight 9 radiance data using two different model transmittance values (τ_1 , τ_2) for the 209- to 365-mb layer and their differences (δ_τ).

Channel		1st-order approx. (τ_0) Eq (10)	Model Value ($\hat{\tau}$)	Final Value (τ) Eq (13)
1	τ_1	0.934	0.903	0.902
	τ_2	<u>.933</u>	<u>.866</u>	<u>.897</u>
	δ_τ	<u>.001</u>	<u>.037</u>	<u>.005</u>
2	τ_1	.988	.997	.988
	τ_2	<u>.988</u>	<u>.994</u>	<u>.988</u>
	δ_τ	<u>.000</u>	<u>.003</u>	<u>.000</u>
3	τ_1	.836	.798	.772
	τ_2	<u>.836</u>	<u>.811</u>	<u>.773</u>
	δ_τ	<u>.000</u>	<u>-.013</u>	<u>-.001</u>
4	τ_1	.693	.653	.639
	τ_2	<u>.694</u>	<u>.661</u>	<u>.638</u>
	δ_τ	<u>-.001</u>	<u>-.008</u>	<u>.001</u>
5	τ_2	.379	.394	.401
	τ_2	<u>.378</u>	<u>.446</u>	<u>.392</u>
	δ_τ	<u>.001</u>	<u>-.052</u>	<u>.009</u>

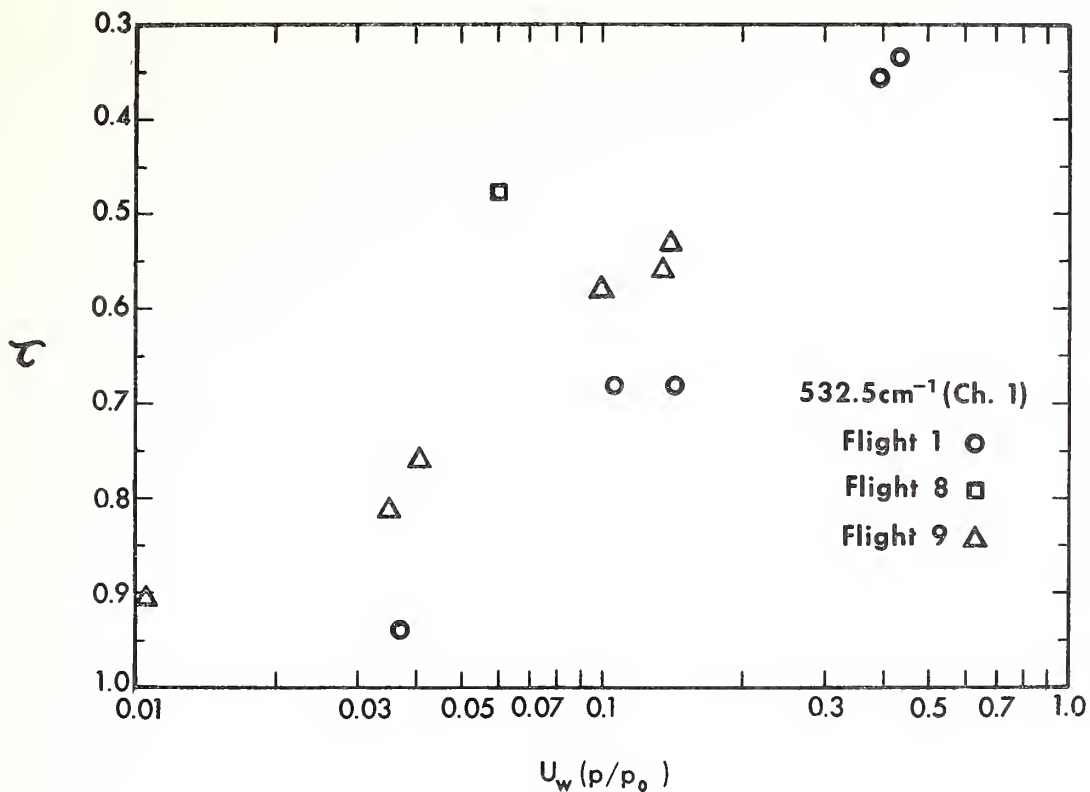


Figure VI-1.--Radiance-derived H₂O transmittance values for channel 1.

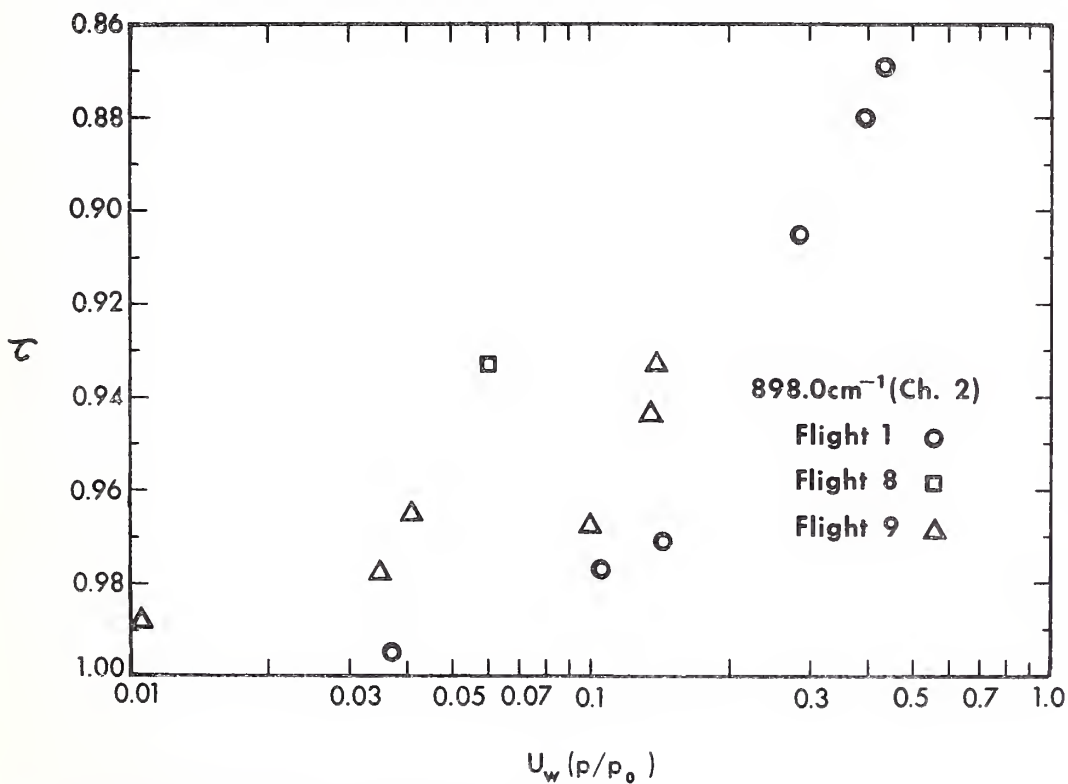
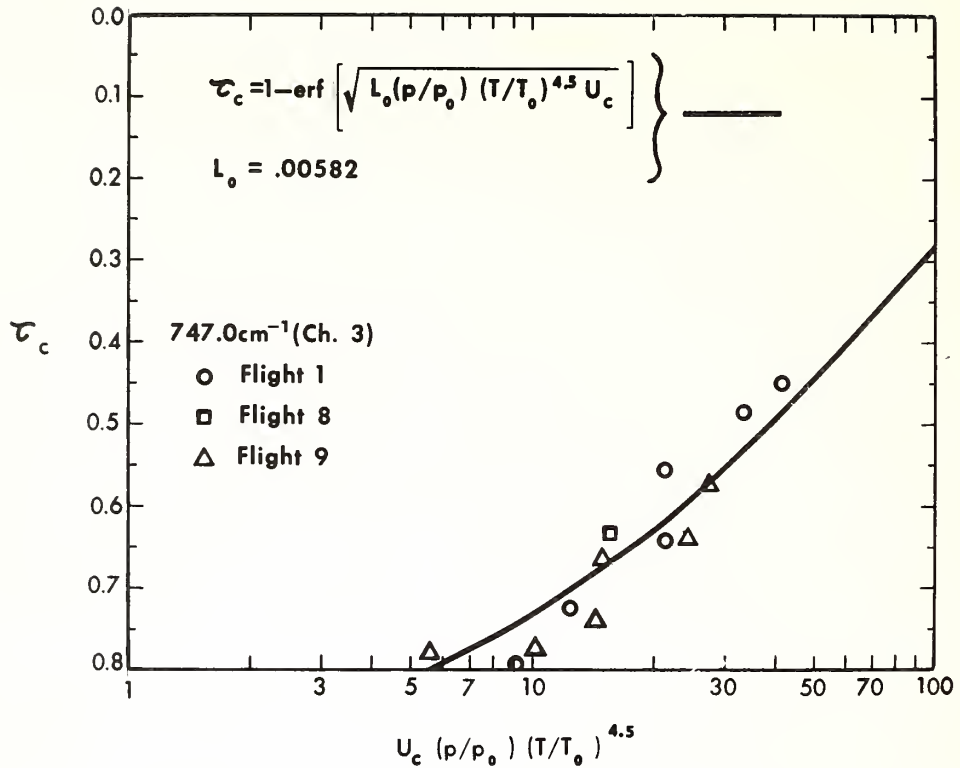
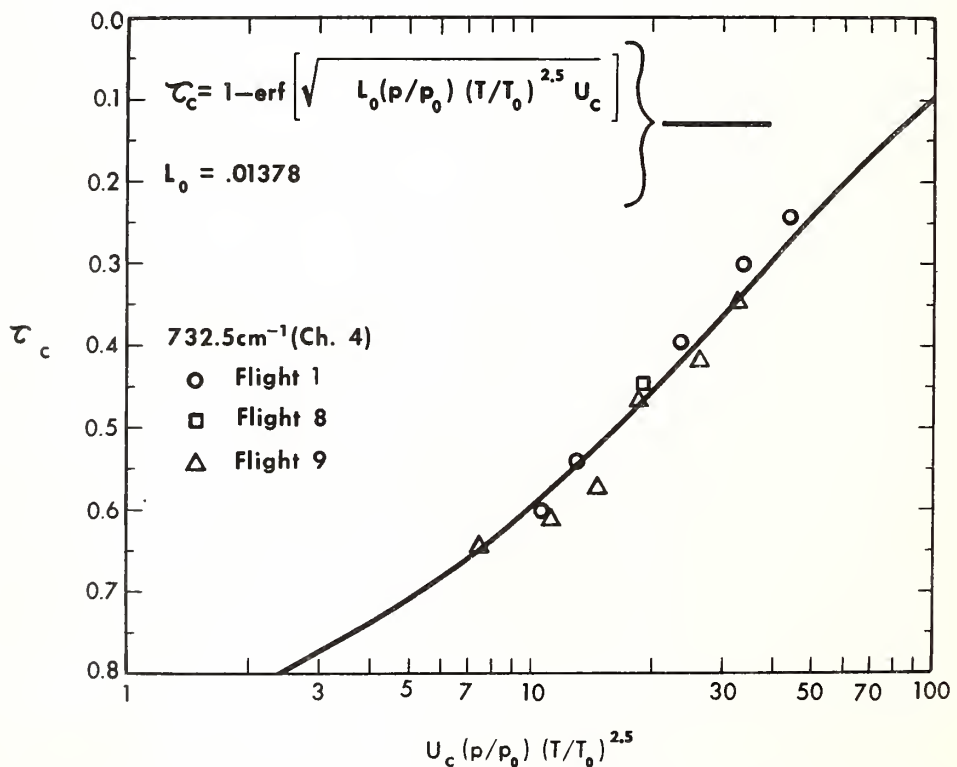


Figure VI-2.--Radiance-derived H₂O transmittance values for channel 2.

Figure VI-3.--Radiance-derived CO₂ transmittance values for channel 3.Figure VI-4.--Radiance-derived CO₂ transmittance values for channel 4.

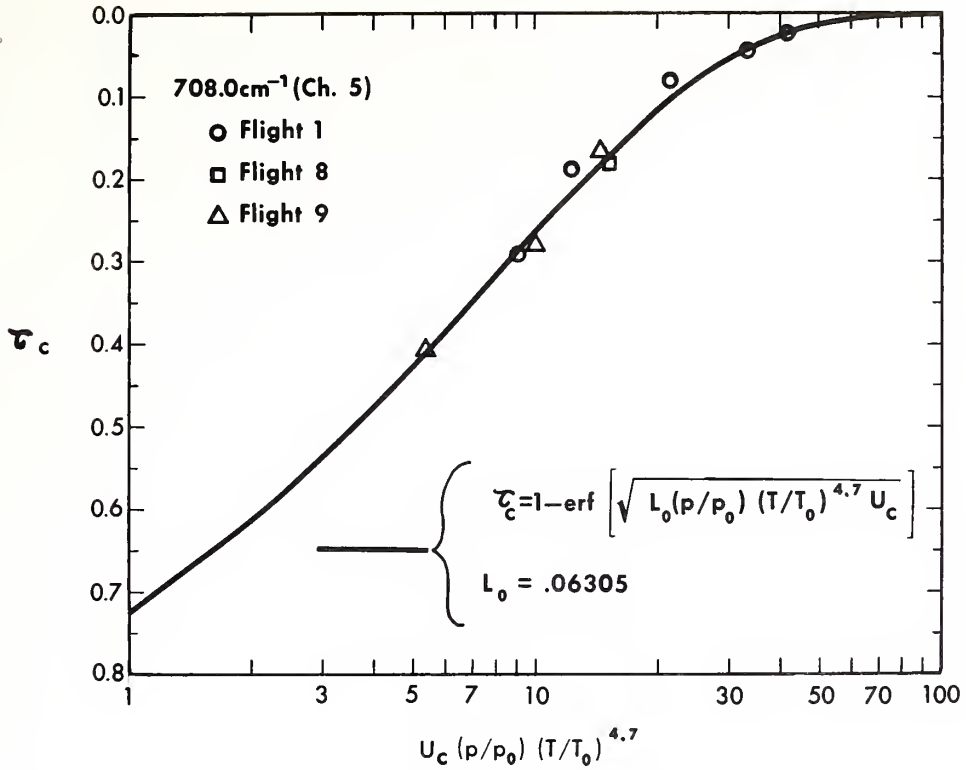


Figure VI-5.--Radiance-derived CO₂ transmittance values for channel 5.

intermediate amount of scatter. (It is noted that for channels 1 and 2 the scatter is caused by errors in U_w , while for channels 3, 4, and 5 the scatter shown is due to errors in τ_c caused by erroneous estimates of τ_w .) In all cases the scatter produced by errors of τ , which are due to radiance errors and temperature profile errors, appear to be small compared to the scatter produced by errors in the estimated water vapor path lengths.

Summary

This study shows that atmospheric transmittances can be determined from airborne radiance profiles through a solution of the differential equation of radiative transfer. Band models may be used to account for the non-monochromatic characteristics of the measured radiation in the solution.

The objective of the transmittance observations is the formulation of models that can be used to estimate atmospheric transmission as a function of absorbing gas concentration, temperature, and pressure for the particular spectral regions sensed by satellite-borne sounding radiometers. Accurate knowledge of the atmospheric transmission functions is needed to determine the temperature and water vapor profiles of the atmosphere from the satellite-measured radiances.

This study indicates that highly accurate water vapor observations are needed to formulate adequate transmission functions for spectral regions whose radiation is absorbed by that gas. The inaccurate water vapor estimates available for this study prevented the formulation of transmission functions for the two spectral regions dominated by water vapor absorption.

It is proposed to use airborne experimental methods, similar to those described here, to help define the atmospheric transmission functions of the spectral channels of future satellite sounding radiometers. The necessary aircraft measurements should be obtained with preflight models of the satellite instruments. This method should decrease much of the current uncertainty about the transmission functions caused by the extrapolation of theory and laboratory observations to the real atmosphere.

VII. DETERMINATION OF CLOUD TRANSMITTANCE

Introduction

The determination of the temperature distribution within the atmosphere to the earth's surface from satellite measurements of the upwelling radiance requires that the atmospheric radiation be emitted from and pass through cloud-free columns of air. However, because the earth always has some cloud cover, it is necessary to estimate an equivalent "clear-column" radiance in the presence of clouds. To aid in the development of procedures for making such estimates it is useful to have information on the spectral transmission characteristics of clouds.

As part of the experimental ITPR testing program, measurements were made of the radiance profile and ambient temperature through various types of clouds with the hope that some of their spectral transmission characteristics

could be determined. Although it was not possible to make an extensive study of these transmittances, two cases were studied in some detail; these cases probably represent high- and middle-level clouds. Many more measurements will be needed for more extensive studies; however, the few results obtained are encouraging, since they indicate that such radiance measurements from aircraft can be utilized in studying the transmittance characteristics of clouds.

Numerical Method

The Schwarzschild equation of radiative transfer in the absence of scattering is generally written in the form,

$$\frac{dI_\nu}{d\tau_\nu} = B_\nu - I_\nu \quad (\text{VII-1})$$

where I_ν is the intensity of the radiation field, B_ν the intensity of the blackbody radiance source, τ_ν is the optical path length in the medium, and ν is the wavenumber of the radiation. The optical path length τ_ν is given by,

$$\tau_\nu = \int_0^z k_\nu(z') dz' \quad (\text{VII-2})$$

where k_ν is the attenuation coefficient and z is the path length in the medium.

For monochromatic radiation, the transmittance in the medium is

$$\tau_\nu(z) = e^{-\int_0^z k_\nu(z') dz'} = e^{-\tau_\nu} \quad (\text{VII-3})$$

Therefore, the optical path length in terms of the transmittance is

$$d\tau_\nu = -\tau_\nu d\tau_\nu \quad (\text{VII-4})$$

Substituting this expression into eq (VII-1), the equation of radiative transfer takes the form

$$\tau_\nu d\tau_\nu - I_\nu d\tau_\nu = -B_\nu d\tau_\nu \quad (\text{VII-5})$$

Integrating eq (VII-5) over a bandwidth $\Delta\nu$, the result is

$$(\tau d\bar{I} - \bar{I} d\bar{\tau}) + \overline{(\tau_\nu' dI_\nu' - I_\nu' d\tau_\nu')} = -\bar{B} d\bar{\tau} - \overline{B_\nu' d\tau_\nu'} \quad (\text{VII-6})$$

where

$$\bar{I} = \frac{\int_0^\infty \phi_\nu I_\nu d\nu}{\int_0^\infty \phi_\nu d\nu}, \quad \bar{B} = \frac{\int_0^\infty \phi_\nu B_\nu d\nu}{\int_0^\infty \phi_\nu d\nu}, \quad \bar{\tau} = \frac{\int_0^\infty \phi_\nu \tau_\nu d\nu}{\int_0^\infty \phi_\nu d\nu},$$

$$I_\nu' = I_\nu - \bar{I}, \quad \tau_\nu' = \tau_\nu - \bar{\tau}, \quad \text{and}$$

ϕ_ν is the instrumental response function. While the correlation terms

in equation VII-6 are important in cloud-free regions of the atmosphere, the scattering and absorption of radiation by water and ice particles in clouds tend to suppress the correlation. Therefore, they shall be neglected in the information. Equation (VII-6) can then be written,

$$\frac{d\bar{\tau}(p_0, p)}{\bar{\tau}(p_0, p)} = + \frac{d\bar{I}(p)}{\bar{I}(p) - \bar{B}(p)} \quad (\text{VII-7})$$

where the explicit dependence upon the pressure levels is shown. p_0 is a reference level, such as the top or base of the cloud.

Integrating both sides of equation (VII-7) from p_0 to p we obtain

$$\ln \bar{\tau}(p_0, p) - \ln \bar{\tau}(p_0, p_0) = + \int_{p_0}^p \frac{d\bar{I}(p')/dp'}{\bar{I}(p') - \bar{B}(p')} dp \quad (\text{VII-8})$$

Since $\bar{\tau}(p_0, p_0) = 1$, we obtain as a final result,

$$\bar{\tau}(p_0, p) = \exp \left\{ - \int_{p_0}^p \frac{d\bar{I}(p')/dp'}{\bar{B}(p') - \bar{I}(p')} dp \right\} \quad (\text{VII-9})$$

Equation (VII-9), therefore, enables one to determine the transmittance $\bar{\tau}$ from a knowledge of the radiance profile, $I(p)$, and the ambient temperature profile, $T(p)$ (i.e., $\bar{B}(T(p))$). In the experiment on the CV-990 flight, the radiances and ambient temperatures were measured at a number of levels in the cloud. Therefore, for practical applications one must approximate equation (VII-9) for a finite number of pressure levels. The approximation that was used may be written,

$$\bar{\tau}(p_0, p_\ell) = \exp \left\{ - \frac{\sum_{m=1}^{\ell} [\bar{I}(p_m) - \bar{I}(p_{m-1})]}{[\tilde{I}(p_m, p_{m-1}) - \tilde{B}(p_m, p_{m-1})]} \right\} \quad (\text{VII-10})$$

$$\text{where } \tilde{I}(p_m, p_{m-1}) = \frac{\bar{I}(p_m) + \bar{I}(p_{m-1})}{2} \quad \text{and} \quad \tilde{B}(p_m, p_{m-1}) = \frac{\bar{B}(p_m) + \bar{B}(p_{m-1})}{2}$$

In this form the transmittances can be readily approximated directly from the measurements.

When scattering cannot be neglected, equation (VII-1) must be generalized

to

$$\frac{dI_v(\mu)}{dt} = -I_v(\mu) + \frac{\omega_v}{2} \int_{-1}^1 p(\mu, \mu') I_v(\mu') d\mu' + (1-\omega_v)B_v \quad (\text{VII-11})$$

where

$$\frac{1}{2} \int_{-1}^1 p(\mu, \mu') d\mu' = 1 \quad (\text{VII-12})$$

$p(\mu, \mu')$ is the scattering phase function which describes how the scattered radiation is distributed with direction, μ' and μ are, respectively, the cosines of the zenith angles of incidence and emergence, and ω_v is the fraction of incident radiation that is scattered by a small volume element.

Since the upward intensity of the radiation was measured, $\mu=1$ in equation (VII-11). Because the size of the scatterers is of the same order as the wavelengths of the radiation, the major contributions to the integral in equation (VII-11) occur in the vicinity of $\mu'=1$, when $\mu=1$. As a result of this and the fact that $I_v(\mu')$ varies only slightly with angle in the angular region near $\mu'=1$, equation (VII-11) can be approximately written

$$\frac{dI_v}{dt} = (1-\omega_v)(B_v - I_v) \quad (\text{VII-13})$$

Similar to the derivation of the transmissivity for the case when scattering was neglected, the transmissivity that results in the presence of scattering is given approximately by

$$\bar{\tau}(p_0, p) = \exp \left\{ - \frac{1}{1-\bar{\omega}} \int_p^{p_0} \frac{[dI(p')/dp']}{\bar{I}(p') - \bar{B}(p')} \right\} \quad (\text{VII-14})$$

where

$$\bar{\omega} = \frac{\int_0^\infty \omega_v \phi_v dv}{\int_0^\infty \phi_v dv} \quad (\text{VII-15})$$

Using equation (VII-9), equation (VII-14) may be written

$$\bar{\tau}(p_0, p) = \bar{\tau}_0(p_0, p) \frac{1}{1-\bar{\omega}} \quad (\text{VII-16})$$

Another useful form that equation (VII-16) may be written is obtained by defining $\bar{\tau}_a(p_0, p)$ to be the transmissivity through the cloud-free atmosphere and $\bar{\omega}_0$ to be the value of $\bar{\omega}$ in the absence of the gaseous

constituents of the atmosphere. Then,

$$\bar{\tau}(p_o, p) = \left(\frac{\bar{\tau}_o(p_o, p)}{\bar{\tau}_a(p_o, p) \bar{\omega}_o} \right)^{\frac{1}{1-\omega}} \quad (\text{VII-17})$$

Results of the Aircraft Measurements

The Convair-990 experimental program included 10 flights. On some of these, measurements of the radiances and ambient temperatures were made as the aircraft flew separate legs above, through, and below one or more cloud decks. In this way we hoped to gather sufficient data to study the spectral transmission characteristics of the clouds. However, because of insufficient data, only two case studies could be examined in detail.

In the first case (flight 2), measurements were made of a deck of clouds described as cirrus. These clouds in the vicinity of Spokane, Wash., had tops at 27,200 feet and bases at about 15,000 feet. The first leg of the cloud study portion of the flight was made beneath the cloud deck, the second and third legs through the deck, and the fourth leg above the deck. This effectively divided the cloud deck into three sublayers.

As the aircraft flew these legs, measurements of the radiances in five separate channels were made every 0.03 seconds, and ambient temperature was measured every minute. The mean radiance for each channel and the mean value of the ambient temperature were computed for each flight leg. These values and the equivalent blackbody temperatures corresponding to the measured radiances are listed in table VII-1. The blackbody radiances corresponding to the ambient temperatures also are shown.

These radiances were then used in equations (VII-10) and (VII-16) to compute estimates of the cloud transmittances, τ_{ca} . The transmittances obtained are shown in figure VII-1 for $\bar{\omega}_o=0$ and in figure VII-2 for $\bar{\omega}_o=0.5$ as a function of the elevation from the base of the cloud. The transmittances for each channel are connected by a smooth curve. While such curves as shown in figure VII-2 are good representations of the actual variations of τ_{ca} in most of the cloud, the variations at the base of the cloud are questionable. It is quite possible that the transmittances approach unity more quickly than indicated and then level off in a manner similar to that shown for the top of the cloud.

Note that values of τ_{ca} in the window channel (2) are significantly higher than those for the other channels, while channel 5, the most opaque CO_2 band, has quite low values. It is interesting that, toward the base of the cloud, transmittances in the water vapor band (1) are lower than those in the CO_2 channels (3 and 4), while the values for channel 1 fall between those of the two CO_2 channels at higher levels. This is probably because of the higher concentration of water vapor at the base.

To isolate the effects of water vapor and CO_2 on the transmittance characteristics of the clouds, estimates were made of transmittances for conditions of zero water vapor and zero CO_2 concentrations. These

Table VII-1.--Temperatures and radiances measured in clouds during flight 2.

Elevation in cloud thousands of feet	Pressure mb	Temperature °K	ergs/cm ² s r cm ⁻¹							
			B ₁	B ₂	B ₃	B ₄	B ₅			
0	587	269.8	111.49	72.15	94.03	95.93	99.00			
2.1	520	264.4	104.84	63.37	86.55	88.43	91.49			
4.6	488	261.6	101.45	62.02	82.80	84.67	87.72			
12.8	332	241.8	78.86	41.27	58.86	60.56	63.40			
Pressure mb	T ₁	T ₂	T ₃	T ₄	T ₅	I ₁	I ₂	I ₃	I ₄	I ₅
587	280.42	304.13	291.99	285.98	277.04	125.14	124.70	128.14	120.28	109.54
520	272.40	295.34	281.42	276.12	268.90	114.75	109.69	111.22	105.11	97.73
488	265.84	279.11	269.25	266.49	263.15	106.60	84.78	93.25	91.30	89.80
332	255.19	267.85	256.01	252.54	248.81	93.88	69.66	75.58	73.10	71.53

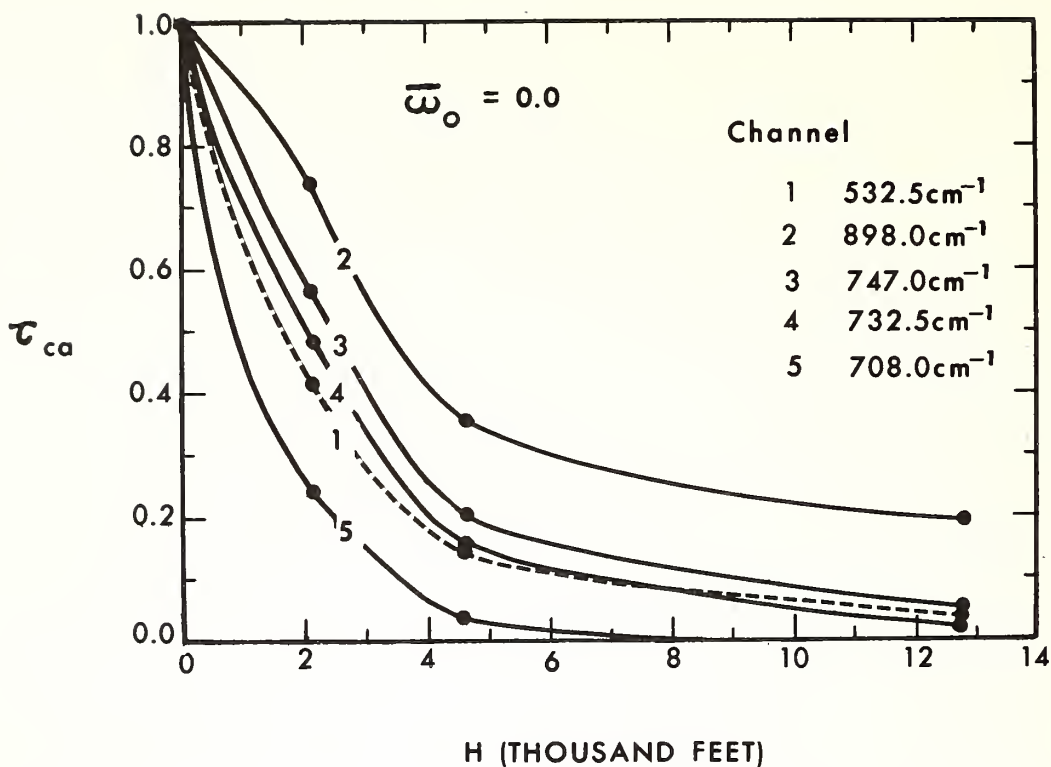


Figure VII-1.--Cloud transmittance (τ_{ca}) vs the elevation (H) above the base of the cloud (Flight 2).

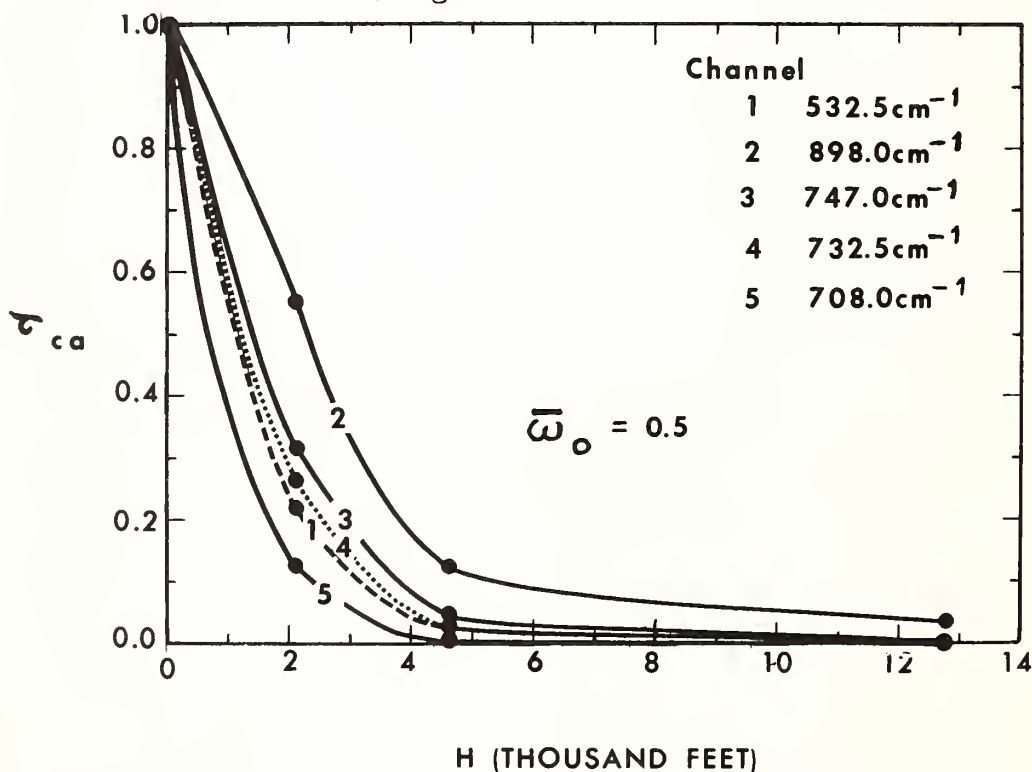


Figure VII-2.--Cloud transmittance (τ_{ca}) vs the elevation (H) above the base of the cloud (Flight 2).

transmittances we shall denote τ_c . The transmittances for the cloud-free regions adjoining the region of measurement were computed for the CO_2 band. These we shall call τ_a . Before the first leg of the flight was made below the cloud deck, the aircraft made a steady descent in the clear air adjacent to the cloud. During this time, radiances were measured, and the clear-air radiance values corresponding to the elevations of the legs were obtained. Using the program discussed in section VI, which is a generalization of Equation (VII-10), transmittances through the cloud-free atmosphere were computed. They are shown in figure VII-3.

The values of τ_{ca} for the cloud for $\bar{\omega}_0 = 0.5$ in the three CO_2 channels were then plotted against the corresponding values of τ_a as shown in figure VII-4. Curves for each cloud level were then extrapolated to where the value of τ_a became unity. The transmittances in the cloud corresponding to these extrapolated values, therefore, are the desired "pure" cloud transmittances, τ_c . The resulting variations of these transmittances with elevation in the cloud are shown in figure VII-5.

Since there is only one channel for the water vapor band and one for the "window", the "pure" cloud transmittances at these spectral intervals must be approximated in a different manner. By assuming that

$$\tau_{ca} \approx \tau_c \times \tau_a \quad (\text{VII-18})$$

the "pure" cloud transmittances may be estimated. The resulting values are also shown in figure VII-5.

It is interesting to note that the transmittances for the CO_2 and water vapor bands are very nearly the same, while those for the window channel are considerably greater in magnitude.

The results presented in figure VII-5 can be explained if the predominant phase of the cloud particles is liquid. Although the cloud was reported as cirrus, it seems quite unlikely that ice particles predominate at levels as low as 15,000 feet. Therefore, assuming that most of the cloud was composed of liquid water drops, the agreement between the transmittances in the CO_2 and water vapor bands can be explained by the fact that the values of the liquid water absorption coefficients are fairly close in the two bands. On the other hand, the magnitude of the absorption coefficient for the window region is less than half that for either the water vapor or CO_2 band. This explains the larger values of τ_c for this channel. The same conclusion may be reached by comparison of the extinction efficiency factors (ratio of the extinction cross section to the geometric cross section) for 10- μm drops. Again, the values for the water vapor and CO_2 bands are close in value while that for the window region is considerably smaller. Table VII-2 lists the absorption coefficients and extinction efficiency factors for the three spectral regions.

The second case for which cloud transmittances were computed was derived from data gathered from cirrus clouds with tops at 37,800 feet and bases at 27,000 feet (flight 10). Table VII-3 lists information on mean radiances and temperatures, similar to that listed in table VII-1. Only one leg of the

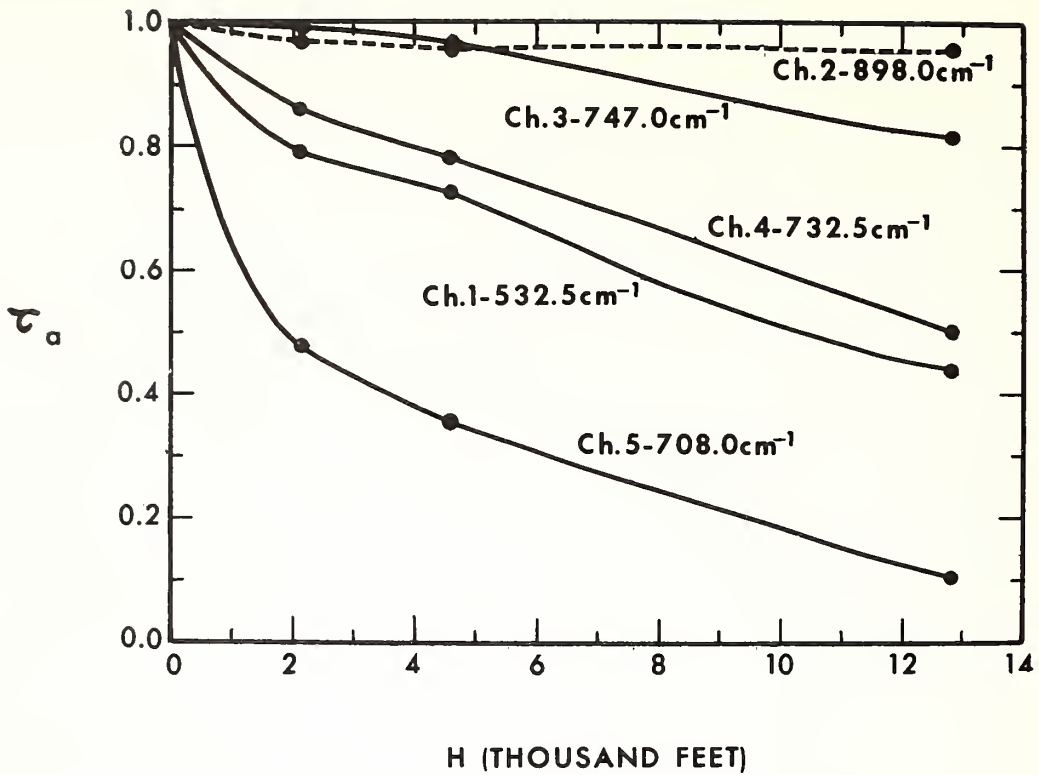


Figure VII-3.--Clear-air transmittance (τ_a) vs the elevation (H) in the clear air above the cloud base (Flight 2).

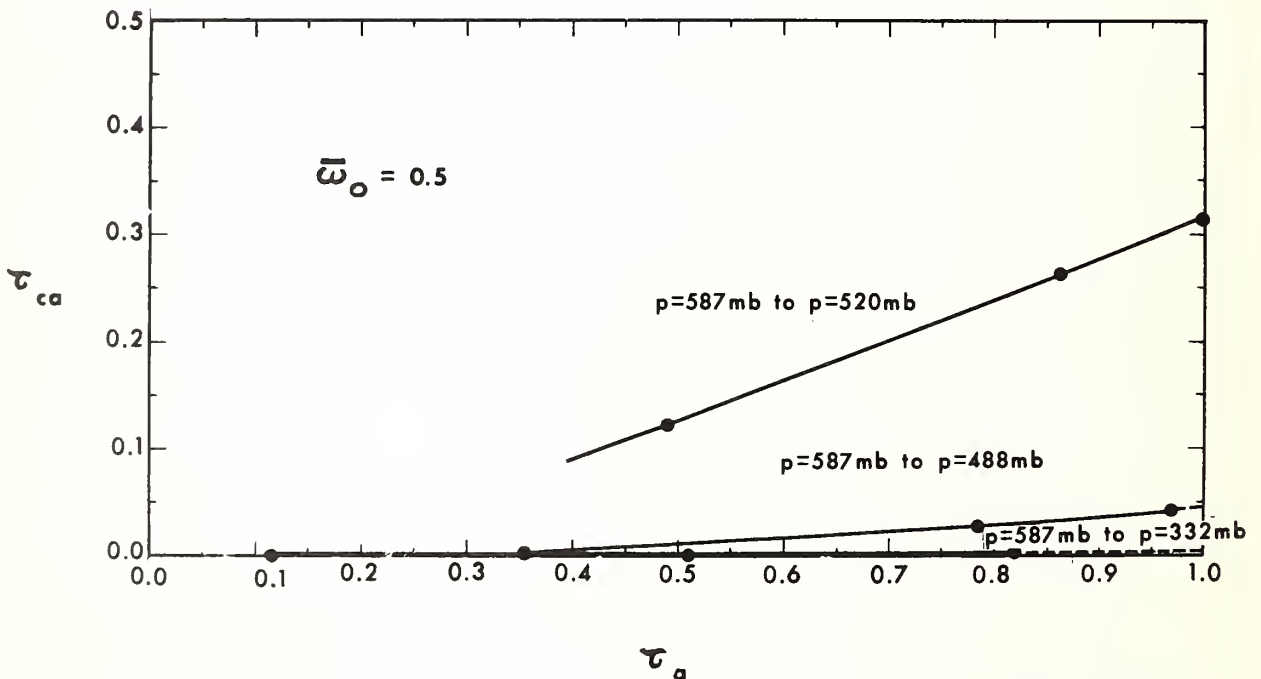


Figure VII-4.--Cloud transmittance (τ_{ca}) vs the clear-air transmittance (τ_a) (Flight 2).

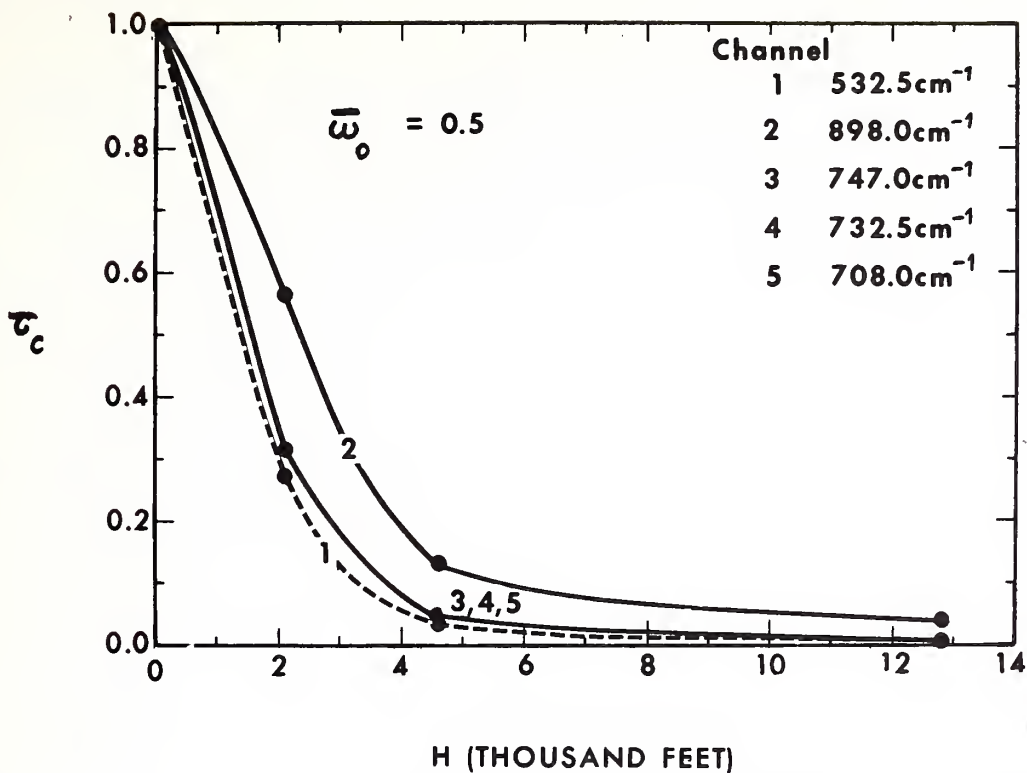


Figure VII-5.--"Pure" cloud transmittance (τ_c) vs the elevation (H) above the base of the cloud (Flight 2).

Table VII-2.--Absorption and extinction factors for liquid water

Channel	Mean wavelength μm	Absorption coeff. in water cm^{-1}	Extinction efficiency factor
1	18.78	2633	2.628
2	11.13	1296	1.789
3	13.72	3083	2.284
4			
5			

Table VII-3.--Temperature and radiances measured in clouds during Flight 10.

Elevation in cloud		Pressure	Temperature	B ₁	B ₂	B ₃	B ₄	B ₅		
thousands of feet		mb	°K	ergs/cm ² s sr cm ⁻¹						
0		314	244.0	81.25	43.32	61.29	63.02	65.90		
5.8		274	236.0	72.71	36.17	52.70	54.34	57.08		
8.8		210	224.0	60.71	26.94	41.19	42.66	45.16		
Pressure	T ₁	T ₂	T ₃	T ₄	T ₅	I ₁	I ₂	I ₃	I ₄	I ₅
mb										
314	273.59	310.56	285.44	274.39	260.29	116.26	136.36	117.51	102.56	85.99
274	261.84	289.55	268.35	260.78	249.78	101.74	100.39	91.97	83.58	72.70
210	246.44	264.17	246.70	243.63	235.74	83.93	65.09	64.36	62.60	56.80

flight was made within the cirrus. Computation results are shown in figures VII-6 and VII-7.

Note that here the window and water vapor channels have transmittances very nearly the same in value. This is probably because of the smaller amount of water vapor at the higher levels.

Since no data from cloud-free regions near the cloud area were available, another means for estimating the "pure" cloud transmittances was used. A relative measure of the absorption coefficients in the CO₂ band were obtained from flight 2 data. By plotting the values of τ_{ca} against the absorption coefficients, one could obtain τ_c by extrapolating the curves to points where the absorption coefficients became zero.

The transmittance values, τ_a , computed for flight 2 were used to estimate an absorption coefficient k for the band, assuming the relation,

$$\tau_a(p_o, p) = e^{-k(p_o - p)} \quad (\text{VII-19})$$

from which

$$k = - \frac{\ln \tau_a(p_o, p)}{p_o - p}$$

Since $(p_o - p)$ is a common factor to all the values of the absorption coefficients, plots of τ_{ca} for $\bar{w} = 0.5$ for this case study were made against $-\ln \tau_a$ determined for the thickest layer from flight 2 (See figure VII-8). The values of τ_{ca} were then extrapolated to a value of zero for $-\ln \tau_a$. The values of τ_{ca} obtained were the desired values of τ_c ; these are plotted in figure VII-9.

The "pure" cloud transmittances for channels 1 and 2 were assumed to be the same as the transmittances with water vapor present. For comparison with the curves of τ_c for the CO₂ band, they are shown in figure VII-9. That the transmittances are much closer in value for all the channels than those for flight 2 can be explained by the fact that ice particles are much larger than cloud water drops. Thus, nearly all the radiation refracted into the crystals is absorbed, and differences in the absorption coefficients are unimportant. For large particles the extinction efficiency factors all tend toward a value of 2. Probably, the small variations in this parameter give rise to the differences in the transmittance curves of figure VII-9.

Conclusions and Recommendations

The results of the cloud transmittances determined from measurements obtained by the airborne ITPR brassboard instrument indicate that much can be learned about the radiative properties of clouds by using such measurements. Although not many cases were studied in quite so great detail as would have been desirable, the results definitely do point toward what can be achieved on future flights.

Therefore, on the basis of this study, we recommend that more extensive

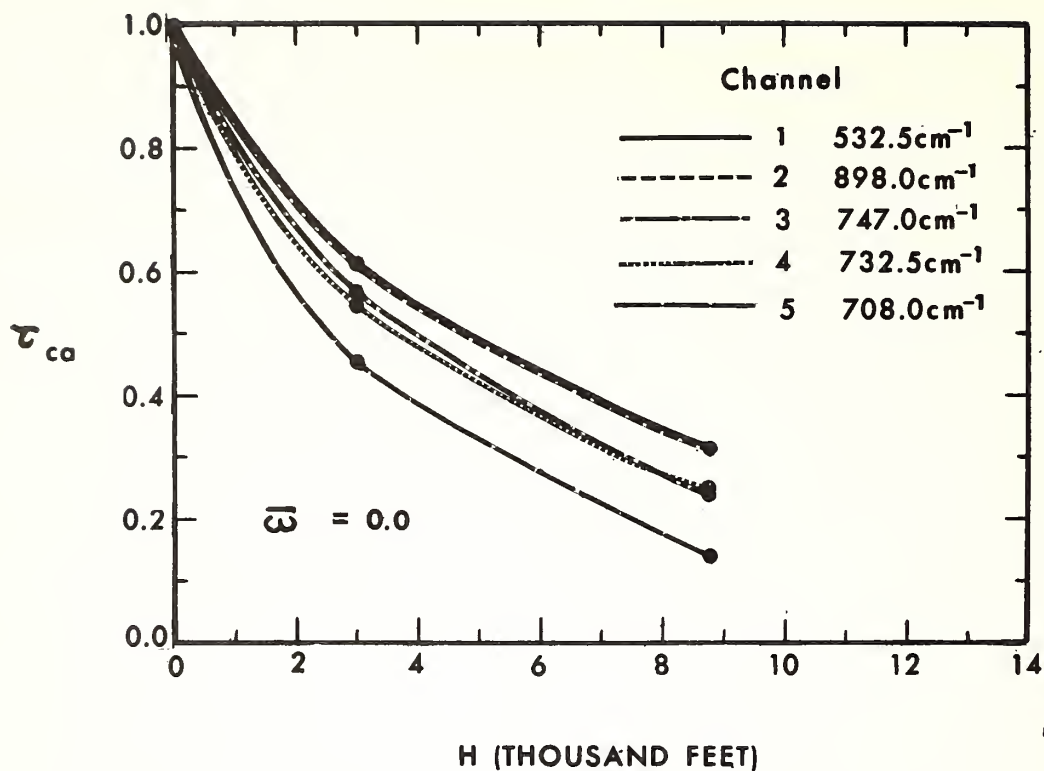


Figure VII-6.--Cloud transmittance (τ_{ca}) vs the elevation (H) above the base of the cloud (Flight 10).

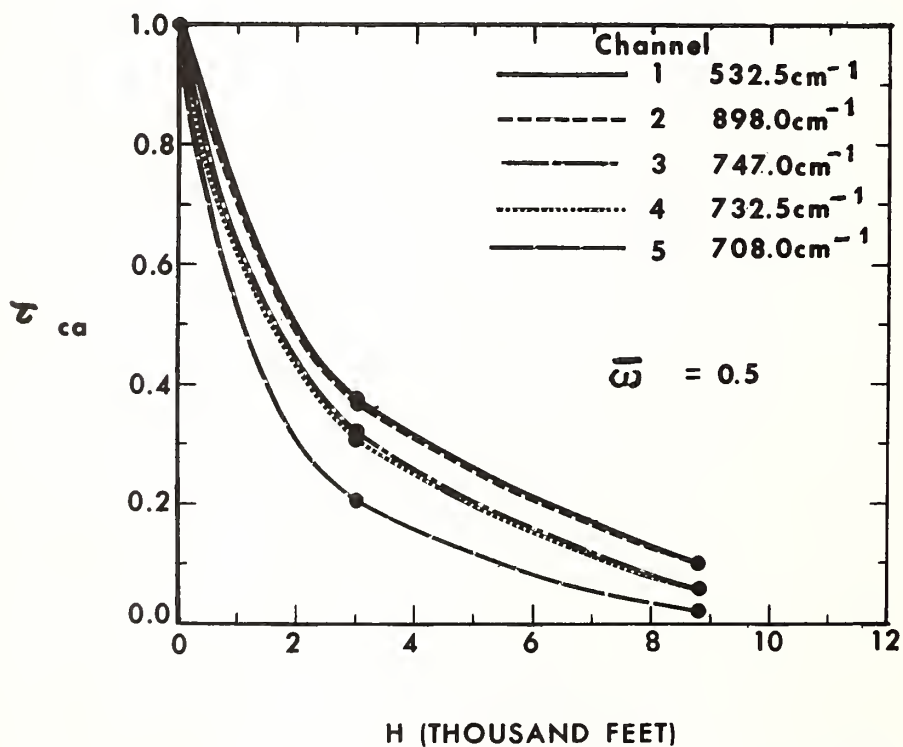


Figure VII-7.--Cloud transmittance (τ_{ca}) vs the elevation (H) above the base of the cloud (Flight 10).

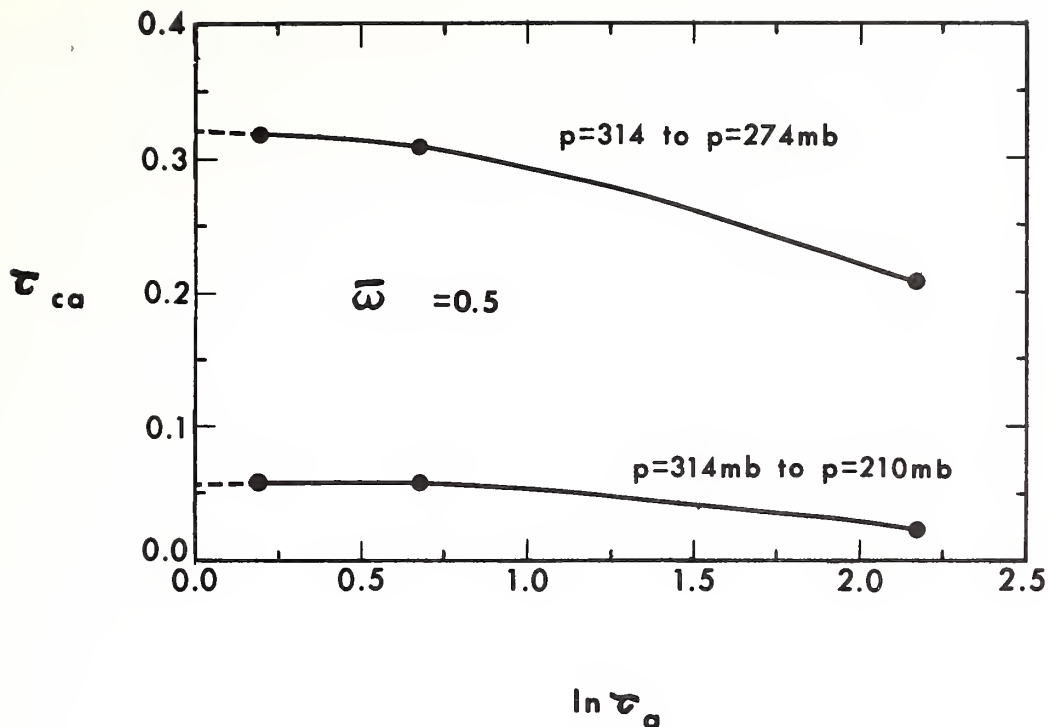


Figure VII-8.--Cloud transmittance (τ_{ca}) for flight 10 vs the negative of the logarithm of the clear air transmittance ($-\ln \tau_a$ for the thickest layer in flight 2).

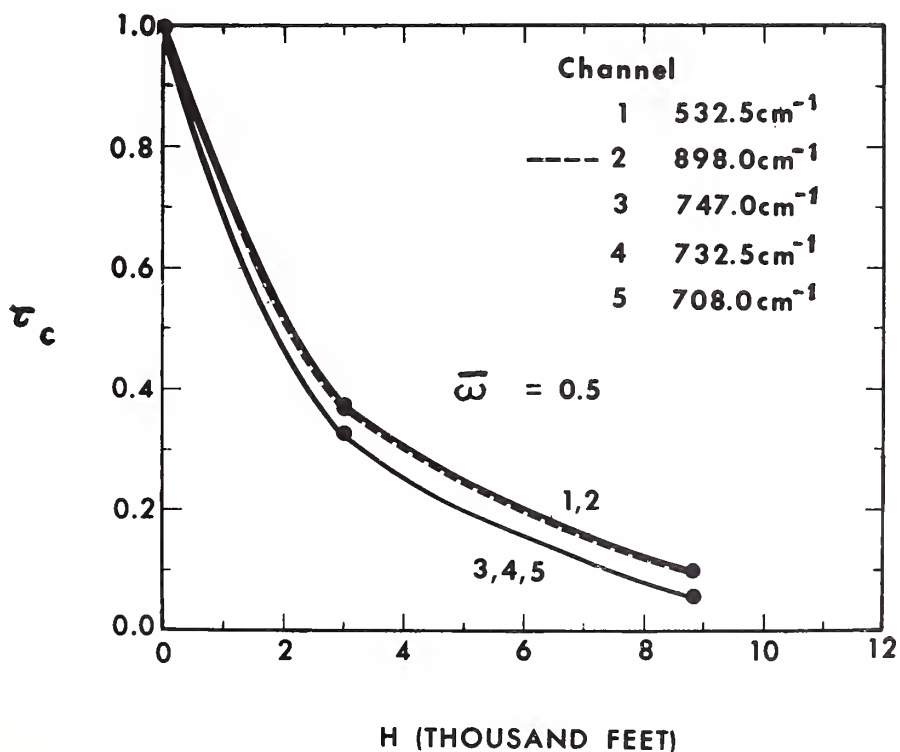


Figure VII-9.--"Pure" cloud transmittance (τ_c) vs the elevation (H) above the base of the cloud (Flight 10).

measurements be made for a variety of cloud situations to assess the accuracy of current results. These measurements should provide for flying a greater number of legs (perhaps six or more) within the clouds and in the adjoining clear regions to permit better definition of transmittance curves. Also, the study of a larger number of cases should lead to a clearer understanding of the factors that influence the transfer of radiation through clouds.

References

- Barnes Engineering Company, "Thermistor Infrared Detectors," Reprinted from NAVORD 5495, June 1, 1958.
- Barnes Engineering Company, "Satellite Spectrometer, Phase II, 1st Quarterly Report 4696 to Contract Cwb 10-419," November 15, 1969.
- Howard, J. N., Burch, D. L., and Williams, D., Near-Infrared Transmission Through Synthetic Atmospheres, Geophysical Research Papers No. 40 (AFCRC-TR-55-213, Cambridge Research Center, U.S.A.F., November 1955, 244 pp.
- Middlebrook, R. D., and Taylor, A. D., "Differential Amplifier with Regulator Achieves High Stability, Low Drift," Electronics Magazine, Vol. 34, July 28, 1961, pp. 56-59.
- Möller, R., and Raschke, E., Evaluation of TIROS III Radiation Data, Ludwig-Maximilians - Universität, Meteorologisches Institut, München, Germany, NASA Research Grant, NSG-305, July 1963, 114 pp.
- Smith, W. L., "An Improved Method for Calculating Tropospheric Temperature and Moisture from Satellite Radiometer Measurements," Monthly Weather Review, Vol. 96, No. 6, June 1968, pp. 387-396.
- Smith, W. L., "A Polynomial Representation of Carbon Dioxide and Water Vapor Transmission," ESSA Technical Report NESC 47, February 1969 (Available from the National Technical Information Service), 20 pp.
- Smith, W. L., "The Improvement of Clear-Column Radiance Determination with a Supplementary 3.8- μm Window Channel," ESSA Technical Memorandum NESCTM-16, U. S. Department of Commerce, National Environmental Satellite Service Center, Washington, D. C., July 1969, 17 pp.
- Smith, W. L., and Jacob, W. J., "Multi-Spectral Window Determination of Surface Temperature and Cloud Properties," (to be submitted for publication).
- Wark, D. Q., Hilleary, D. T., Anderson, S. P., and Fischer, J. C., "NIMBUS Satellite Infrared Spectrometer Experiment," IEEE Transactions on Geoscience Electronics, Vol. GE-8, No. 4, October 1970, pp. 264-270.

APPENDIX

Flight plan and ITPR data for June 12, 1970 (flight 7)

I. Flight Plan

The flight plan is to leave Eielson AFB for a point southeast of Fairbanks and execute a pass over the glacier Gloco at 14 K. After Anchorage is passed, the aircraft will proceed to a point of 49° N. and 150° W. at 31 K in order to pass over a front. The aircraft will then turn left at Medford, Oregon, pass over the cold section of the front, there execute a 30-minute delay. The aircraft will then attempt to reach the cirrus shield associated with the warm front, and if time permits, to execute a 15-minute delay with clear skies below the cirrus. Afterwards, the aircraft will go down the coast about 200 miles offshore until Moffett AFB is reached.

II. Flight Data

DATA FORMAT

Time: Hours: Minutes: Seconds (GMT)

Pressure Altitude (mb)

Brightness Temperatures ($^{\circ}$ K)

T1 (532.5 cm^{-1})

T2 (898.5 cm^{-1})

T3 (747.0 cm^{-1})

T4 (732.5 cm^{-1})

T5 (708.0 cm^{-1})

HR	MIN	SEC	ALT	I1	I2	I3	I4	I5	ALT	I1	I2	I3	I4	I5
15	46	57	285	261.80	283.14	254.56	254.63	243.84	287	255.62	265.01	251.61	247.05	242.92
19	47	17	285	260.31	277.22	260.19	251.33	242.62	286	259.89	275.35	259.14	250.78	242.60
19	47	37	286	260.54	274.20	261.94	251.83	243.01	285	259.65	276.32	259.23	250.30	242.47
19	47	49	287	260.22	275.89	259.55	251.25	242.77	288	260.24	273.13	250.65	251.53	242.61
19	48	0	285	258.51	277.17	258.41	249.93	241.92	287	257.43	275.26	256.41	248.35	242.16
19	48	13	288	259.83	273.76	259.31	251.14	243.43	287	259.58	273.93	259.59	256.37	242.93
19	48	25	287	257.97	272.74	257.39	249.42	242.21	287	256.61	277.17	257.71	249.31	241.44
19	48	37	288	253.90	272.11	252.68	245.97	240.37	285	258.90	279.30	259.54	251.30	242.72
19	48	57	283	259.29	277.75	258.95	251.07	243.03	287	259.79	273.63	260.14	251.50	242.98
19	49	9	285	258.53	275.25	257.18	250.31	242.72	286	258.92	275.26	258.00	251.00	243.25
19	49	21	284	261.73	285.74	264.72	254.03	243.75	286	261.25	282.29	262.99	253.36	243.56
19	49	32	287	251.47	273.49	262.56	253.13	244.22	288	260.73	277.74	260.44	252.34	243.68
19	49	45	287	260.46	277.68	260.74	252.45	243.73	284	255.33	260.55	251.21	247.28	242.50
19	49	59	286	257.01	267.36	254.11	248.90	243.01	288	257.77	273.29	256.31	250.14	243.26
19	50	11	289	254.34	259.74	254.11	247.27	242.47	286	254.20	253.16	250.80	247.25	242.67
19	50	23	287	255.32	261.45	251.67	247.73	242.65	286	255.65	261.03	252.19	248.09	242.94
19	50	35	287	253.86	268.14	259.86	247.41	241.58	286	259.10	254.09	245.57	242.32	240.15
19	50	51	285	247.07	252.15	243.91	241.23	239.22	288	247.39	251.14	244.40	242.45	239.30
19	51	3	289	240.00	251.61	245.97	243.27	240.37	285	249.62	253.34	246.06	243.09	240.54
19	51	15	286	248.16	252.16	244.95	242.50	239.94	286	245.52	253.54	246.19	243.38	240.72
19	51	27	287	249.93	255.16	247.33	244.14	240.96	287	248.61	255.07	245.50	242.32	240.16
19	51	39	285	249.80	253.57	246.32	244.07	240.93	288	245.84	252.94	246.53	244.14	240.87
19	51	51	286	248.42	251.66	245.20	243.15	240.36	288	248.27	251.60	244.83	243.33	240.22
19	52	3	288	249.11	252.94	245.73	243.62	240.63	280	247.35	252.31	246.49	244.23	240.99
19	52	15	287	251.14	256.67	248.23	245.57	241.63	295	251.74	259.01	248.82	245.78	241.67
19	52	27	286	250.74	256.39	247.62	245.12	241.35	286	249.82	253.79	246.71	244.48	240.93
19	52	39	284	248.91	251.43	245.60	243.41	240.43	286	248.70	251.43	245.56	243.41	240.82
19	52	51	285	247.98	251.61	244.42	243.23	240.35	285	247.40	251.38	243.33	242.31	239.79
19	53	3	287	245.72	243.71	247.16	241.35	239.13	288	245.83	247.36	242.71	241.55	239.20
19	53	15	287	244.96	247.44	242.45	240.95	238.88	289	244.99	247.07	240.60	239.30	238.27
19	53	27	284	243.93	246.89	240.76	237.65	238.23	286	243.45	246.73	240.86	239.36	238.03
19	53	39	285	245.59	244.41	247.29	241.33	238.88	288	245.63	243.01	242.30	241.15	239.18
19	54	3	287	243.42	245.22	240.51	238.77	238.03	286	243.38	245.71	243.16	239.37	237.74
19	54	15	286	243.06	246.25	239.81	238.44	237.53	286	245.09	248.74	242.08	240.37	238.63
19	54	27	285	247.02	251.74	244.19	242.54	239.32	286	246.37	250.04	243.55	242.12	239.13
19	54	39	287	246.55	243.59	243.18	242.22	239.32	286	246.22	243.48	243.45	242.35	239.38
19	54	51	287	246.82	247.45	241.42	240.59	238.44	286	245.74	243.20	242.34	241.46	238.94
19	54	59	286	245.16	247.44	241.66	241.00	238.57	288	245.21	247.73	242.33	241.41	238.86
19	55	0	287	243.67	245.91	240.61	240.21	237.96	285	242.53	245.17	239.16	239.46	237.28
19	55	12	284	242.11	244.60	232.48	238.99	237.11	287	242.47	244.74	239.84	239.11	237.42
19	55	24	286	242.42	244.01	239.48	238.21	237.27	287	242.48	245.03	239.73	239.23	237.33
19	55	36	283	243.74	247.16	242.55	240.14	237.90	287	244.96	246.24	242.33	240.94	239.19
19	55	48	286	246.11	249.47	247.63	242.73	239.38	285	246.91	250.31	244.43	243.55	239.57
19	55	59	287	247.27	250.49	244.54	243.35	239.37	289	247.63	250.39	244.57	243.00	240.00
19	56	3	289	247.87	251.42	244.18	243.11	239.73	287	247.82	251.63	244.46	243.28	239.79
19	56	15	286	247.44	251.25	245.13	244.60	240.01	286	247.79	251.61	244.97	243.71	239.91
19	56	27	285	248.08	251.44	245.43	244.35	240.94	285	247.33	251.53	244.44	243.45	239.73
19	56	39	287	246.82	243.93	242.34	243.11	239.43	286	247.05	243.91	244.43	243.47	239.29
19	56	51	285	245.65	243.36	243.29	243.61	239.20	287	245.94	246.96	243.32	243.74	239.30
19	56	59	286	246.52	243.85	243.35	243.45	239.46	288	247.15	250.76	244.90	244.32	240.00
19	57	0	286	247.15	251.22	244.62	244.62	240.01	286	247.11	251.92	245.39	245.53	240.33
19	57	12	285	246.90	250.82	244.11	242.61	239.59	286	247.23	250.75	244.81	244.18	240.15
19	57	24	287	247.91	251.32	244.92	244.35	240.30	287	247.82	251.46	245.35	244.29	240.53
19	57	36	284	247.39	252.53	245.31	243.91	240.06	287	247.94	249.18	243.62	241.45	242.05
19	57	48	286	244.75	247.63	241.77	243.64	238.83	286	246.82	247.01	241.92	243.57	238.81
19	57	59	283	245.24	247.74	242.10	240.22	239.13	288	249.45	249.93	242.17	243.26	239.08
19	58	3	285	245.84	248.53	244.14	242.61	239.34	285	245.84	248.14	242.61	242.18	239.34
19	58	15	284	246.11	249.47	247.63	242.73	239.38	287	246.64	247.17	241.88	241.31	238.36
19	58	27	286	247.27	250.49	244.54	243.35	239.37	287	247.62	251.14	244.58	244.11	240.08
19	58	39	285	248.08	251.44	245.43	244.35	240.94	286	248.01	250.26	243.90	242.99	239.42
19	58	51	284	247.39	252.53	245.31	243.91	240.06	286	248.41	252.54	245.66	244.32	240.28
19	58	59	285	246.55	243.36	243.29	243.61	239.20	286	247.44	250.76	245.11	243.72	239.99
19	59	0	286	246.52	243.93	242.34	243.11	239.43	287	246.00	248.93	243.01	242.54	239.36
19	59	12	285	245.65	243.36	243.29	243.61	239.20	287	246.58	249.43	243.92	244.10	239.60
19	59	24	286	246.52	243.85	243.35	243.45	239.46	288	247.26	250.96	244.19	244.50	239.85
19	59	36	284	247.39	252.53	245.31	243.91	240.06	285	247.47	250.99	245.10	245.10	239.92
19	59	48	286	248.01	251.32	244.92	244.35	240.30	286	248.27	251.43	245.63	244.06	240.33
19	59	59	287	248.93	255.16	247.33	244.14	240.96	286	248.01	250.26	243.90	242.99	239.42
20	0	3	285	247.98	251.61	244.42	243.23	240.35	286	248.73	251.63	244.97	243.71	239.91
20	0	15	286	248.75	247.63	241.77	243.64	238.83	286	248.41	249.93	242.17	243.26	239.08
20	0	27	284	245.24	247.74	242.10	240.22	239.13	286	248.01	249.93	242.17	243.26	239.08
20	0	39	285	245.84	248.53	244.14	242.61	239.34	285	245.84	248.14	242.61	242.18	239.34
20	0	51	284	246.11	249.47	247.63	242.73	239.38	287	246.64	247.17	241.88	241.31	238.36
20	0	59	286	247.27	250.49	244.54	243.35	239.37	287	247.62	251.14	244.58	244.11	240.08
20	1	0	285	248.08	251.44	245.43	244.35	240.94	287	247.67	251.57	245.58	244.26	240.22
20	1	12	284	247.39	252.53	245.31	243.91	240.06	288	249.90	248.34	243.31	243.55	239.50
20	1	24	286	244.75	247.63	241.77	243.64	238.83	287	249.90	248.34	243.31	243.55	239.50
20	1	36	283	245.24	247.74	242.10	240.22	239.13	287	248.01	249.93	242.17	243.26	239.08
20	1	48	285	245.84	248.53	244.14	242.61	239.34	287	248.01	249.93	242.17	243.26	239.08
20	1	59	284	246.11	249.47	247.63	242.73	239.38	287	248.01	249.93	242.17	243.26	239.08
20</														

HR	MN	SC	ALT	I1	I2	I3	I4	I5	ALT	I1	I2	I3	I4	I5	ALT	I1	I2	I3	I4	I5
20	10	55	287	248.82	251.64	246.91	244.52	241.53	287	248.70	251.79	246.23	244.41	241.29	285	249.51	253.14	247.50	245.36	241.98
20	11	7	285	249.25	252.42	246.83	244.95	241.71	287	249.22	252.53	247.19	244.37	241.82	285	249.19	252.43	246.97	244.68	241.55
20	11	19	287	249.32	252.53	247.93	245.23	241.93	288	248.78	252.36	246.78	244.76	241.39	285	249.15	252.45	247.21	244.91	241.74
20	11	31	287	249.69	253.79	247.78	245.23	241.33	286	249.74	253.61	247.79	245.56	241.87	286	249.68	253.58	247.45	245.31	241.69
20	11	43	287	249.74	253.69	248.32	245.42	241.85	285	249.45	253.95	249.11	246.56	241.97	288	249.25	253.07	246.99	244.79	241.58
20	11	55	286	249.72	253.53	248.06	245.47	241.99	287	249.51	253.20	247.43	245.14	241.60	289	249.64	253.95	247.92	245.52	241.91
20	12	7	289	249.23	253.74	247.91	245.25	241.74	288	248.91	253.20	247.14	244.31	241.50	286	248.82	253.17	247.09	244.80	241.62
20	12	19	285	248.50	252.71	246.94	245.57	241.13	286	248.34	252.21	246.63	244.34	240.99	283	248.27	252.01	246.69	244.43	241.03
20	12	31	285	248.91	252.69	246.95	244.67	241.17	287	248.86	253.15	246.93	244.34	241.38	287	248.44	252.99	246.34	244.28	240.93
20	12	43	287	248.81	252.79	246.77	244.31	241.00	289	247.95	251.24	245.83	243.40	240.63	287	248.32	251.85	246.58	244.21	241.09
20	12	55	286	248.10	251.81	246.51	244.17	240.77	288	248.84	252.96	247.18	244.75	241.09	285	248.83	252.99	246.59	244.43	240.89
20	13	7	286	248.57	252.84	247.32	244.71	240.37	287	248.40	252.47	246.19	243.33	240.63	285	247.93	251.95	246.46	244.07	240.50
20	13	19	286	247.11	251.88	246.31	243.13	239.94	288	247.08	250.42	245.01	242.39	239.80	287	247.48	251.84	245.52	243.30	239.96
20	13	31	286	247.38	251.41	245.39	243.11	239.71	286	246.82	251.23	244.61	242.64	239.39	286	246.33	249.33	244.56	242.37	239.19
20	13	43	287	245.26	244.84	243.32	241.48	238.49	288	245.25	248.22	243.47	241.28	238.53	285	245.36	248.40	243.18	241.23	238.56
20	13	55	283	248.90	247.77	242.95	240.83	238.27	287	244.90	246.12	242.73	240.34	238.43	285	244.81	247.67	242.72	240.92	238.34
20	14	7	287	245.36	243.81	243.60	241.23	238.40	287	245.36	243.81	243.60	241.23	238.40	287	245.67	249.08	244.12	241.94	239.06
20	14	19	288	245.34	243.65	242.24	241.51	238.59	286	245.34	243.85	243.22	241.43	238.66	283	245.70	249.07	244.61	241.68	238.74
20	14	31	287	245.73	243.01	243.06	241.73	238.86	289	245.79	243.57	243.28	241.33	239.54	286	245.42	248.17	243.89	241.54	238.64
20	14	43	287	244.48	242.33	242.58	240.61	237.96	286	245.35	243.99	243.27	241.33	239.53	286	244.69	247.86	242.53	240.74	237.68
20	14	55	287	244.20	242.12	242.00	240.13	237.96	287	244.20	242.12	241.91	240.08	237.95	285	244.20	247.00	242.13	240.07	237.56
20	15	7	287	242.64	246.77	241.05	239.71	237.33	287	242.64	246.77	241.76	239.41	237.09	286	243.19	245.83	240.72	239.23	237.01
20	15	19	287	242.65	246.42	240.74	239.71	236.91	287	242.03	244.39	239.66	238.30	236.34	287	242.30	244.82	240.03	238.54	236.59
20	15	31	285	242.05	244.62	239.58	238.25	236.59	285	242.16	244.38	239.87	238.42	236.44	286	242.49	245.22	240.47	238.84	236.69
20	15	43	288	242.25	244.77	240.91	239.43	237.18	286	242.80	245.31	240.86	239.14	237.16	287	242.83	245.07	240.45	238.94	236.85
20	15	55	288	242.12	244.99	240.91	239.43	237.18	286	242.05	245.31	240.86	239.14	237.16	288	242.65	245.21	240.89	239.06	237.00
20	16	7	284	242.03	244.44	241.02	238.45	236.59	286	242.01	243.11	238.75	237.39	235.74	287	242.18	244.99	240.26	238.72	236.88
20	16	19	285	242.32	244.44	238.42	236.59	236.59	288	242.73	245.09	240.59	238.42	236.85	287	242.29	244.54	239.96	238.79	236.69
20	16	31	285	241.73	243.90	239.48	238.45	236.59	285	240.84	243.93	238.22	237.41	235.72	287	241.55	243.68	239.33	237.91	236.27
20	16	43	287	241.16	243.22	238.57	237.45	235.89	286	241.82	244.31	239.85	238.21	236.49	286	241.45	243.65	239.06	238.01	236.22
20	16	55	287	241.82	244.19	239.44	238.42	236.46	286	241.34	243.39	239.19	238.00	236.05	287	241.21	243.44	239.39	237.89	236.33
20	17	7	285	240.45	242.40	234.11	237.14	235.49	288	240.39	242.62	238.14	236.37	235.49	290	240.28	242.43	238.07	237.04	235.48
20	17	19	285	240.28	242.14	238.25	237.00	235.52	287	240.44	242.76	238.35	237.13	235.73	289	240.28	242.25	237.96	236.74	235.37
20	17	31	286	239.63	241.19	237.76	236.30	234.96	286	239.75	240.44	235.25	233.42	232.26	285	239.63	242.11	238.14	236.66	235.34
20	17	43	287	239.64	241.20	237.49	236.51	235.17	287	239.59	241.42	237.64	236.31	235.21	285	239.45	239.69	236.23	235.41	234.19
20	17	55	283	238.26	239.65	235.61	234.35	233.93	286	238.12	238.65	233.24	235.37	234.22	287	238.10	240.00	235.85	235.23	234.36
20	18	7	284	238.94	241.49	236.76	235.33	234.73	288	238.88	240.21	236.96	235.33	234.98	288	238.89	239.47	236.68	235.69	234.83
20	18	19	285	238.78	240.19	236.24	235.55	234.83	287	238.37	239.73	235.94	235.42	234.61	286	239.11	240.51	236.46	235.86	235.08
20	18	31	289	239.44	241.10	237.14	236.33	235.50	286	239.74	239.47	236.20	235.31	234.77	289	239.35	240.52	237.33	236.46	235.29
20	18	43	286	239.21	241.30	236.81	236.25	235.15	286	239.47	241.31	237.45	236.58	235.47	286	239.01	240.32	236.71	236.36	235.01
20	18	55	287	239.77	241.56	237.96	237.77	236.59	287	239.24	240.43	236.80	236.37	235.15	289	239.70	241.40	238.20	236.86	235.89
20	19	7	288	239.12	241.27	237.33	236.57	235.25	285	239.49	241.31	237.57	236.31	235.84	287	239.46	240.44	237.57	236.88	235.72
20	19	19	287	239.25	241.51	237.16	236.61	235.49	286	238.86	240.45	237.43	236.25	235.33	286	239.19	240.47	237.46	236.26	235.17
20	19	31	285	239.08	240.91	236.95	236.13	234.99	287	239.11	240.95	237.08	236.11	234.98	287	239.56	240.35	237.47	236.49	235.20
20	19	43	288	238.24	239.54	236.09	235.43	234.24	288	238.42	239.43	235.98	235.43	234.29	289	238.84	240.10	237.13	236.53	234.75
20	19	55	286	238.74	239.47	236.00	235.33	234.14	286	239.47	241.31	237.45	236.58	235.47	286	239.01	240.32	236.71	236.36	235.01
20	20	7	287	239.47	241.56	237.96	237.77	236.59	287	239.24	240.43	236.80	236.37	235.15	289	239.70	241.40	238.20	236.86	235.89
20	20	19	285	239.12	241.27	237.33	236.57	235.25	285	239.49	241.31	237.57	236.31	235.84	287	239.46	240.44	237.57	236.88	235.72
20	20	31	286	239.25	241.51	237.16	236.61	235.49	286	239.16	240.45	237.43	236.25	235.33	286	239.19	240.47	237.46	236.26	235.17
20	20	43	285	239.08	240.91	236.95	236.13	234.99	287	239.11	240.95	237.08	236.11	234.98	287	239.56	240.35	237.47	236.49	235.20
20	20	55	288	238.24	239.54	236.09	235.43	234.24	288	238.42	239.43	235.98	235.43	234.29	289	238.84	240.10	237.13	236.53	234.75
20	21	7	286	238.74	239.47	236.00	235.33	234.14	286	239.47	241.31	237.45	236.58	235.47	286	239.01	240.32	236.71	236.36	235.01
20	21	19	287	239.47	241.56	237.96	237.77	236.59	287	239.24	240.43	236.80	236.37	235.15	289	239.70	241.40	238.20	236.86	235.89
20	21	31	285	239.12	241.27	237.33	236.57	235.25	285	239.49	241.31	237.57	236.31	235.84	287	239.46	240.44	237.57	236.88	235.72
20	21	43	286	239.25	241.51	237.16	236.61	235.49	286	239.16	240.45	237.43	236.25	235.33	286	239.19	240.47	237.46	236.26	235.17
20	21	55	285	239.08	240.91	236.95	236.13	234.99	287	239.11	240.95	237.08	236.11	234.98	287	239.56	240.35	237.47	236.49	235.20
20	22	7	288	238.24	239.54	236.09	235.43	234.24												

HR	MN	SC	ALT	T1	T2	T3	T4	T5	ALT	T1	T2	T3	T4	T5
20	26	33	275	253.32	259.55	251.99	247.75	241.72	276	253.69	252.42	251.62	247.50	241.42
20	26	43	271	250.74	254.75	248.45	245.22	240.04	274	249.63	253.47	247.54	244.39	240.05
20	26	55	271	247.65	251.13	245.63	243.04	238.61	270	248.78	252.73	246.22	243.47	239.10
20	27	01	268	249.86	254.27	247.68	244.41	239.26	270	250.52	255.65	248.37	244.34	239.63
20	27	19	267	252.07	258.65	250.26	246.12	240.07	270	257.15	262.44	253.27	248.65	241.58
20	27	31	266	255.71	263.36	253.94	248.93	241.73	267	256.30	268.80	255.84	250.19	242.21
20	27	43	267	255.91	264.33	254.90	249.22	241.79	264	253.62	260.80	251.99	247.27	240.45
20	27	55	263	249.91	255.98	247.86	244.07	238.72	263	246.42	251.37	244.76	241.42	237.05
20	28	07	261	249.04	256.45	247.10	243.19	238.05	260	245.91	254.30	245.59	241.33	237.25
20	28	19	258	248.56	255.63	246.42	242.57	237.32	255	249.24	255.77	247.48	243.21	237.59
20	28	31	253	250.12	257.37	248.46	243.80	237.65	252	249.49	257.08	247.02	242.37	237.09
20	28	43	246	251.03	259.09	248.92	244.39	237.94	248	251.67	258.13	249.33	244.61	238.20
20	28	55	247	253.81	261.54	251.33	246.22	239.34	246	256.23	263.71	253.43	247.94	239.61
20	29	07	244	249.32	256.53	247.15	242.57	236.49	241	248.51	259.55	245.73	241.68	236.27
20	29	19	244	256.26	262.73	252.80	246.82	239.16	244	254.56	261.87	251.94	246.19	238.46
20	29	31	243	254.71	262.39	251.75	246.29	238.91	246	255.17	262.08	252.61	246.75	238.91
20	29	43	243	258.21	265.59	255.61	249.05	240.06	244	254.36	261.38	251.32	245.62	238.50
20	29	55	242	261.88	270.40	259.45	251.47	241.44	242	264.72	273.25	261.65	253.44	242.70
20	30	07	243	261.55	269.89	259.75	251.12	241.29	242	264.03	273.18	261.14	253.15	242.28
20	30	19	241	266.11	275.67	263.75	254.32	243.32	240	267.38	277.21	264.81	257.74	243.59
20	30	29	242	269.09	279.75	266.46	256.84	244.03	238	269.60	279.49	267.02	257.33	244.49
20	30	41	239	269.50	273.93	266.33	257.27	244.28	238	265.82	278.34	266.92	257.33	244.49
20	30	53	239	269.34	273.03	266.22	256.74	244.06	238	269.25	278.26	266.58	257.07	244.40
20	31	05	239	269.26	278.40	266.35	257.00	244.36	239	269.36	278.08	266.41	257.32	244.29
20	31	17	238	269.15	277.18	265.66	256.44	243.79	239	268.84	276.98	265.40	256.24	243.86
20	31	29	239	269.64	277.88	266.33	256.32	244.13	239	269.36	278.33	266.47	257.07	244.14
20	31	41	239	270.13	278.18	266.47	257.15	244.41	237	270.16	273.70	266.91	257.39	244.48
20	31	53	240	269.83	277.94	266.11	256.39	244.35	238	269.91	277.67	266.20	256.35	244.39
20	32	05	240	270.46	279.70	266.79	257.37	244.36	240	270.49	278.92	266.95	257.37	244.50
20	32	17	237	270.46	273.60	266.38	257.23	244.35	237	270.50	278.46	266.65	257.16	244.24
20	32	29	239	270.74	273.89	266.74	257.17	244.52	240	270.59	278.57	266.91	257.31	244.54
20	32	41	241	270.53	273.62	266.79	257.23	244.41	239	270.69	278.30	267.01	257.41	244.54
20	32	53	238	270.89	279.41	267.74	257.61	244.70	240	271.13	279.46	267.54	257.67	244.57
20	33	05	240	270.81	273.92	267.31	257.51	244.50	239	270.88	279.47	267.44	257.51	244.43
20	33	15	240	271.06	279.76	267.99	257.75	244.69	238	271.03	279.44	267.59	257.70	244.44
20	33	27	239	271.35	273.72	267.79	257.71	244.68	239	271.30	279.68	267.78	257.71	244.65
20	33	39	239	271.27	279.61	267.51	257.73	244.67	239	271.20	279.62	267.58	257.59	244.44
20	33	51	239	271.31	279.53	267.52	257.74	244.44	239	271.25	279.57	267.45	257.51	244.31
20	34	03	237	271.05	279.10	267.12	257.44	244.32	240	271.54	279.57	267.83	257.34	244.76
20	34	15	240	271.34	279.47	267.57	257.73	244.53	239	271.36	279.51	267.36	257.32	244.43
20	34	27	238	271.08	279.07	267.02	257.26	244.23	240	271.42	279.56	267.85	257.34	244.69
20	34	39	238	271.00	278.89	267.34	257.44	244.26	240	271.44	279.32	267.29	257.52	244.65
20	34	51	239	270.80	278.54	266.97	257.30	244.44	238	271.06	278.90	267.01	257.49	244.60
20	35	03	239	270.88	278.75	266.77	257.25	244.31	238	270.89	278.30	267.14	257.43	244.39
20	35	15	239	271.23	279.41	267.26	257.45	244.49	237	271.61	279.11	267.94	257.91	244.61
20	35	27	239	271.54	280.26	267.97	257.80	244.77	239	271.19	279.44	267.49	257.28	244.18
20	35	39	239	271.39	279.94	267.46	257.57	244.60	239	271.33	279.54	267.59	257.71	244.49
20	35	51	239	271.50	273.73	267.22	257.42	244.72	238	271.19	279.47	267.23	257.54	244.18
20	36	03	238	271.24	279.39	267.43	257.48	244.39	238	271.12	279.41	267.65	257.59	244.28
20	36	15	240	271.26	279.42	267.66	257.65	244.52	239	271.15	279.41	267.11	257.27	244.39
20	36	27	239	270.75	278.74	267.94	257.14	244.16	238	271.03	278.84	267.22	257.36	244.62
20	36	39	239	270.89	278.75	267.28	257.41	244.63	237	270.71	278.60	266.78	257.11	244.33
20	36	51	239	270.77	278.47	266.42	257.21	244.29	239	270.80	278.96	267.21	257.57	244.61
20	37	03	238	270.73	278.93	267.17	257.37	244.45	237	270.68	279.06	267.08	257.24	244.37
20	37	15	239	270.61	279.21	267.21	257.24	244.52	237	270.58	279.20	267.21	257.57	244.49
20	37	27	240	270.62	279.13	267.22	257.57	244.64	239	270.54	279.07	267.04	257.29	244.41
20	37	39	239	270.48	278.97	267.13	257.25	244.46	239	270.64	279.27	267.45	257.57	244.68
20	37	51	239	270.60	279.42	267.52	257.71	244.71	239	270.44	278.95	267.21	257.18	244.42
20	38	03	239	270.52	279.21	267.27	257.45	244.55	239	270.55	279.09	267.31	257.41	244.51
20	38	15	240	270.66	279.15	267.60	257.63	244.72	238	270.56	278.78	267.06	257.32	244.41
20	38	27	240	270.69	278.96	267.20	257.42	244.51	238	270.62	278.86	267.20	257.59	244.40
20	38	39	241	270.83	278.63	267.35	257.55	244.64	237	270.78	278.47	266.94	257.31	244.47
20	38	51	239	270.77	278.65	267.23	257.47	244.51	238	270.85	278.74	267.06	257.38	244.46
20	39	03	239	270.48	278.74	267.03	257.27	244.32	239	270.59	278.70	267.35	257.30	244.45
20	39	15	239	270.81	278.73	267.41	257.55	244.45	239	270.76	279.03	267.17	257.33	244.58
20	39	27	240	270.66	278.92	267.33	257.64	244.68	238	270.49	278.57	266.90	257.25	244.30
20	39	39	239	270.56	279.04	267.00	257.27	244.43	237	267.30	274.78	265.09	256.43	244.44
20	39	51	238	267.00	274.43	264.31	255.55	243.64	238	266.93	274.41	264.12	256.50	243.67
20	40	03	239	267.43	275.02	264.17	256.34	243.86	238	267.06	274.53	263.65	254.90	243.45
20	40	15	239	266.89	274.43	263.58	254.91	243.37	240	267.17	274.76	263.60	254.93	243.53
20	40	27	239	267.26	274.87	264.03	255.26	243.62	239	267.22	274.33	263.29	254.70	243.25
20	40	39	238	267.05	273.51	262.99	254.44	243.16	239	267.14	273.60	263.14	254.64	243.39
20	40	51	241	267.27	274.10	263.35	254.84	243.56	241	267.09	273.49	262.89	254.59	243.17
20	41	03	242	267.17	273.91	263.13	254.69	243.21	243	267.60	273.19	263.48	255.39	243.72
20	41	15	244	267.44	273.82	263.47	255.15	243.76	243	267.21	273.24	262.89	254.82	243.50
20	41	27	243	267.41	273.34	262.82	254.73	243.56	244	267.51	273.72	263.48	255.08	243.97
20	41	39	246	267.61	273.63	263.23	255.02	243.83	246	267.62	273.95	263.73	255.19	243.88
20	41	51	245	267.56	273.61	263.49	255.23	244.09	247	267.40	273.79	263.29	255.12	244.08
20	42	03	246	267.67	273.65	263.67	255.43	244.17	247	267.58	273.42	263.43	255.13	243.96
20	42	15	247	267.62	273.52	263.47	255.24	243.97	247	267.62	273.47	263.68	255.47	24

HR	MN	SC	ALT	T1	T2	T3	T4	T5	ALT	T1	T2	T3	T4	T5	ALT	T1	T2	T3	T4	T5
21	3	25	264	266.95	278.36	265.71	256.67	245.03	261	266.10	277.64	264.85	256.16	244.67	261	266.42	277.74	265.37	256.50	245.00
21	3	37	261	268.25	277.16	264.79	256.06	244.77	261	266.48	277.71	265.34	256.33	244.96	261	266.63	278.90	265.67	256.66	245.08
21	3	49	262	266.67	273.41	265.74	256.57	244.96	261	266.60	278.42	265.41	256.43	244.75	260	266.80	278.63	265.82	256.67	244.91
21	4	0	262	268.67	273.55	265.67	256.50	244.79	260	266.81	278.54	265.71	256.71	244.97	262	266.82	278.60	265.69	256.51	244.92
21	4	13	262	266.89	278.54	265.89	256.75	245.04	262	266.58	278.25	265.51	256.46	244.74	263	266.86	278.86	265.96	257.02	245.19
21	4	25	263	266.44	278.55	265.37	256.44	244.73	261	266.95	278.85	265.90	256.89	245.20	262	266.83	278.52	265.61	256.51	244.85
21	4	37	262	266.94	278.36	265.46	256.71	244.97	262	266.87	277.87	265.34	256.46	244.97	261	266.42	276.74	264.49	256.10	244.85
21	4	49	261	268.52	276.94	264.68	256.11	244.92	259	266.67	277.12	264.86	256.25	245.14	262	266.50	276.96	264.67	256.16	244.84
21	5	9	262	266.77	276.93	264.96	256.38	245.21	263	266.30	275.78	264.11	255.89	244.78	264	266.49	275.82	264.28	255.96	245.04
21	5	10	262	268.19	275.45	263.88	255.78	244.87	261	266.77	276.16	264.63	256.42	245.40	262	266.27	275.16	263.83	255.67	244.79
21	5	23	261	266.44	275.20	264.19	255.98	245.27	261	266.13	275.40	263.93	255.67	244.77	261	266.41	275.87	264.19	256.07	245.13
21	5	35	262	268.17	275.99	263.96	255.73	244.76	260	266.40	276.05	264.51	256.19	244.97	263	266.17	275.22	263.66	255.60	244.67
21	5	47	261	266.85	276.82	264.92	256.35	245.11	262	266.77	277.41	264.90	256.16	244.90	262	266.06	278.33	265.63	256.69	245.24
21	5	59	262	267.38	277.94	265.60	256.74	244.97	263	267.15	278.08	265.40	256.52	244.95	264	266.94	276.53	265.00	256.48	245.15
21	6	10	261	266.41	274.40	263.52	255.70	244.67	261	266.59	274.21	264.12	256.14	245.07	263	266.17	273.20	263.33	255.48	244.60
21	6	23	262	268.45	274.17	263.84	255.79	245.05	260	266.22	273.93	263.42	255.62	244.94	264	266.33	273.67	263.61	255.82	244.99
21	6	35	261	266.44	273.49	263.60	255.75	244.99	263	266.38	273.97	263.69	255.87	245.06	262	266.43	274.08	263.60	255.69	244.98
21	6	47	263	268.47	274.34	263.76	255.84	244.74	261	266.37	274.50	263.86	255.88	244.80	261	266.48	275.07	264.21	256.13	245.08
21	6	59	262	266.85	275.11	264.56	256.35	245.20	261	266.70	275.90	264.60	256.20	244.90	263	266.89	275.74	265.08	256.36	245.12
21	7	10	261	268.57	275.52	264.62	256.11	244.84	263	267.18	275.97	265.04	256.62	245.24	261	267.06	276.13	264.96	256.49	245.17
21	7	23	262	267.05	275.77	264.91	256.46	245.09	262	266.68	275.18	264.57	256.18	244.98	263	267.07	275.82	264.76	256.39	244.96
21	7	35	261	267.04	275.77	265.08	256.63	245.10	261	266.94	275.49	264.62	256.11	244.85	261	267.06	276.14	264.91	256.28	245.06
21	7	47	261	266.92	275.74	264.79	256.34	245.04	262	266.92	275.99	264.80	256.28	244.90	260	267.19	276.61	264.87	256.31	244.86
21	7	59	262	267.28	275.57	264.88	256.35	244.92	260	267.02	275.47	264.60	256.25	244.89	261	267.37	276.06	265.05	256.60	245.14
21	8	10	260	267.05	275.80	264.86	256.21	244.88	269	267.45	275.83	265.21	256.63	245.17	261	267.35	275.76	264.97	256.41	245.06
21	8	20	262	267.17	276.06	264.88	256.35	245.01	263	267.29	275.88	265.12	256.52	245.17	261	267.11	276.61	264.76	256.22	244.90
21	8	33	261	267.34	275.85	265.10	256.36	245.09	261	267.34	276.00	264.97	256.46	245.03	260	267.26	275.49	264.72	256.30	244.82
21	8	45	263	267.37	275.82	265.05	256.53	245.05	263	267.47	275.78	265.22	256.47	245.09	261	267.30	275.54	264.64	256.30	244.87
21	8	57	261	267.62	275.92	265.22	256.43	245.34	262	267.36	275.62	264.64	256.21	244.94	261	267.46	275.57	264.74	256.32	245.01
21	9	8	261	267.58	275.91	265.16	256.64	245.24	261	267.38	275.52	265.01	256.40	244.95	262	267.42	275.65	264.86	256.43	245.02
21	9	20	261	267.40	275.65	264.86	256.51	245.20	263	267.77	276.17	265.33	256.73	245.37	262	267.30	275.72	264.87	256.26	244.94
21	9	33	261	267.45	275.94	265.14	256.67	245.36	263	267.43	275.69	264.86	256.37	245.10	261	267.57	275.75	265.18	256.62	245.19
21	9	45	261	267.48	275.75	265.07	256.42	245.17	262	267.62	275.68	265.07	256.46	245.14	260	267.33	275.51	264.71	256.26	244.85
21	9	57	262	267.57	276.17	265.25	256.73	245.42	261	267.25	275.45	264.82	256.20	244.85	261	267.67	275.65	265.08	256.45	245.22
21	10	8	263	267.34	275.69	264.76	256.27	245.07	262	267.54	275.48	265.07	256.58	245.20	261	267.57	275.65	264.61	256.30	245.01
21	10	20	261	267.56	276.21	265.20	256.91	245.33	262	267.60	275.27	264.43	256.24	244.76	262	267.53	275.74	265.17	256.63	245.27
21	10	33	262	267.63	275.68	265.08	256.60	245.45	262	267.55	275.67	265.23	256.71	245.37	262	267.39	275.48	264.82	256.45	245.14
21	10	45	261	267.57	275.79	265.33	256.95	245.39	262	267.39	275.63	264.71	256.28	244.91	262	267.74	276.08	265.32	256.62	245.33
21	10	57	262	267.37	275.87	264.92	256.59	245.19	262	267.21	275.64	264.80	256.59	245.10	260	267.28	275.69	264.79	256.45	245.20
21	11	9	263	267.39	275.82	265.21	256.74	245.29	262	267.18	275.93	264.75	256.43	245.07	262	267.60	276.52	265.37	256.87	245.48
21	11	20	261	267.32	275.98	264.87	256.45	245.02	261	267.22	275.68	265.06	256.48	245.13	262	267.21	276.30	264.97	256.30	245.10
21	11	33	261	267.09	275.98	265.17	256.65	245.17	262	267.13	276.20	264.76	256.48	245.10	262	267.47	276.35	265.29	256.63	245.32
21	11	45	262	267.17	276.59	264.88	256.23	245.07	262	267.45	276.46	265.37	256.65	245.22	262	267.54	276.83	265.39	256.76	245.25
21	11	57	261	267.41	276.50	265.24	256.53	245.13	260	267.28	276.35	265.06	256.53	245.14	261	267.53	277.37	265.61	256.80	245.16
21	12	7	262	267.48	277.81	265.63	256.73	245.16	262	267.46	277.64	265.78	256.71	245.16	263	267.46	278.18	265.87	256.86	245.38
21	12	19	263	267.35	277.14	265.63	256.70	244.99	260	267.29	278.06	265.69	256.71	245.07	263	267.11	276.99	265.46	256.59	245.02
21	12	31	262	267.08	276.88	264.85	256.35	244.95	262	267.33	276.82	265.33	256.55	245.10	263	267.07	276.85	264.93	256.30	244.69
21	12	43	262	267.27	277.09	265.32	256.55	245.02	262	267.12	277.57	265.28	256.37	244.94	262	267.42	277.40	265.27	256.65	245.13
21	12	55	261	267.39	277.32	265.27	256.38	244.96	262	267.47	277.83	265.39	256.63	245.25	261	267.34	277.70	265.32	256.43	244.88
21	13	7	262	267.73	278.26	265.99	256.89	245.28	261	267.50	278.34	265.71	256.67	244.87	261	267.77	278.76	265.82	256.86	245.36
21	13	19	261	267.71	278.76	265.96	256.36	245.30	262	267.65	278.53	265.98	256.32	245.16	261	267.56	279.00	265.67	256.76	245.10
21	13	31	260	267.77	278.90	266.11	256.07	245.39	262	267.57	279.06	266.02	257.00	245.17	262	267.90	279.01	266.01	256.97	245.26
21	13	43	262	268.07	279.29	266.04	257.02	245.23	260	267.94	279.00	265.83	256.33	245.19	264	267.99	279.04	266.06	257.05	245.29
21	13	55	267	267.82	278.81	266.04	256.88	245.05	263	268.11	279.14	266.66	257.28	245.47	264	267.67	278.92	265.81	256.91	245.06
21	14	7	262	267.95	278.99	266.18	257.27	245.36	261	267.74	279.24	266.20	257.19	245.25	261	267.90	278.82	266.20	257.04	245.14
21	14	19	260	267.85	279.17	266.04	257.06	245.22	261	268.13	279.12	266.55	257.30	245.35	263	267.58	278.98	265.86	256.64	245.03
21	14	31	262	268.07	279.00	266.22	257.12	245.58	262	267.70	278.58	265.								

FLIGHT NO 7 6/ 12/ 70

Table with columns: HR MN SC, ALT, T1, T2, T3, T4, T5, ALT, T1, T2, T3, T4, T5, ALT, T1, T2, T3, T4, T5. Contains flight data for 24 hours from 21:23:13 to 21:44:57.

HR	MIN	SC	ALT	T1	T2	T3	T4	T5	ALT	T1	T2	T3	T4	T5	ALT	T1	T2	T3	T4	T5
21	45	8	263	271.13	281.42	268.75	260.12	249.45	260	270.93	283.08	258.84	260.13	248.51	262	270.62	279.84	268.72	259.99	248.32
21	45	9	261	270.66	279.64	268.43	259.82	249.23	262	270.45	273.89	268.52	259.33	248.29	262	270.45	279.43	268.42	259.74	248.26
21	45	31	261	270.14	279.45	268.23	259.53	249.24	262	270.28	273.33	268.26	259.73	248.81	262	269.69	278.81	267.78	259.19	247.88
21	45	43	261	268.53	277.53	267.09	258.67	247.83	262	267.29	276.50	266.32	257.71	247.05	263	268.47	277.67	266.80	258.58	247.90
21	45	55	261	268.19	277.21	266.62	258.43	247.50	262	267.15	276.41	265.92	258.25	247.40	262	267.15	277.61	265.78	257.71	247.11
21	46	7	262	267.15	275.63	265.95	257.92	247.21	263	267.94	277.35	266.79	258.45	247.56	262	268.15	277.53	267.22	258.61	247.74
21	46	19	261	267.57	277.79	266.71	258.24	247.34	263	267.59	277.39	266.64	258.37	247.34	263	265.73	275.35	264.64	256.92	246.77
21	46	31	261	266.94	276.77	265.84	257.73	247.21	262	267.13	276.93	266.96	257.77	247.13	262	267.57	277.62	266.92	258.36	247.49
21	46	43	261	267.99	278.19	266.47	258.91	247.61	263	267.07	280.16	266.33	259.34	248.28	261	268.44	279.36	267.48	258.99	247.70
21	46	55	260	268.80	279.78	265.29	259.43	248.95	262	268.24	279.15	267.51	258.38	247.74	261	265.11	275.13	264.43	256.64	246.41
21	47	7	260	268.89	269.60	264.96	257.32	248.69	262	265.25	267.92	258.24	252.36	244.48	262	265.63	266.46	257.36	251.84	244.34
21	47	19	262	268.64	265.72	267.65	261.33	249.22	262	263.03	267.21	268.43	262.39	244.71	263	263.44	268.14	268.66	262.50	244.75
21	47	31	262	261.34	277.36	260.75	258.38	249.46	263	263.03	267.21	268.43	262.39	244.71	263	264.02	273.48	268.63	256.04	246.58
21	47	43	262	266.58	277.07	265.84	258.33	247.74	262	266.51	276.48	266.19	258.16	247.57	262	265.35	275.60	264.81	257.19	247.10
21	47	55	262	266.98	277.41	265.99	258.23	247.51	262	268.66	280.08	268.62	259.43	248.56	262	267.89	279.48	267.61	259.02	247.90
21	48	7	262	267.44	278.58	267.36	259.32	247.91	261	267.84	273.79	267.76	259.29	248.17	260	267.58	278.34	267.39	258.87	247.93
21	48	19	262	268.03	279.66	264.14	259.51	248.06	263	267.81	278.98	267.56	259.14	248.30	263	265.92	276.25	265.35	257.46	247.21
21	48	29	262	263.69	273.12	262.59	255.32	245.38	261	262.18	271.79	261.55	254.44	245.73	263	264.42	274.85	263.77	256.20	246.71
21	48	41	261	266.33	277.66	265.29	258.08	247.53	261	267.35	273.25	267.35	259.33	248.15	264	267.77	280.17	268.03	259.37	248.30
21	48	53	261	267.64	279.71	267.55	259.16	248.59	263	268.09	280.11	269.95	259.43	249.66	261	267.90	280.02	268.19	259.53	248.37
21	49	4	262	267.05	280.33	264.17	259.47	248.59	263	267.74	283.21	267.99	259.40	248.36	261	267.57	279.09	267.37	259.24	248.23
21	49	17	260	267.57	279.42	267.12	259.21	248.10	261	267.82	281.75	268.30	259.31	243.52	260	268.00	280.23	268.23	259.68	248.35
21	49	29	263	268.13	279.79	264.14	259.74	248.62	263	268.29	273.29	267.96	259.69	248.72	262	268.39	279.98	268.59	259.68	248.64
21	49	41	262	268.26	279.66	267.17	259.55	248.46	262	268.74	273.55	268.19	259.75	248.56	262	268.12	280.02	268.03	259.53	248.37
21	49	53	262	268.63	280.35	264.31	259.66	248.60	263	268.23	280.42	268.69	259.31	248.50	261	268.14	280.23	268.25	259.78	248.59
21	50	5	262	268.07	280.11	263.65	259.71	248.53	262	268.00	273.58	267.99	259.43	249.39	261	267.95	278.87	267.66	259.33	248.40
21	50	17	261	268.06	278.71	267.64	259.41	248.43	261	267.92	279.24	267.44	259.36	248.34	261	267.45	277.81	266.75	258.64	247.88
21	50	29	263	268.82	277.12	265.20	258.32	247.89	261	266.21	275.94	265.73	257.19	247.61	260	266.45	276.88	265.96	258.22	247.71
21	50	41	263	268.06	278.63	267.77	259.44	248.60	262	268.32	273.11	267.11	259.36	248.39	261	268.45	279.98	268.58	259.94	248.81
21	50	53	261	269.64	281.15	268.10	262.13	248.83	262	265.04	281.23	263.01	260.31	243.83	262	268.41	280.12	268.49	259.91	248.74
21	51	4	263	267.68	277.05	266.49	259.33	248.63	262	267.50	277.59	266.44	258.72	249.36	261	267.30	277.97	266.86	259.08	248.67
21	51	17	261	268.12	278.55	265.20	257.82	248.07	262	265.66	274.49	264.69	257.52	247.92	262	267.03	277.17	266.28	258.69	248.32
21	51	29	263	266.73	278.75	265.46	258.31	248.36	262	266.69	273.38	264.67	258.33	248.43	262	268.48	278.37	267.92	259.68	248.79
21	51	41	263	268.55	273.29	268.06	255.82	248.69	260	265.92	276.16	266.11	258.37	248.35	261	265.89	273.47	264.57	257.70	248.09
21	51	51	261	265.79	272.71	264.39	257.82	248.13	261	265.55	274.21	266.22	258.23	248.49	262	266.57	274.90	265.38	258.26	248.23
21	52	3	262	266.93	275.13	265.76	258.43	248.63	260	264.43	274.83	265.26	258.27	248.36	261	266.61	274.45	265.41	258.36	248.47
21	52	15	261	266.41	273.95	265.03	258.01	248.28	260	267.08	273.46	265.84	258.47	248.70	260	267.19	276.74	266.01	258.69	248.48
21	52	27	262	267.37	277.11	265.57	258.03	248.59	262	266.84	276.11	265.92	258.35	248.35	262	267.89	278.29	267.30	259.34	248.80
21	52	39	262	267.06	278.33	267.21	259.15	248.62	261	268.94	279.37	268.81	260.23	249.18	262	268.39	280.18	268.33	259.91	248.77
21	52	51	262	269.51	281.15	268.13	263.03	248.99	261	269.49	280.34	269.08	260.38	249.98	262	269.40	281.61	269.53	260.62	249.21
21	53	3	263	267.06	277.87	267.65	259.44	248.71	263	267.46	277.26	266.73	259.27	249.71	263	266.83	277.13	266.37	258.88	248.46
21	53	15	263	266.84	275.74	266.18	258.31	248.82	263	265.99	275.26	268.39	258.33	248.33	261	265.45	274.75	264.37	257.56	248.03
21	53	27	263	265.12	275.31	264.91	257.12	247.87	260	265.11	272.32	263.37	257.15	247.92	262	264.48	274.16	263.93	256.33	247.30
21	53	39	262	264.58	278.49	265.85	256.67	247.86	261	264.81	274.55	264.82	258.35	247.33	260	265.01	273.67	262.95	256.97	247.80
21	53	51	262	268.80	276.24	265.87	258.23	248.74	261	265.17	274.59	264.46	258.11	248.00	264	265.83	276.96	265.83	258.36	248.19
21	54	3	262	266.75	273.52	267.00	259.33	248.34	261	266.55	273.42	267.27	259.20	248.63	262	265.15	273.55	265.12	257.96	247.81
21	54	15	263	265.72	273.46	265.51	258.13	248.69	261	265.14	276.92	265.75	258.27	248.63	262	263.88	273.47	264.20	257.31	247.67
21	54	27	262	260.54	263.63	260.74	254.91	246.72	261	260.54	268.15	260.35	254.41	248.48	263	261.33	268.41	261.56	255.01	246.83
21	54	39	261	261.90	272.11	262.76	256.13	246.85	262	260.30	268.94	260.18	254.35	246.31	261	260.25	267.47	261.35	254.75	246.84
21	54	51	262	268.43	266.55	268.95	263.06	248.34	262	265.28	262.98	259.12	250.12	243.26	262	265.29	264.57	255.55	250.35	243.43
21	55	0	261	268.47	268.77	265.26	249.46	248.14	262	265.61	267.38	257.02	251.22	244.00	263	265.34	265.56	255.85	250.78	243.76
21	55	13	262	264.02	261.23	264.67	248.31	242.31	261	262.62	263.18	262.31	247.32	242.15	261	262.32	269.25	262.03	247.59	241.95
21	55	25	262	263.71	262.73	263.40	244.74	242.43	262	265.68	267.16	260.78	249.95	243.75	262	266.32	268.30	258.09	251.71	243.87
21	55	37	265	266.73	263.93	261.91	244.13	244.19	262	267.13	263.47	258.65	262.34	244.62	262	267.07	270.33	259.62	253.00	244.99
21	55	49	262	267.86	269.45	264.96	252.94	248.77	262	268.94	271.98	260.11	263.67	245.64	261	269.03	271.50	260.39	253.87	245.91
21	56	0	262	260.35	274.23	262.46	256.41	246.41	261	261.26	276.24	263.76	266.41	246.95	262	261.52	272.30	262.45	255.42	246.67
21	56	4	261	269.31	268.11	269.33	263.83	246.41	263											

FLIGHT NO 7 6/ 12/ 70

HR	MIN	SC	ALT	I1	I2	I3	I4	I5	ALT	I1	I2	I3	I4	I5	ALT	I1	I2	I3	I4	I5
22 8 29	732	278.24	282.42	282.28	280.71	277.62	739	277.35	279.70	282.08	280.73	277.21	743	277.45	279.56	281.94	280.67	277.38		
22 8 41	752	277.82	273.43	282.02	280.93	277.55	752	275.05	282.29	282.74	281.30	278.56	758	277.98	279.49	282.40	281.16	278.06		
22 8 53	765	279.29	282.31	283.04	281.65	279.04	771	278.39	279.69	282.55	281.53	278.52	769	278.23	279.34	282.39	281.43	278.55		
22 9 9	772	278.09	273.52	282.50	281.46	273.44	773	278.33	279.83	282.52	281.32	278.48	772	279.16	279.16	282.13	281.28	278.45		
22 9 17	769	278.96	281.89	282.55	281.45	278.95	774	278.39	282.59	282.76	281.63	279.18	771	277.90	280.08	282.29	281.00	278.31		
22 9 29	775	278.94	283.12	282.95	281.51	279.13	767	277.59	281.42	282.16	281.13	278.35	767	273.21	281.97	282.93	281.52	279.34		
22 9 41	767	278.51	280.61	282.17	281.15	278.44	765	275.52	284.21	283.01	281.72	279.37	773	279.41	284.07	283.00	281.64	279.34		
22 9 53	767	279.16	283.95	282.79	281.45	279.19	765	279.59	284.10	283.14	281.73	279.53	772	279.63	285.14	282.80	281.61	279.54		
22 10 5	777	279.73	283.74	282.87	281.71	279.57	765	279.93	284.32	282.93	281.73	279.69	774	281.23	283.63	282.88	281.65	279.95		
22 10 29	758	282.20	284.61	282.26	281.19	281.87	720	280.68	286.13	283.62	282.31	280.50	770	280.00	285.39	283.17	282.02	280.09		
22 10 49	771	280.48	285.57	283.30	282.23	280.27	770	280.15	285.32	283.02	282.17	280.07	774	280.26	284.83	283.08	282.10	279.98		
22 11 4	775	279.81	284.50	282.88	281.82	279.82	768	280.51	285.13	283.29	282.84	280.31	771	279.02	282.10	282.36	281.58	279.60		
22 11 11	771	280.57	285.28	283.29	282.21	280.29	770	280.34	284.87	283.02	282.16	280.18	769	279.31	282.01	282.66	281.78	279.84		
22 11 23	771	279.07	281.86	282.27	281.53	279.33	772	280.70	284.37	283.24	282.23	280.49	771	279.24	281.75	282.33	281.58	279.86		
22 11 35	770	280.21	284.30	283.04	282.02	280.31	769	279.10	281.49	282.15	281.60	279.53	771	280.28	284.41	282.91	282.24	280.46		
22 11 47	772	279.20	281.32	283.17	281.33	279.42	766	280.59	284.44	283.07	282.27	280.57	769	279.31	281.25	282.07	281.51	279.64		
22 11 59	769	279.44	281.36	281.94	281.53	279.74	774	279.21	281.69	281.37	281.14	279.39	767	279.62	280.68	281.29	280.94	279.44		
22 12 10	773	279.83	281.15	280.99	280.54	279.12	767	275.33	280.57	281.43	281.17	279.50	770	279.24	280.67	281.17	280.86	279.40		
22 12 23	770	279.30	280.71	281.42	281.04	279.64	768	279.52	281.79	281.13	280.37	279.54	769	279.76	280.57	281.33	281.11	279.59		
22 12 35	772	279.44	280.78	281.02	280.73	279.44	767	279.67	280.14	281.13	280.76	279.55	769	279.24	280.10	280.65	280.51	279.45		
22 12 47	770	280.67	281.40	281.40	281.42	280.46	770	279.24	280.31	280.88	280.53	279.39	771	279.40	279.95	280.82	280.59	279.46		
22 12 59	771	279.62	280.22	280.54	280.62	279.45	767	279.38	280.32	281.12	280.30	279.56	771	279.32	280.14	280.68	280.53	279.28		
22 13 11	772	279.44	280.41	281.09	280.74	279.80	771	279.37	281.42	280.70	280.48	279.35	769	279.73	280.43	281.33	281.02	279.63		
22 13 23	771	279.63	281.62	281.29	280.34	273.60	769	279.41	280.51	281.15	280.88	279.52	770	279.44	280.90	280.91	280.77	279.45		
22 13 35	769	279.77	281.10	281.63	281.15	279.72	770	279.83	281.37	281.35	281.16	279.69	767	279.57	280.65	280.77	280.75	279.54		
22 13 47	770	279.38	281.29	280.54	280.51	273.36	770	279.19	280.53	280.95	280.33	279.42	771	279.32	280.63	280.78	280.60	279.47		
22 13 59	769	279.67	280.67	280.94	280.75	274.55	770	279.41	280.75	280.83	280.61	279.46	771	279.57	280.85	280.93	280.85	279.76		
22 14 10	771	279.67	281.19	281.08	280.35	279.73	768	279.62	280.73	281.16	280.32	279.66	770	279.46	280.63	281.08	280.74	279.45		
22 14 20	767	279.56	281.97	281.10	280.30	274.59	769	279.70	281.47	281.35	281.15	279.78	768	279.55	280.97	280.76	280.53	279.51		
22 14 33	767	279.55	281.45	281.10	280.35	279.63	769	279.83	282.03	281.25	281.15	279.69	766	280.31	282.89	282.18	281.68	280.03		
22 14 45	771	279.89	283.23	283.30	281.79	273.94	770	279.79	283.47	282.87	282.20	280.18	767	279.87	283.75	282.75	282.05	279.91		
22 14 57	773	279.47	283.25	282.58	282.34	280.60	768	279.23	282.20	281.36	281.16	279.59	769	279.65	281.98	281.68	281.33	279.70		
22 15 8	770	279.68	281.82	281.20	281.11	273.56	773	280.02	282.83	282.53	282.17	280.14	767	280.01	283.45	282.73	282.17	280.02		
22 15 20	759	280.02	282.82	282.26	282.49	280.27	772	280.05	283.88	283.13	282.37	280.25	771	280.17	283.99	283.22	282.68	280.36		
22 15 33	771	279.79	283.09	283.13	282.34	280.66	770	280.05	284.00	283.42	282.67	280.33	774	280.17	283.95	283.20	282.50	280.20		
22 15 45	772	279.81	283.63	282.79	282.23	280.02	769	280.32	283.37	283.14	282.56	280.21	766	279.81	283.89	283.05	282.50	280.25		
22 15 57	771	279.69	283.02	283.03	282.25	280.03	772	279.88	284.33	283.37	282.63	280.18	771	279.81	284.34	283.14	282.44	280.03		
22 16 9	765	280.03	284.64	283.43	283.43	280.31	769	280.22	284.47	283.29	282.59	280.16	766	280.15	284.30	283.33	282.67	280.31		
22 16 20	770	279.99	284.08	283.07	282.46	280.10	768	279.75	284.53	282.99	282.65	280.29	767	279.95	284.75	283.31	282.59	280.22		
22 16 33	768	282.57	284.73	283.27	282.62	280.87	765	280.30	285.54	285.78	285.35	285.00	769	285.17	285.57	285.70	285.16	284.88		
22 16 49	769	285.28	285.81	285.81	285.41	285.03	766	286.06	285.39	286.11	286.24	286.50	769	280.46	283.53	282.62	282.31	280.72		
22 22 13	771	280.46	284.10	283.41	283.01	280.90	765	280.48	284.66	283.68	283.20	281.05	770	280.34	284.54	283.82	283.13	280.93		
22 22 25	770	280.16	283.99	282.54	282.64	280.58	766	280.50	284.45	283.68	283.12	280.80	775	280.27	284.27	283.50	282.98	280.68		
22 22 37	772	280.05	283.55	282.45	282.85	280.58	769	280.19	284.38	283.68	283.12	280.67	771	280.26	283.62	283.12	282.87	280.68		
22 22 49	772	280.00	282.64	282.46	282.24	280.39	767	280.30	283.50	282.79	282.63	280.61	774	280.35	284.17	283.16	282.90	280.70		
22 23 0	774	280.02	282.95	282.53	282.33	281.36	769	279.93	282.64	282.95	282.38	280.40	769	280.24	281.82	281.73	281.94	280.26		
22 23 13	777	279.84	282.22	281.93	282.03	280.07	766	280.07	283.33	282.66	282.55	280.44	769	280.31	283.87	282.89	282.71	280.52		
22 23 25	765	280.11	283.71	282.63	282.41	280.36	770	280.10	283.75	282.87	282.57	280.46	770	279.99	283.60	282.69	282.41	280.41		
22 23 37	777	280.02	283.17	282.57	282.36	280.32	764	279.93	283.03	282.42	282.16	280.44	775	280.16	283.12	282.56	282.25	280.32		
22 23 49	774	280.16	283.19	282.53	282.41	280.33	767	280.20	282.95	282.17	282.19	280.30	769	280.10	282.10	281.59	281.76	280.18		
22 23 59	774	280.04	282.75	282.24	282.15	280.39	771	279.92	282.73	281.80	281.78	280.19	771	280.51	283.79	282.82	282.62	280.68		
22 24 10	777	279.65	282.19	281.72	281.63	280.17	767	280.12	282.04	281.65	281.69	280.30	771	279.71	280.33	280.57	280.89	279.83		
22 24 23	773	279.48	281.47	280.72	280.94	279.48	774	280.05	282.91	281.86	282.12	280.32	767	280.39	283.52	282.36	282.22	280.40		
22 24 35	770	280.06	282.49	282.29	282.03	280.35	772	280.12	282.53	281.88	281.37	280.39	767	280.34	283.25	282.36	282.22	280.40		
22 24 47	770	280.11	283.43	282.56	282.45	280.43	767	279.60	282.56	281.73	281.50	279.90	766	279.77	282.84	281.62	281.69	280.03		
22 24 59	770	279.65	282.49	281.35	281.39	279.91	768	279.56	282.14	281.15	281.54	279.76	772	279.82	282.44	281.38	281.61	279.97		
22 25 11	768	279.75	282.12	281.43	281.23	279.77	772</													

HR	MN	SC	ALT	T1	T2	T3	T4	T5	ALT	T1	T2	T3	T4	T5	ALT	T1	T2	T3	T4	T5
22 41	33	934	284.05	283.41	284.29	284.73	284.73	940	285.13	283.35	284.53	285.09	284.93	935	285.31	283.63	284.37	284.98	284.90	
22 41	45	937	284.90	283.33	284.46	284.92	284.84	925	285.07	283.74	284.39	285.12	284.96	935	285.35	283.77	284.82	285.22	285.06	
22 41	57	938	284.82	283.62	284.59	284.93	284.84	942	285.44	284.28	284.80	285.29	285.14	941	285.41	284.21	284.97	285.45	285.14	
22 42	9	938	285.14	283.87	285.11	285.42	285.14	935	285.45	284.44	284.86	285.34	285.27	941	285.37	284.10	285.15	285.47	285.32	
22 42	19	940	284.95	284.11	284.91	285.35	285.16	935	285.23	284.48	284.99	285.46	285.27	942	285.40	284.22	285.13	285.39	285.06	
22 42	31	947	285.25	284.21	284.71	285.14	284.31	947	285.20	284.23	285.02	285.35	285.04	933	284.82	284.52	284.89	285.28	285.06	
22 42	43	939	285.32	284.21	285.07	285.40	285.00	939	285.05	284.51	285.07	285.51	285.04	945	285.21	284.50	285.32	285.59	285.07	
22 42	55	944	284.79	283.67	284.78	285.13	284.73	951	285.36	284.47	285.21	285.52	285.13	952	284.93	284.41	284.93	285.26	284.92	
22 43	7	946	284.93	284.14	284.80	285.12	284.90	955	284.98	284.41	285.01	285.24	284.98	954	285.53	284.53	284.85	285.29	284.97	
22 43	19	952	285.32	284.43	285.29	285.32	285.76	958	285.28	284.21	284.75	285.11	284.76	953	285.34	284.59	285.13	285.52	285.10	
22 43	31	962	285.03	284.20	284.63	284.93	284.63	957	285.18	284.17	284.73	285.16	284.82	957	285.04	284.25	284.63	285.00	284.77	
22 43	43	955	284.94	284.19	284.37	284.83	284.83	955	284.90	284.12	284.41	284.39	284.65	959	285.06	284.63	284.53	285.07	284.87	
22 43	55	967	284.73	284.26	284.44	285.06	284.76	965	284.62	284.20	284.38	284.39	284.73	968	285.21	284.33	284.73	285.12	284.89	
22 44	7	965	285.24	284.40	284.50	285.02	284.76	963	285.35	284.24	284.52	285.13	284.78	961	285.17	284.35	284.22	284.89	284.73	
22 44	19	968	284.70	284.16	284.33	284.76	284.51	968	284.92	284.28	284.26	284.59	284.52	974	285.00	284.18	284.62	285.00	284.72	
22 44	31	974	284.66	284.15	284.17	284.73	284.51	977	284.80	284.37	284.47	284.36	284.76	976	284.56	284.13	284.11	284.64	284.46	
22 44	43	973	284.67	284.07	284.30	284.82	284.55	975	284.56	284.27	284.19	284.74	284.53	974	284.86	284.27	284.46	284.87	284.73	
22 44	55	978	284.85	284.13	284.16	284.65	284.57	977	285.11	284.57	284.13	284.36	284.78	980	285.27	284.26	284.44	284.84	284.75	
22 45	7	980	284.63	283.99	284.16	284.63	284.57	982	285.11	284.37	284.81	285.10	284.82	982	285.10	284.20	284.45	284.87	284.79	
22 45	19	977	285.04	284.37	284.50	284.94	284.87	984	285.05	284.83	284.39	285.13	284.95	987	285.13	284.30	284.50	284.94	284.74	
22 45	31	932	284.80	284.33	284.08	284.56	284.43	981	285.04	284.34	284.39	284.45	284.65	983	285.03	284.36	284.31	284.74	284.61	
22 45	43	988	284.48	283.77	283.95	284.41	284.38	995	285.00	284.15	284.04	284.46	284.56	994	284.65	283.95	284.00	284.38	284.38	
22 45	55	992	284.82	283.71	283.94	284.29	284.31	995	284.49	284.12	283.56	284.14	284.32	995	284.27	283.95	283.91	284.41	284.26	
22 46	7	993	284.21	283.47	283.65	284.07	284.03	1002	284.22	283.62	283.56	284.13	284.16	997	284.26	283.72	283.79	284.14	284.19	
22 46	19	996	283.82	283.39	283.46	283.76	283.97	1000	284.17	283.25	283.51	283.77	283.80	1001	284.14	283.23	283.11	283.58	283.88	
22 46	29	1001	283.75	282.71	283.03	283.43	283.66	1005	283.40	282.48	282.41	283.21	283.42	999	284.12	282.76	282.93	283.49	283.50	
22 46	40	995	283.61	282.68	282.84	283.13	283.34	1007	283.57	282.74	282.95	283.46	283.46	1001	284.11	283.31	283.09	283.63	283.62	
22 46	53	992	284.03	283.13	283.06	283.53	283.62	1000	282.32	282.03	283.18	283.59	283.63	999	283.74	283.21	283.03	283.59	283.70	
22 47	5	994	284.31	283.24	283.50	283.73	283.81	999	283.87	283.05	283.26	283.46	283.59	1007	284.18	283.19	283.31	283.76	283.79	
22 47	17	1001	284.00	283.15	283.43	283.31	283.63	1003	283.68	283.02	283.06	283.37	283.63	997	284.31	283.20	283.24	283.69	283.82	
22 47	29	998	284.30	283.43	283.17	283.72	283.79	1004	284.10	282.82	283.23	283.55	283.63	1003	284.35	282.95	283.06	283.94	283.71	
22 47	41	1004	284.07	282.55	283.10	283.47	283.63	1001	284.02	283.03	282.72	283.25	283.61	1000	283.66	282.77	283.14	283.64	283.65	
22 47	53	1003	283.96	282.98	282.46	283.41	283.59	1005	283.88	282.69	282.63	283.26	283.48	998	283.79	282.59	282.86	283.39	283.54	
22 48	5	1006	284.01	282.86	283.10	283.50	283.75	1004	283.74	282.50	282.69	283.14	283.32	1001	283.80	282.54	282.68	283.24	283.44	
22 48	17	1007	283.84	282.46	282.53	283.07	283.37	1005	283.81	282.42	282.41	282.33	283.38	1003	283.76	282.46	282.68	283.10	283.38	
22 48	29	1009	283.28	282.11	282.36	282.91	283.13	1001	283.20	282.50	282.23	282.34	283.21	1007	283.26	282.35	282.50	282.87	283.20	
22 48	41	1001	283.44	282.22	282.91	282.75	283.06	1008	283.32	282.29	282.21	282.79	283.13	1007	283.55	282.13	282.41	282.78	283.08	
22 48	53	1004	283.15	281.63	282.10	282.49	282.60	1009	283.32	282.10	282.29	282.63	282.95	1003	283.57	282.26	282.11	282.58	283.06	
22 49	3	1003	283.27	281.98	282.42	282.75	282.98	998	283.17	282.38	282.04	282.67	282.97	1007	283.41	282.01	282.34	282.65	283.08	
22 49	15	1011	283.08	282.14	281.89	282.44	282.64	1007	283.52	282.57	282.28	282.33	283.29	1011	283.58	282.18	282.50	282.83	283.14	
22 49	27	1010	282.99	282.16	282.47	282.45	282.93	1003	283.27	282.42	282.42	282.31	283.16	1005	283.57	282.73	282.34	282.84	283.26	
22 49	39	1012	283.43	282.11	282.42	282.71	283.29	1019	283.69	282.43	282.24	282.75	283.18	1005	283.49	282.48	282.57	282.96	283.38	
22 49	51	1011	283.32	282.21	282.81	282.61	282.98	1008	283.81	282.41	282.39	282.31	283.25	1019	283.57	282.56	282.65	283.01	283.26	
22 50	3	1011	283.81	282.27	282.16	282.73	283.26	1002	283.65	282.42	282.44	282.32	283.21	1007	283.60	282.25	282.67	283.01	283.14	
22 50	15	1005	283.56	282.56	282.52	283.05	283.27	1003	283.74	282.50	282.75	282.39	283.40	1011	283.71	282.59	282.20	282.69	283.25	
22 50	27	1005	283.77	282.65	282.64	283.11	283.44	1019	283.82	282.73	282.94	283.17	283.38	1002	283.44	282.55	282.50	282.95	283.28	
22 50	39	1014	283.84	282.65	282.67	283.13	283.42	1004	283.77	282.39	282.73	283.15	283.56	1012	283.53	282.60	282.72	282.88	283.37	
22 50	51	1008	283.74	282.55	282.57	283.11	283.44	1010	283.96	282.85	283.03	283.23	283.62	1008	284.22	282.68	282.76	283.06	283.45	
22 51	3	1011	284.20	282.42	282.64	283.17	283.47	1011	284.17	283.21	283.00	283.31	283.61	1003	283.65	282.78	282.75	283.02	283.49	
22 51	15	1005	284.07	282.62	282.81	283.30	283.95	1000	284.03	283.00	282.66	283.16	283.56	1008	284.05	283.17	283.32	283.44	283.91	
22 51	27	1011	283.79	282.32	282.81	283.03	283.54	1010	283.63	282.61	282.76	283.19	283.58	1003	283.98	282.74	283.30	283.36	283.78	
22 51	39	1012	284.06	282.75	282.95	283.13	283.70	1002	284.27	282.01	283.48	283.26	283.76	1003	284.29	283.34	283.07	283.62	283.93	
22 51	51	1004	284.34	282.72	283.14	283.50	283.77	1003	284.16	282.61	282.81	283.21	283.60	1005	283.74	282.97	283.14	283.48	283.81	
22 52	0	1006	284.26	283.23	283.44	283.61	283.87	1008	284.10	283.10	282.97	283.24	283.70	1004	283.92	283.12	283.20	283.52	283.80	
22 52	13	1004	283.47	283.14	283.31	283.43	283.79	1008	283.79	283.10	283.21	283.47	283.75	1011	283.70	283.26	282.92	283.42	283.87	
22 52	25	1014	284.26	283.24	283.24	283.50	283.87	1009	284.04	282.91	283.05	283.32	283.62	1014	283.63	282.63	282.76	283.19	283.58	
22 52	37	1007	283.83	283.27	283.28	283.53	283.82	1006	283.87	283.31	283.05	283.53	283.83	1009	283.86	282.98	283.03	283.37	283.73</	

FLIGHT NO 7 6/ 12/ 70

HR	MN	SC	ALT	T1	T2	T3	T4	T5	ALT	T1	T2	T3	T4	T5	ALT	T1	T2	T3	T4	T5
23	17	27	254	247.60	256.18	244.52	242.41	240.24	251	247.31	250.29	244.19	241.31	239.66	248	246.43	255.45	242.98	240.90	239.08
23	17	27	254	247.74	257.45	244.94	242.17	239.46	245	245.23	250.13	246.78	243.61	240.34	245	250.35	252.19	248.10	244.54	240.81
23	17	39	243	249.46	260.37	246.94	243.67	240.43	242	249.19	259.67	246.30	243.18	240.21	241	248.67	258.83	246.03	242.97	240.14
23	17	51	233	250.50	262.18	248.28	244.61	241.54	238	250.19	262.23	247.82	244.23	241.30	237	250.57	262.48	247.75	244.09	239.89
23	18	1	236	250.02	261.62	247.69	243.76	239.56	234	247.95	258.23	244.59	241.46	238.35	234	247.45	257.79	243.90	240.95	238.15
23	18	15	235	246.72	255.22	243.00	240.25	237.60	235	244.43	251.13	239.79	237.37	236.46	234	244.58	251.12	240.49	238.15	236.38
23	18	27	234	245.08	261.53	240.46	238.41	236.82	233	246.99	254.53	242.90	240.13	237.48	234	250.29	259.52	246.74	243.01	238.84
23	18	39	235	253.12	262.83	250.31	245.64	239.97	233	252.42	260.43	249.52	245.18	239.96	234	253.06	260.99	249.73	245.46	240.27
23	18	51	233	253.78	262.35	251.28	246.42	240.69	233	255.11	265.82	252.67	247.57	241.14	234	255.37	267.55	253.81	248.28	241.50
23	19	3	232	255.32	263.34	253.25	247.93	241.33	230	258.19	272.04	257.19	250.55	242.56	232	259.71	274.03	258.96	252.17	243.01
23	19	13	231	260.42	274.59	260.00	252.63	243.30	230	260.38	274.44	259.57	252.25	243.14	230	259.88	273.47	258.93	251.93	242.86
23	19	25	228	259.18	272.64	258.09	251.26	242.43	230	258.64	272.00	257.89	250.49	242.01	228	258.60	272.22	257.02	250.49	241.77
23	19	37	227	259.33	273.15	258.32	251.42	242.43	225	260.41	274.59	259.67	252.42	242.91	226	260.83	275.35	260.51	253.08	243.33
23	19	49	224	261.31	275.75	260.68	253.21	243.58	224	260.83	275.07	260.27	252.36	243.12	226	260.13	274.93	259.26	252.09	242.48
23	20	0	222	259.85	273.68	259.02	251.90	242.34	222	256.24	272.84	258.12	251.07	241.68	220	259.93	272.62	258.04	250.85	241.63
23	20	13	212	258.12	273.47	258.13	250.93	241.70	218	259.11	273.19	258.51	251.10	241.57	217	259.09	273.01	258.14	250.90	241.39
23	20	25	216	258.83	273.11	257.71	250.54	241.75	214	257.49	271.08	256.83	249.33	240.84	214	258.27	272.23	256.85	250.02	241.20
23	20	37	212	260.18	274.84	259.29	251.93	242.04	212	261.18	275.39	256.67	252.39	242.40	212	261.37	272.14	260.94	252.95	242.45
23	20	49	212	260.88	275.95	260.38	252.46	242.16	210	260.73	275.48	260.06	252.17	241.97	210	258.16	272.61	257.09	249.86	240.44
23	21	0	211	264.53	268.51	252.27	246.22	238.74	210	258.69	275.34	262.84	246.39	239.84	210	252.98	266.66	250.11	244.71	239.04
23	21	13	211	252.14	268.73	248.84	243.43	237.58	210	250.27	260.92	246.56	242.21	237.16	210	249.49	259.18	245.42	241.64	236.78
23	21	25	211	246.85	262.88	244.45	239.24	236.21	210	249.98	251.62	240.50	238.34	235.79	209	246.73	259.91	241.86	239.06	235.66
23	21	37	209	247.64	255.73	248.06	239.81	236.03	209	246.69	253.33	241.63	238.83	235.63	207	245.52	251.44	240.89	238.24	235.28
23	21	49	207	242.73	245.97	236.30	235.53	233.92	207	242.80	247.43	237.02	235.55	234.12	205	244.11	251.46	239.09	237.22	234.95
23	22	0	205	244.48	251.66	239.70	237.66	235.30	206	244.84	252.53	240.58	237.92	235.42	205	246.04	254.30	242.14	239.26	236.00
23	22	13	205	245.00	252.74	239.70	237.42	235.24	204	245.22	252.39	240.52	238.37	235.44	203	244.23	250.16	239.24	237.30	234.96
23	22	25	202	244.59	250.90	239.60	237.44	235.18	203	244.08	250.38	238.77	236.75	234.49	201	243.36	248.65	238.15	236.21	234.00
23	22	37	202	243.28	243.82	237.84	235.95	233.90	201	242.75	250.38	238.22	236.23	233.86	200	244.88	253.31	235.87	233.33	231.45
23	22	49	199	245.51	254.11	240.64	238.13	235.03	200	240.63	255.04	240.83	238.32	235.20	198	246.28	255.91	241.57	238.68	235.44
23	22	59	199	247.16	257.91	242.72	239.61	235.64	200	239.67	261.46	245.54	241.32	238.35	198	246.88	257.84	242.29	238.91	235.11
23	23	11	197	249.39	261.35	245.81	241.37	236.33	199	246.58	257.12	242.25	238.75	236.50	198	246.14	256.23	241.44	238.05	234.78
23	23	23	197	246.99	257.95	242.57	239.07	234.80	198	245.72	255.41	240.99	237.78	234.59	198	244.89	256.67	233.80	237.23	234.33
23	23	35	197	243.09	244.78	232.79	235.43	233.51	198	243.95	251.85	238.55	236.52	233.01	198	243.59	250.58	238.85	236.26	233.49
23	23	47	194	244.43	253.44	239.67	236.94	233.86	197	245.05	255.10	240.27	237.30	234.11	198	246.19	256.67	241.84	238.64	235.85
23	23	59	197	244.98	253.75	240.72	237.75	234.43	199	245.55	255.44	241.13	238.44	234.93	196	247.65	258.84	243.85	240.27	235.65
23	24	10	197	248.48	260.62	245.20	241.63	235.38	197	246.12	259.62	244.56	240.43	235.97	194	247.79	259.52	243.66	240.19	235.83
23	24	23	196	248.63	261.75	245.69	241.33	236.25	196	248.07	257.72	244.49	240.45	235.82	193	246.71	257.12	243.40	239.56	235.09
23	24	35	194	244.67	253.67	240.05	237.44	234.27	194	247.69	253.07	244.23	240.17	235.41	193	247.81	259.83	243.65	239.87	235.38
23	24	47	192	248.21	261.70	244.53	240.45	235.25	192	247.84	253.74	244.17	240.12	235.36	191	249.26	262.98	247.18	242.31	235.94
23	24	59	191	248.50	260.90	244.98	240.73	235.57	192	248.80	264.86	247.10	242.31	236.09	191	246.88	263.14	246.73	241.64	235.89
23	25	11	192	253.70	263.00	251.19	245.02	237.42	190	254.69	268.92	252.54	246.11	237.64	190	252.79	271.45	254.92	247.76	238.41
23	25	23	190	253.22	267.24	253.80	244.61	236.94	190	257.59	272.98	255.38	248.12	238.98	189	260.34	275.09	259.25	250.88	239.83
23	25	35	189	260.34	275.11	259.11	250.91	239.65	190	260.34	275.14	255.33	250.19	239.83	188	260.52	275.52	259.17	250.94	239.78
23	25	47	189	260.51	275.49	259.61	251.24	239.96	188	260.35	275.47	259.19	250.37	239.74	188	261.29	274.97	259.27	250.90	239.63
23	25	59	189	259.91	274.84	258.83	250.49	239.41	187	255.56	264.46	257.53	248.34	234.93	189	260.08	274.78	259.13	250.53	239.31
23	26	0	183	259.78	274.74	258.75	250.26	238.15	188	259.55	274.50	258.73	250.19	239.09	188	259.04	273.40	257.91	249.67	238.84
23	26	11	183	258.88	273.79	257.49	249.61	238.88	187	258.26	273.01	256.60	248.79	238.14	189	258.63	273.51	257.57	249.46	238.70
23	26	23	184	257.68	272.46	256.50	248.60	237.94	186	257.82	272.71	256.88	248.43	237.97	187	258.20	273.16	256.90	248.98	238.32
23	26	35	188	257.07	272.99	257.11	248.97	238.33	188	257.85	272.67	256.42	248.60	237.92	187	257.91	272.43	256.49	248.42	237.99
23	26	47	187	256.84	271.15	255.32	247.62	237.07	185	256.11	271.42	254.85	247.11	236.95	182	256.27	270.75	254.74	247.11	237.14
23	26	59	185	256.63	270.54	255.25	247.46	237.27	182	256.46	262.49	254.66	249.46	237.24	182	256.50	273.22	258.89	250.97	239.05
23	27	0	181	253.50	262.37	256.44	247.37	233.83	183	259.25	273.85	258.96	250.70	239.02	182	259.34	273.81	258.53	250.46	238.96
23	27	13	182	259.56	273.88	258.37	250.30	248.86	161	256.54	273.76	258.11	250.10	238.40	184	259.49	273.54	258.11	249.93	238.71
23	27	25	182	259.43	273.41	257.38	249.40	238.46	182	258.92	272.64	256.97	248.93	238.13	182	258.48	271.86	256.27	248.33	237.71
23	27	37	181	258.78	272.94	256.36	248.44	237.40	181	259.82	272.45	257.07	248.73	237.95	184	258.90	270.79	258.73	251.31	239.46
23	27	49	181	259.27	271.98	258.63	250.99	239.17	182	258.63	273.24	259.14	250.37	239.06	181	259.75	273.54	258.75	250.52	238.75
23	28	0	181	259.39	273.11	259.46	249.42													

HR	MN	SC	ALT	T1	T2	T3	T4	T5	T1	T2	T3	T4	T5	ALT	T1	T2	T3	T4	T5
23 43	35	182	256.91	270.37	255.68	248.50	238.25	181	252.77	264.22	250.23	244.34	236.29	182	257.72	271.10	256.40	249.12	238.76
23 43	59	182	259.55	275.36	253.44	251.15	239.72	182	260.10	275.92	260.22	251.78	239.96	183	261.46	278.34	261.97	252.97	240.70
23 44	23	181	261.61	279.25	262.33	253.20	240.77	182	261.67	277.13	261.77	253.10	240.67	182	261.81	277.48	262.02	252.30	240.84
23 44	47	182	262.13	278.16	262.50	253.42	241.12	182	262.04	277.45	262.23	253.43	241.18	182	262.28	277.10	262.46	253.62	241.18
23 45	8	182	262.13	277.34	262.29	253.31	240.92	183	262.21	277.90	262.52	253.55	241.06	181	262.24	277.70	262.65	253.66	241.15
23 45	29	182	262.38	277.71	262.49	253.67	241.05	183	262.41	277.21	262.41	253.58	241.15	182	262.25	276.84	262.36	253.65	241.21
23 45	57	182	262.38	277.87	262.49	253.61	241.17	182	262.15	277.07	262.40	253.46	241.23	182	261.93	276.82	262.38	253.67	240.94
23 46	21	182	262.27	276.83	262.54	253.67	241.26	182	262.13	277.42	262.72	253.75	241.31	182	262.27	278.16	263.03	253.85	241.27
23 46	45	181	262.46	277.53	262.75	253.77	241.28	182	262.51	276.98	262.56	253.70	241.33	181	262.26	276.91	262.53	253.89	241.21
23 47	9	182	262.39	277.30	262.91	253.95	241.46	183	262.44	276.75	262.74	253.35	241.33	182	262.35	276.76	262.77	254.00	241.45
23 47	29	183	262.29	276.62	262.49	253.73	241.31	182	262.21	276.46	262.31	253.60	241.08	182	262.46	276.95	262.83	254.00	241.48
23 47	41	182	262.15	276.60	262.52	253.64	241.11	182	262.28	276.63	262.60	253.63	241.22	183	262.45	276.84	262.85	253.74	241.43
23 47	53	183	262.46	276.84	262.78	253.82	241.29	183	262.41	276.98	262.75	253.36	241.31	182	262.48	277.15	262.94	254.11	241.46
23 48	3	183	262.49	277.24	262.87	253.97	241.38	181	262.65	277.31	263.12	254.23	241.57	182	262.69	277.62	262.91	254.17	241.56
23 53	17	183	263.63	279.61	263.33	253.60	240.80	183	263.73	281.52	264.08	253.32	240.91	181	263.40	280.45	263.45	253.61	240.76
23 53	39	182	263.62	282.15	264.43	253.83	241.75	182	263.49	281.32	263.37	253.43	240.68	182	263.98	282.25	264.44	253.75	240.68
23 53	59	181	263.94	282.63	264.46	253.83	240.75	182	263.04	282.06	264.61	253.37	240.75	182	263.79	282.44	264.39	253.75	240.60
23 54	11	182	263.88	282.24	264.60	253.95	240.88	183	263.79	282.25	264.64	254.16	240.84	183	263.59	280.71	263.92	253.70	240.75
23 54	23	182	263.58	279.60	263.29	253.45	240.67	182	263.58	279.53	263.29	253.56	240.73	182	263.58	280.31	263.71	253.59	240.81
23 54	35	182	263.55	280.40	263.94	253.78	240.74	182	263.67	281.46	263.96	253.77	240.74	182	263.98	282.39	264.91	254.18	240.87
23 54	47	183	263.55	281.05	263.93	253.72	240.98	182	263.55	279.95	263.52	253.61	240.82	181	263.41	279.14	263.95	253.60	240.79
23 54	59	182	263.23	278.94	262.99	253.44	240.81	181	263.02	277.83	262.83	253.24	240.53	182	263.02	277.14	262.71	253.40	240.70
23 55	10	183	263.07	277.39	262.46	253.33	240.50	182	263.35	277.33	262.92	253.50	240.77	183	263.12	276.48	262.50	253.22	240.57
23 55	23	182	263.22	276.86	262.79	253.44	240.75	183	263.14	276.88	262.74	253.23	240.73	183	263.21	276.71	262.65	253.36	240.76
23 55	35	182	263.61	277.07	262.84	253.54	240.83	182	263.72	277.04	263.08	253.34	241.08	183	263.44	276.46	262.92	253.38	240.75
23 55	47	182	263.54	276.60	262.85	253.40	240.86	182	263.70	277.10	262.65	253.41	240.82	183	263.69	276.79	263.08	253.69	240.93
23 55	59	183	263.59	275.67	262.83	253.47	240.92	183	263.86	277.41	263.03	253.66	241.04	183	264.05	277.73	263.25	253.76	240.98
23 56	27	181	264.39	277.21	263.47	253.91	241.28	182	264.44	277.45	263.88	254.00	241.34	183	264.46	278.38	263.48	254.00	241.17
23 56	51	181	264.66	278.92	263.95	254.29	241.24	183	264.65	278.87	263.80	253.17	241.29	184	264.71	277.71	263.65	253.95	241.17
23 57	13	181	264.42	278.24	263.61	254.05	241.15	182	264.77	278.13	263.84	254.10	241.25	184	264.60	278.05	263.60	254.11	241.19
23 57	27	182	264.54	277.86	263.62	254.21	241.25	182	264.61	278.47	263.75	254.14	241.25	183	264.68	278.22	263.72	254.30	241.47
23 57	57	182	264.63	277.80	263.69	254.13	241.48	182	264.71	278.21	263.75	254.27	241.47	183	264.83	278.27	263.74	254.20	241.32
23 58	8	183	264.64	278.84	263.95	254.44	241.49	183	264.76	279.19	264.05	254.27	241.65	184	264.47	278.43	263.74	254.18	241.49
23 58	20	182	264.86	278.04	264.24	254.41	241.69	182	264.54	278.34	264.03	254.38	241.68	183	264.62	278.21	263.99	254.43	241.57
23 58	33	182	264.87	278.01	263.72	254.43	241.63	183	264.88	277.95	264.03	254.51	241.67	182	264.72	278.31	263.96	254.53	241.51
23 58	45	182	264.76	278.12	264.05	254.43	241.68	181	264.77	277.79	263.89	254.35	241.54	183	264.73	277.29	263.69	254.32	241.49
23 58	57	181	264.70	277.69	263.53	254.21	241.49	182	265.06	277.46	264.07	254.56	241.74	182	264.92	277.22	263.99	254.44	241.56
23 59	8	182	265.19	277.24	263.97	254.64	241.83	183	264.92	277.10	263.78	254.83	241.76	182	264.97	277.31	263.79	254.51	241.70
23 59	20	182	264.84	277.78	263.70	254.33	241.58	183	264.81	277.52	263.85	254.49	241.59	183	264.77	277.46	263.73	254.47	241.60
23 59	33	182	264.97	277.62	264.08	254.57	241.79	182	265.03	277.28	263.96	254.39	241.72	184	265.11	277.77	264.02	254.59	241.73
23 59	45	182	265.22	278.29	264.17	254.70	241.65	182	265.11	279.13	263.78	254.33	241.83	182	265.24	278.12	264.38	254.72	241.86
23 59	57	182	265.03	277.88	263.86	254.55	241.48	183	265.13	277.82	263.38	254.72	241.91	182	265.14	277.69	264.09	254.58	241.89
0 0	7	182	265.15	277.29	263.78	254.57	241.67	182	265.37	277.57	264.07	254.97	242.00	182	265.42	277.28	264.27	254.75	241.96
0 0	19	183	265.11	277.35	263.83	254.55	241.75	182	265.43	277.40	263.91	254.70	242.00	183	265.30	277.39	264.02	254.73	242.02
0 0	31	183	265.29	277.35	264.13	254.41	241.99	182	265.45	277.43	264.13	254.32	241.94	182	265.44	277.67	264.20	254.96	242.24
0 0	43	182	265.40	277.51	264.08	254.37	242.11	182	265.63	277.64	264.20	254.49	242.16	182	265.27	277.33	263.71	254.77	241.80
0 0	55	182	265.60	277.41	264.19	254.83	241.97	182	265.51	277.21	264.10	254.84	242.08	183	265.45	277.26	264.15	254.92	242.17
0 1	7	182	265.45	277.68	264.11	254.80	242.11	182	265.44	277.62	264.36	255.12	242.12	182	265.52	277.71	264.18	254.93	242.13
0 1	19	182	265.52	277.84	264.39	254.93	242.15	183	265.69	277.83	264.50	255.17	242.17	183	265.42	277.79	264.18	254.82	241.91
0 1	31	182	265.52	277.84	264.49	254.96	242.12	182	265.46	277.82	264.14	254.13	242.03	183	265.43	277.63	264.32	254.92	242.08
0 1	43	182	265.39	277.97	264.37	255.07	242.17	181	265.53	277.79	264.29	254.36	242.10	182	265.52	277.87	264.37	255.02	242.12
0 1	55	183	265.52	277.61	264.34	254.97	242.05	182	265.65	277.97	264.52	254.38	242.17	182	265.69	277.80	264.48	255.07	242.24
0 2	7	182	265.21	277.82	264.38	254.92	242.02	182	266.27	277.84	266.06	256.18	242.06	182	266.63	278.45	266.06	255.82	242.03
0 2	19	183	266.49	279.64	265.67	255.33	241.55	183	266.61	279.03	265.52	255.20	241.67	182	266.67	278.83	265.06	254.65	241.28
0 2	31	182	266.57	279.62	265.11	254.53	241.29	182	266.50	279.24	264.75	254.14	240.92	182	266.85	280.57	265.32	254.51	241.21
0 2	43	182	266.56	279.88	264.95	254.25	240.91	182	266.66	279.66	264.84	254.25	240.97	181	266.67	279.18	264.46	254.17	240.91
0 2	55	182	266.54	279.37	264.40	254.13	240.84	184	266.62	278.69	264.05	253.32	240.75	182	266.81	279.82	264.68	254.09	241.03
0 2	57	183	266.72	279.99	264.58	254.16	240.87	183	266.93	280.62	265.02								

HR	MN	SC	ALT	T1	T2	T3	T4	T5	ALT	T1	T2	T3	T4	T5	ALT	T1	T2	T3	T4	T5
0	17	20	183	269.54	278.82	266.35	256.19	243.01	183	269.18	278.82	265.96	255.37	242.63	183	269.48	279.17	266.31	256.15	242.96
0	17	33	182	269.46	279.71	266.54	256.19	242.81	182	269.27	279.42	266.01	255.38	242.58	182	269.67	280.70	266.76	256.24	242.96
0	17	45	182	269.94	283.31	267.98	256.78	242.93	182	269.68	282.71	267.54	256.56	242.78	183	269.52	281.50	266.63	256.43	243.17
0	17	57	182	269.78	282.29	267.28	256.64	242.93	183	269.59	282.15	267.19	256.51	242.88	183	269.49	280.13	266.36	256.26	242.96
0	18	8	183	269.53	281.26	266.87	256.29	242.76	182	269.45	280.26	266.30	256.12	242.84	182	269.30	279.42	266.10	256.19	242.88
0	18	20	182	269.28	279.07	266.47	256.13	242.95	183	269.31	280.23	266.05	255.35	242.88	182	269.77	280.29	266.69	256.29	243.12
0	18	33	182	269.80	281.37	266.88	256.24	242.86	184	270.13	282.84	267.81	256.64	243.04	183	270.47	283.70	268.33	257.03	243.20
0	18	45	183	270.30	283.52	268.02	256.95	243.14	182	270.42	283.79	268.21	257.02	243.19	182	270.52	283.67	268.36	256.92	243.07
0	18	57	182	270.41	283.79	268.52	256.98	242.99	182	270.37	284.09	268.40	256.34	243.16	181	270.16	283.97	268.37	256.98	243.02
0	19	9	182	270.34	283.93	268.27	257.01	243.04	183	270.47	284.23	268.29	257.16	243.22	182	270.42	283.94	268.33	256.98	243.05
0	19	19	183	270.42	283.96	268.46	256.92	243.02	183	270.53	284.32	268.30	256.39	243.22	183	270.82	284.78	268.57	257.29	243.42
0	19	31	183	270.70	284.48	268.42	257.18	243.32	182	270.78	284.65	268.32	257.10	243.22	183	270.75	284.60	268.36	257.07	243.23
0	19	43	184	270.63	284.61	268.45	256.15	243.32	181	270.50	284.13	268.20	256.85	242.88	183	270.70	284.44	268.46	257.09	243.28
0	19	55	183	270.24	282.75	267.31	256.33	242.95	182	270.35	283.32	267.83	256.30	243.21	181	270.08	281.76	268.95	256.40	243.02
0	20	7	183	270.62	282.74	267.61	256.88	243.36	182	270.13	281.77	267.12	256.51	242.96	181	270.23	280.55	266.86	256.36	243.41
0	20	19	183	270.16	280.63	266.92	256.13	243.20	182	270.40	280.93	266.68	256.31	243.16	183	270.00	280.28	266.97	256.36	243.41
0	20	31	182	269.46	280.73	266.71	256.53	243.39	182	269.91	281.17	266.75	256.26	243.01	183	269.92	280.04	266.91	256.29	243.22
0	20	43	185	269.89	279.73	266.26	256.27	243.23	183	269.89	280.04	266.32	256.33	243.10	182	270.23	281.41	266.99	256.54	243.27
0	20	55	184	270.33	282.40	267.44	256.66	243.09	181	270.37	281.87	267.22	256.64	243.26	182	270.80	284.05	268.57	257.34	243.69
0	21	7	182	270.50	283.71	268.08	256.88	243.18	182	270.71	283.89	268.07	257.30	243.29	183	270.87	284.28	268.17	257.08	243.42
0	21	19	183	270.99	284.36	268.54	257.24	243.48	182	270.91	284.13	268.39	257.02	243.26	183	270.94	283.11	267.77	256.89	243.36
0	21	30	183	270.42	282.02	267.17	256.75	243.46	183	270.48	281.91	267.33	256.32	243.36	182	270.25	281.67	267.26	256.52	243.21
0	21	43	183	270.84	283.25	266.64	256.44	243.30	182	270.53	281.62	267.42	256.82	243.39	183	269.94	278.64	265.99	256.96	243.03
0	21	55	183	270.30	279.93	266.71	256.33	243.41	182	270.56	281.21	267.04	256.61	243.28	182	270.95	282.65	267.86	256.96	243.37
0	22	7	184	271.19	284.06	268.58	257.18	243.39	182	271.24	283.69	268.42	257.21	243.60	183	270.86	283.59	268.35	257.06	243.40
0	22	19	182	270.72	281.28	266.81	256.62	243.46	181	271.11	283.11	268.08	257.12	243.50	182	271.16	282.78	268.05	257.16	243.53
0	22	28	182	271.32	284.25	269.72	257.37	243.35	182	271.53	284.52	268.94	257.44	243.66	183	271.25	284.63	268.82	257.39	243.48
0	22	41	182	271.35	284.61	268.74	257.24	243.45	182	271.56	284.52	268.94	257.24	243.66	183	271.42	284.41	268.56	257.40	243.66
0	22	53	182	271.27	284.14	268.62	257.26	243.57	183	271.20	283.67	268.44	257.23	243.68	183	271.44	284.45	268.71	257.33	243.52
0	23	4	183	271.65	284.78	269.21	257.63	243.82	182	271.46	284.54	268.89	257.22	243.48	182	271.75	284.88	268.16	257.67	243.69
0	23	17	182	271.56	284.77	269.04	257.44	243.60	181	271.62	284.84	269.06	257.52	243.65	182	271.56	284.93	268.97	257.52	243.71
0	23	29	183	271.69	285.01	269.29	257.73	243.95	182	271.59	284.67	268.84	257.45	243.54	183	271.56	284.92	269.28	257.66	243.93
0	23	40	183	271.49	284.64	268.78	257.37	243.95	182	271.43	284.74	268.80	257.59	243.65	182	271.46	284.98	268.87	257.55	243.84
0	23	53	184	271.81	285.14	269.42	257.83	244.15	183	271.57	284.98	268.96	257.37	243.75	182	271.38	284.76	268.96	257.45	243.65
0	24	4	182	271.50	285.01	269.19	257.61	243.91	182	271.54	284.74	268.97	257.65	243.88	181	271.56	284.46	268.90	257.44	243.89
0	24	17	183	271.57	284.19	268.89	257.44	243.62	183	271.42	283.83	268.45	257.39	243.49	182	271.71	284.65	269.10	257.59	243.86
0	24	28	183	271.78	284.72	268.31	257.21	243.73	182	271.48	283.63	268.48	257.25	243.69	182	271.19	282.52	267.95	257.03	243.60
0	24	41	182	271.56	283.00	268.36	257.28	243.86	181	271.38	283.25	268.23	257.20	243.67	181	271.71	284.25	268.89	257.54	243.84
0	24	53	183	271.33	283.05	268.14	257.13	243.81	183	270.98	283.81	267.10	256.34	243.61	182	270.79	279.81	266.68	256.65	243.59
0	25	5	182	271.51	282.83	268.17	257.28	243.96	181	271.67	284.05	268.69	257.43	243.74	182	271.66	284.14	269.11	257.46	243.70
0	25	17	182	271.70	283.53	268.27	257.26	243.74	182	271.26	282.64	267.95	257.19	243.85	182	271.49	282.33	268.01	257.01	243.72
0	25	29	183	271.72	283.84	268.31	257.33	243.95	183	271.59	283.38	268.59	257.22	243.61	181	271.59	283.20	268.26	257.26	243.90
0	25	39	183	271.46	283.98	268.53	257.20	243.95	184	271.50	284.00	268.75	257.36	243.76	181	271.72	284.39	268.89	257.52	243.91
0	25	51	183	271.73	284.65	269.05	257.53	243.89	183	271.76	284.67	268.84	257.42	243.62	182	271.75	284.31	269.04	257.61	243.81
0	26	2	183	271.51	284.53	269.02	257.53	243.89	183	271.70	284.77	268.82	257.47	243.80	182	271.67	284.47	268.79	257.42	243.77
0	26	15	182	271.53	283.86	268.29	257.47	243.96	183	271.62	284.21	267.75	256.43	243.54	181	269.51	282.27	269.96	258.50	246.04
0	26	33	184	271.41	283.49	268.48	257.30	243.20	182	271.74	283.44	269.21	257.37	243.00	182	271.86	283.56	268.89	257.30	242.81
0	26	45	184	272.06	283.47	269.00	257.16	242.73	182	272.16	283.45	268.54	256.73	242.63	182	272.26	283.26	268.51	256.69	242.62
0	26	57	183	272.25	283.45	268.93	256.60	242.81	182	272.10	282.97	268.24	256.41	242.39	183	271.86	283.21	268.19	256.31	242.48
0	27	8	183	272.61	283.12	268.12	256.23	242.38	183	271.63	283.02	267.80	256.36	242.24	183	271.87	283.29	267.95	256.22	242.48
0	27	20	183	271.94	283.07	267.93	256.09	242.46	182	271.53	282.95	267.74	256.00	242.26	183	271.48	282.63	267.79	256.91	242.12
0	27	33	182	271.73	282.56	267.54	255.83	242.19	182	271.78	282.49	267.55	255.37	242.21	182	272.03	282.05	267.52	255.95	242.28
0	27	43	183	272.17	282.20	267.67	255.81	242.40	182	271.79	281.91	267.53	255.34	242.21	182	271.83	282.06	267.52	255.96	242.25
0	27	55	183	271.94	282.05	267.30	255.81	242.20	183	271.66	281.79	267.07	255.84	241.91	182	272.07	282.02	267.59	256.16	242.32
0	28	7	183	272.12	281.81	267.13	255.94	242.13	182	271.99	281.49	267.27	255.30	242.07	183	272.22	281.83	267.47	256.02	242.22
0	28	19	184	272.21	281.60	267.40	256.01	242.18	183	272.10	281.62	267.30	255.35	242.19	183	271.94	281.64	267.26	255.75	242.06
0	28	30	184	271.92	281.56	267.38	256.13	242.18	182	272.35	281.72	267.47	256.11	242.27						

HR	MN	SC	ALT	I1	I2	I3	I4	I5	ALT	I1	I2	I3	I4	I5	ALT	I1	I2	I3	I4	I5
0	51	31	325	272.34	281.75	271.05	261.48	250.32	325	272.42	281.82	271.23	262.11	250.44	327	272.60	281.79	271.15	262.17	250.70
0	51	33	330	272.18	281.58	270.87	261.45	250.52	329	271.88	281.56	271.03	262.14	250.67	329	271.73	281.57	271.21	262.12	250.79
0	51	55	333	271.74	281.73	271.09	262.03	250.84	332	271.88	282.09	271.23	262.19	250.84	333	271.88	282.23	271.44	262.32	250.99
0	52	7	335	271.68	282.33	270.92	262.12	250.93	336	271.99	283.24	271.49	262.27	251.36	338	271.94	282.49	273.00	262.92	251.22
0	52	19	341	272.35	284.12	272.28	262.87	251.42	340	272.37	282.73	271.79	262.68	251.58	345	272.23	282.50	271.82	262.85	251.64
0	52	30	343	271.98	282.12	271.39	262.51	251.58	346	272.16	282.27	271.60	262.30	251.89	347	271.78	282.07	271.53	262.69	251.64
0	52	43	347	271.77	281.72	271.46	262.51	251.75	351	271.80	282.12	271.60	262.31	251.91	350	271.89	282.20	271.56	262.90	251.91
0	52	55	353	271.91	281.74	271.35	262.85	251.68	352	271.95	281.79	271.47	263.17	251.95	358	271.89	282.05	271.61	263.15	252.17
0	53	7	358	272.01	281.77	271.63	263.08	252.02	359	272.17	281.93	271.75	263.16	252.25	363	272.13	281.91	271.99	263.24	252.42
0	53	19	362	271.97	281.91	271.82	263.25	252.35	362	271.93	281.39	271.77	263.40	252.46	365	271.79	282.19	271.91	263.52	252.62
0	53	31	367	271.71	281.67	271.69	263.23	252.43	366	271.69	282.10	271.80	263.45	252.76	369	271.32	281.98	271.76	263.46	252.78
0	53	43	368	270.99	281.89	271.85	263.33	252.73	373	271.24	281.96	272.05	263.69	252.97	374	271.41	282.10	272.10	263.78	253.16
0	53	55	377	271.65	281.95	271.91	263.67	253.11	375	272.24	282.22	272.58	264.23	253.57	378	272.25	282.00	272.40	264.08	253.57
0	54	7	379	272.26	282.10	272.41	264.16	253.71	382	272.00	282.02	272.45	264.18	253.65	384	272.07	282.22	272.55	264.43	254.05
0	54	19	385	272.05	282.15	272.12	264.23	253.95	390	272.19	282.23	272.45	264.51	254.25	389	271.87	281.89	272.32	264.31	254.13
0	54	31	392	271.86	282.12	272.53	264.52	254.32	396	271.77	282.22	272.54	264.58	254.44	393	271.94	282.05	272.83	264.89	254.51
0	54	40	394	271.70	282.17	272.69	264.75	254.67	400	271.74	282.22	272.83	264.92	254.82	400	271.87	282.33	272.94	265.08	255.07
0	54	53	404	271.63	282.27	272.99	265.02	255.13	409	271.51	282.33	272.77	265.03	255.19	406	271.78	282.29	273.00	265.32	255.43
0	55	4	407	271.67	282.32	272.98	265.30	255.55	412	272.02	282.37	273.39	265.35	255.97	415	271.67	282.00	273.19	265.67	255.80
0	55	17	416	271.67	282.12	273.39	265.81	256.13	419	271.44	282.35	273.33	265.92	256.41	422	271.94	281.96	273.54	266.04	256.43
0	55	28	425	271.42	282.15	273.39	266.11	256.64	427	271.95	282.05	273.68	266.29	256.88	428	272.06	282.12	273.78	266.48	257.09
0	55	40	429	271.96	281.59	273.35	266.43	257.14	426	272.26	282.45	274.14	266.38	257.47	436	271.74	282.27	273.97	266.84	257.38
0	55	53	437	271.69	282.49	274.32	267.13	257.71	441	271.60	282.40	273.96	266.40	257.69	442	271.86	282.33	274.22	267.43	258.03
0	56	4	444	272.03	282.34	274.39	267.49	258.12	448	272.38	282.35	274.55	267.55	258.27	450	272.09	282.35	274.17	267.49	258.39
0	56	17	448	272.10	282.54	274.64	267.86	258.59	454	271.98	282.35	274.30	267.66	258.58	453	272.10	282.49	274.72	268.08	258.79
0	56	29	455	271.84	282.12	274.67	267.79	258.72	460	272.07	282.18	274.71	267.33	258.73	460	271.77	282.25	274.60	267.91	258.76
0	56	40	462	271.04	282.17	274.52	267.95	258.93	465	270.76	282.16	274.28	267.40	259.01	466	271.04	282.32	274.63	268.12	259.20
0	56	53	466	270.70	282.19	274.46	267.93	259.26	468	271.00	282.26	274.83	268.36	259.46	468	270.52	282.09	274.29	268.14	259.44
0	57	4	474	270.99	282.24	274.89	268.36	259.79	474	271.02	282.26	274.65	268.36	259.67	474	271.06	282.06	274.86	268.64	259.86
0	57	17	476	271.10	282.16	274.63	268.51	259.83	479	271.22	282.02	274.87	268.70	260.01	479	270.82	281.58	274.61	268.44	259.83
0	57	29	479	271.02	282.19	275.03	268.73	260.35	480	271.92	282.08	274.75	268.49	260.31	485	270.95	281.71	274.80	268.64	260.37
0	57	40	483	272.27	284.70	275.51	269.44	261.60	451	271.28	281.92	274.99	269.10	260.85	489	271.34	282.09	275.35	269.25	261.09
0	57	51	491	272.58	284.52	275.49	269.43	262.05	495	271.78	281.94	275.38	269.54	261.40	495	271.55	282.05	275.24	269.44	261.40
0	58	3	498	273.07	284.98	276.12	270.32	262.56	501	271.63	282.24	275.45	269.49	261.68	503	271.31	282.22	275.65	269.81	261.74
0	58	15	509	272.17	285.14	276.05	270.25	262.92	507	272.60	282.97	275.30	269.67	261.93	511	270.35	288.37	277.69	270.50	261.95
0	58	35	517	267.08	277.92	270.65	266.46	261.13	521	265.00	281.02	271.64	267.75	262.80	524	269.39	280.93	274.02	269.10	262.48
0	58	47	525	270.55	282.74	276.01	270.74	263.21	529	272.09	285.55	276.76	271.41	264.42	531	270.75	282.75	276.35	270.97	263.54
0	58	59	531	270.67	282.79	276.27	270.83	263.57	536	271.01	283.02	276.65	271.51	263.96	533	271.70	285.65	276.88	271.72	264.80
0	59	10	546	270.33	283.70	276.70	271.46	264.14	541	271.30	286.77	277.38	272.06	265.13	542	276.95	284.13	276.87	271.56	264.30
0	59	23	547	270.66	286.00	276.35	271.73	265.10	549	265.37	275.42	269.13	266.34	262.40	549	264.98	273.11	265.99	264.88	262.68
0	59	35	545	264.20	269.32	264.74	263.66	262.28	553	264.04	269.41	264.55	263.60	262.67	559	271.05	286.48	278.53	272.96	265.67
0	59	51	561	272.88	290.15	279.47	273.93	265.94	563	271.39	288.34	279.58	273.71	266.02	567	272.83	290.35	279.64	274.11	267.10
1	0	5	567	273.27	289.92	279.78	274.23	267.36	572	272.07	290.19	279.70	274.50	267.56	574	272.69	290.10	279.68	274.36	267.57
1	0	15	572	272.63	291.44	279.74	274.29	267.63	577	269.92	289.13	275.13	271.18	266.43	580	270.63	288.26	276.13	271.98	266.86
1	0	27	582	269.44	285.44	276.17	271.70	266.30	587	271.45	290.31	278.74	273.67	267.71	587	271.60	290.32	278.72	273.80	267.68
1	0	39	589	271.93	291.63	279.84	274.50	268.03	591	272.90	291.68	280.55	275.33	268.67	597	272.32	290.43	280.05	274.76	268.33
1	0	51	601	271.58	288.89	277.79	273.50	268.26	601	272.58	291.08	280.06	275.15	268.98	604	270.69	288.58	277.33	273.13	268.20
1	1	3	607	270.99	287.26	276.45	272.73	269.31	606	272.39	292.45	281.23	276.10	269.65	608	273.42	293.64	282.05	276.50	269.84
1	1	13	607	273.93	293.60	282.14	276.53	269.43	609	273.77	293.53	281.97	276.38	269.70	611	273.79	292.97	282.17	276.56	269.86
1	1	24	612	273.46	291.87	281.24	276.25	269.72	611	274.29	293.12	282.18	276.56	269.91	617	274.36	294.79	282.97	277.00	269.97
1	1	37	616	274.75	294.78	283.76	277.03	270.35	617	274.44	294.56	282.61	277.11	270.30	621	274.41	294.11	282.55	276.99	270.28
1	1	49	621	274.83	292.23	281.33	277.31	270.83	629	274.63	291.52	281.97	276.36	270.84	634	274.89	291.06	281.55	276.92	271.07
1	1	2	631	275.13	293.57	287.91	277.62	271.29	636	275.47	296.65	284.49	278.58	271.79	641	275.19	293.11	282.91	277.89	271.65
1	1	13	639	275.73	294.34	287.72	278.44	272.14	645	275.48	292.13	282.89	278.08	272.11	650	275.38	293.99	283.69	278.37	272.14
1	1	25	647	275.39	294.05	283.77	278.57	272.40	649	274.97	292.50	282.96	278.25	272.12	654	274.76	291.30	282.56	277.89	271.99
1	1	37	652	275.33	292.32	282.34	278.25	272.37	652	275.34	294.58	284.37	279.19	272.77	655	275.60	294.68	284.23	278.90	272.56
1	1	49	653	276.19	295.53	284.36	279.57	273.14	657	276.03	295.58	284.49	279.71	273.05	661	276.22	295.84	285.06	279.74	272.99
1	1	3</																		

FLIGHT NO 7 6/ 12/ 70

HR	MM	SC	ALT	T1	T2	T3	T4	T5	ALT	T1	T2	T3	T4	T5	ALT	T1	T2	T3	T4	T5
1	11	31	747	279.74	283.16	284.85	282.12	277.98	745	280.16	289.68	285.14	282.44	278.13	750	280.52	292.13	286.68	283.49	278.56
1	11	43	753	280.64	281.45	282.55	281.45	278.86	755	280.99	291.58	286.82	283.71	279.26	764	281.79	289.71	285.85	283.18	279.11
1	11	55	769	281.14	288.88	285.44	283.22	279.34	772	282.30	292.54	287.66	285.14	280.41	774	282.81	296.03	290.38	286.83	281.19
1	12	7	732	282.82	282.63	283.61	286.05	281.18	782	282.47	288.18	286.07	284.39	281.15	791	282.83	289.02	286.97	284.96	281.79
1	12	19	797	283.11	283.97	284.83	285.39	281.90	810	283.09	288.06	286.60	285.14	282.19	810	283.54	288.39	287.02	285.50	282.76
1	12	30	813	284.27	283.34	287.34	286.11	283.36	826	284.85	281.33	287.88	286.41	283.71	830	285.04	289.48	288.63	287.05	284.09
1	12	43	833	285.88	291.28	289.77	288.08	285.09	845	286.00	291.49	290.01	288.31	285.15	847	285.96	290.79	289.77	288.26	285.32
1	12	55	852	286.23	290.79	289.79	288.58	285.61	865	287.16	292.22	290.91	289.58	286.48	866	288.70	297.10	294.13	291.88	287.33
1	13	7	873	288.70	296.87	294.14	292.07	287.39	875	288.09	294.08	292.63	291.33	287.41	877	288.86	294.45	293.03	291.44	287.82
1	13	19	887	290.21	297.15	295.04	293.03	288.79	891	290.98	300.00	297.08	294.58	289.49	895	290.70	298.08	295.82	293.83	289.45



(Continued from inside front cover)

- NESC 53. Archiving and Climatological Applications of Meteorological Satellite Data, John A. Leese, Arthur L. Booth, and Frederick A. Godshall, July 1970. (COM-71-00076)
- NESC 54. Estimating Cloud Amount and Height From Satellite Infrared Radiation Data, P. Krishna Rao, July 1970. (PB-194 685)
- NESC 56. Time Longitude Sections of Tropical Cloudiness (December 1966-November 1967), J. M. Wallace, July 1970.

NOAA Technical Reports

- NESS 55. The Use of Satellite-Observed Cloud Patterns in Northern Hemisphere 500-mb Numerical Analysis, Roland E. Nagle and Christopher M. Hayden. April 1971.
- NESS 57. Table of Scattering Function of Infrared Radiation for Water Clouds, Giichi Yamamoto, Masayuki Tanaka, and Shoji Asano, April 1971. (COM-71-50312)

PENN STATE UNIVERSITY LIBRARIES



A000072018286